Spring 5-19-2017

# Evidence of fault movement during the Holocene in Southern Louisiana: integrating 3-D seismic data with shallow high resolution seismic data

Joseph P. Frank
*University of New Orleans*, jpfrank2@uno.edu

# Evidence of fault movement during the Holocene in Southern Louisiana: integrating 3-D seismic data with shallow high resolution seismic data

A Thesis

Submitted to the Graduate Faculty of the
University of New Orleans
in partial fulfillment of the
requirements for the degree of

Master of Science
in
Earth and Environmental Sciences
Coastal Geology

by

Joseph Frank

B.S. The Pennsylvania State University, 2013

May, 2017

# Acknowledgements

I sincerely want to thank my advisor Dr. Mark A. Kulp for his support and guidance throughout my graduate career. I also thank Dr. Ioannis Georgiou and Dr. Royhan Gani for being on my advisory committee. I must also extend my gratitude to Chris McClindon for his help with acquiring the seismic data as well his guidance with the project. My thanks also go to Michael Brown and Andrew Courtois for their help with performing the field work necessary to complete this study.

# Table of Contents

# List of Figures

# List of Tables

# Abstract

The Baton Rouge fault system of Louisiana is a well-known recently active system consisting of en echelon, east trending, down-to-the-south normal faults across the northeast periphery of the Mississippi River delta plain. Two, industry-donated, 3-D seismic surveys across 860 $km^2$ image deep-seated faults below Lake Borgne, along an east strike that parallels previously well mapped segments of the Baton Rouge system. Four major faults (> 6 km fault trace) are imaged within the seismic surveys across the Lake. The industry seismic data were not processed for reliable imaging at depths (<600 m). To bridge the depth gap in seismic, high resolution, shallow seismic data has been acquired in areas where faults are projected to intercept the surface. Integration of high resolution data with industry 3-D seismic data is fundamental to evaluating whether these faults are recently active (Holocene) and if they are strike aligned to nearby, linear wetland loss patterns.



Keywords: Faulting, Southern Louisiana, Holocene, Seismic, Chirp, Marsh Land Loss.

# Chapter 1. Introduction, Organization, and Significance

## *1.1 Introduction*

This study uses large-scale industry seismic data as a novel approach to understand whether deep-seated structures of the Baton Rouge Fault System (BRFS) in Louisiana have affected shallow Holocene strata and geomorphology. The study focuses additionally on identifying the strike-parallel extent of the fault system across a portion of eastern coastal Louisiana.

The BRFS consists of *en echelon,* east-trending faults across the northern border of where Holocene Mississippi River delta plain strata and coastal wetlands onlap Pleistocene and older uplands to the north (Russell, 1940) (Fisk, 1944). The Baton Rouge system trends from west of Baton Rouge to at least as far as eastern Lake Pontchartrain (Fig. 1), whether the system continues farther east has not yet been published outside of internal industry documents. This system dominantly consists of normal, down-to-the-south faults that, to date, have been of primary interest (e.g. Durham and Peeples, 1956; Lopez, 1991; Saucier, 1994; Gagliano et al., 2003; Dokka 2006, 2011; Heinrich, 2006; McCulloh et al., 2012; Yeager et al., 2012 and Haggar, 2014) because of documented property damageabove the system (McCulloh, 2001) and suggestions that it serves as a brine pathway into shallow aquifers (Bray and Hanor, 1990) (Tomaszewski, 1996) (Stoesell and Prochaska, 2005).

Penland et al. (2002) and Gagliano et al. (2003) questioned whether faults can be a mechanism of land-surface elevation change and consequently drive relative sea level rise that can lead to land loss in Louisiana. Gagliano et al. (2003) suggested that the effect of active faults on surface morphology manifests with different signatures, including distinct straight lines and scarps along or across the marsh platform, aligned natural channels, and ballooned channels (Fig.

2) (Gagliano et al. 2003). Previous work suggested that only 0.57% of all wetland loss in Louisiana from 1932 to 1990 is driven by active faults (Penland et al., 2002). Industry level seismic data to truly image deep structures toward the surface was however not available to fully appreciate the magnitude of large, deep-seated, fault slip on near surface geology. Lopez et al. (1991) studied and suggested rates of slip for a small segment of the BRFS. Questions still remain about the eastward extent of the BRFS below the land bridge into Lake Borgne, the slip history, and whether modern surface morphology has geomorpholically responded to fault motion.

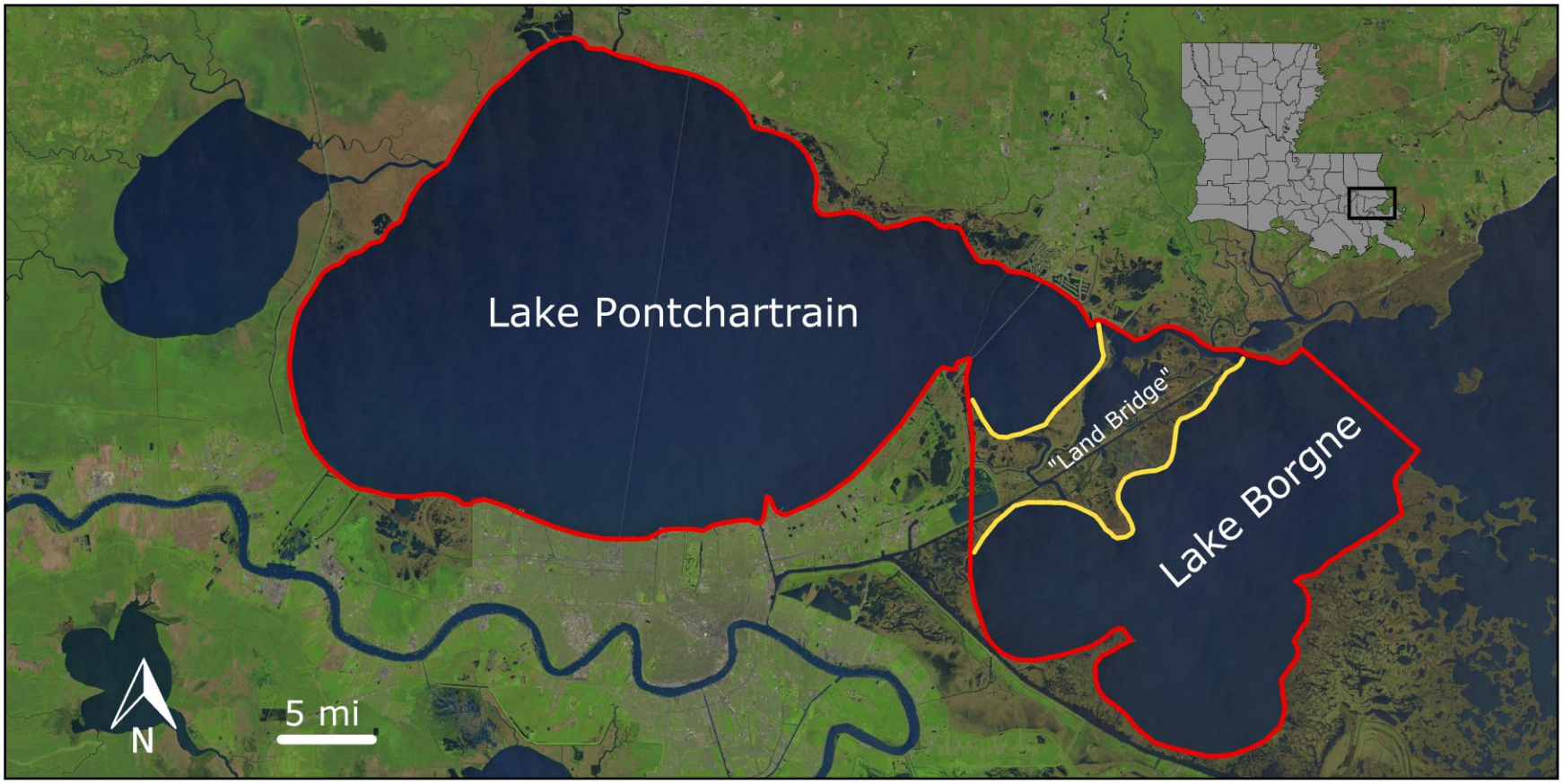


**Figure 1.** Satellite image showing the location of the study area (outlined in red) and the New Orleans "Land Bridge" (outlined in yellow) (image from USGS *Landsat Look Viewer March 27, 2015).*

## *1.2 Purpose and Hypothesis*

### 1.2.1 Purpose

This study consisted of two primary phases: 1) the analysis of deep (2,000 – 24,000ft) (609 – 7,315m) industry-standard seismic data and 2) the collection and interpretation of shallow (30ft) (9m) high-resolution seismic data (Chirp).

The first phase focused on determining whether deep-seated faults are present within the industry seismic and if they are present can they be mapped up section to the limit of the processed industry data. Once deep seated faults were identified efforts focused on using shallow, high-resolution seismic to determine if deep faults of the study area (Fig. 1) have affected Holocene strata and geomorphology of the last 50 years.

### 1.2.2 Hypothesis

The hypotheses are that: 1) the well-known east-trending, normal faults of Lake Pontchartrain extend along strike into Lake Borgne, 2) If the BRFS extends into Lake Borgne, a similar offset to that of Lake Pontchartrain will be seen there, and 3) Linear marsh features reflect sub surface fault motion.

## *1.3 Importance*

The effects of Hurricane Katrina landfall along the northern Gulf in 2005 resulted in the Hurricane and Storm Damage Risk Reduction System (HSDRRS) for New Orleans, the program reinforced weak points in the flood protection system and created flood protection in unprotected areas (Reid, 2013). This required approximately 133mi (214km) of enhanced flood protection (Reid, 2013).

The closest portion of the HSDDRRS to this study area is the Inner Harbor Navigation Channel surge barrier. This surge barrier is 26ft (8m) high and approximately 1.8 mi long (2.9km). While this project is located along the boundaries of the study area, if faults are found to be active in the study area there is the potential for branching faults to reach the project area.It is important to understand the subsurface geology, considering the large investment ($1.7 million) in the project.

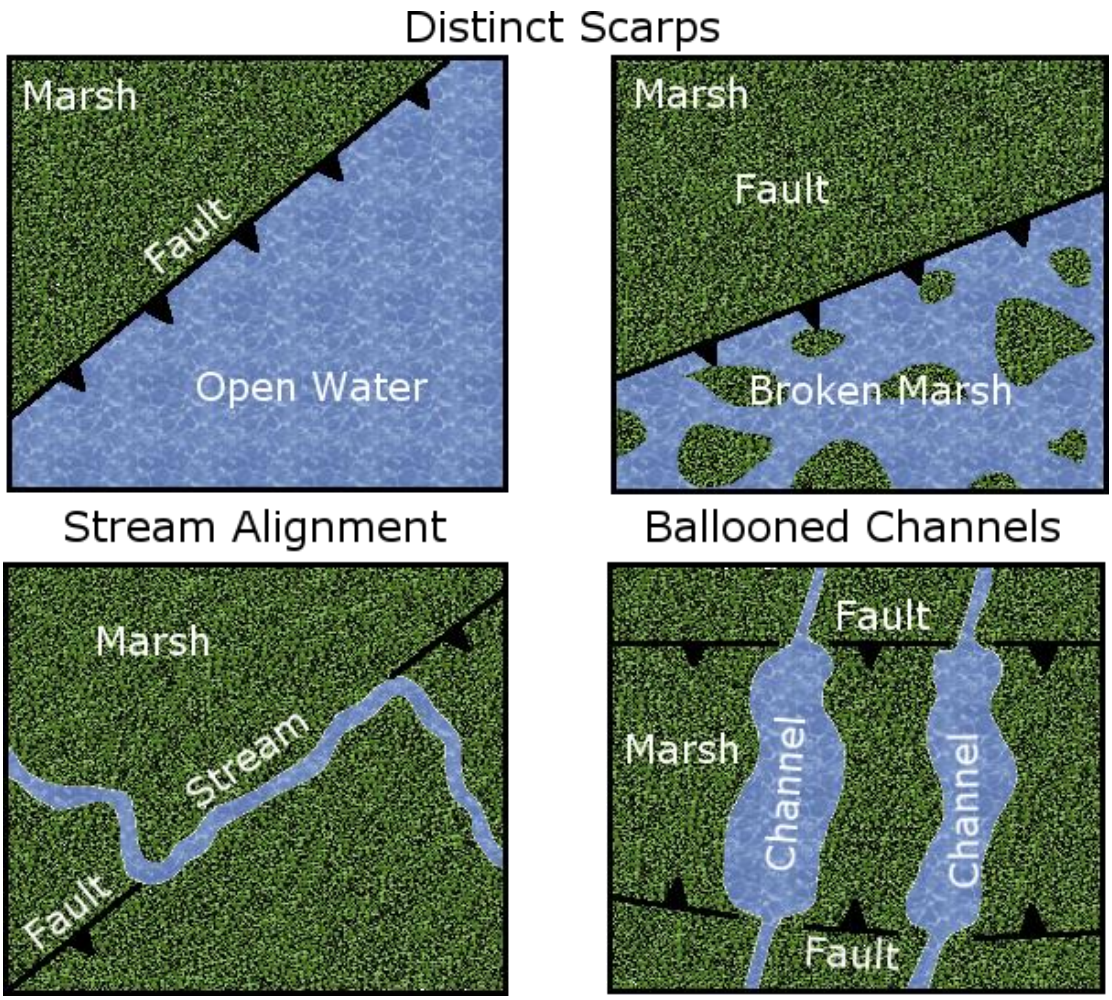


**Figure 2.** Conceptual model showing some of the different geomorphic responses to active surface faulting (modified from Gagliano et al., 2003), including inundation, marsh fragmentation, distributary alignment and bay enlargement. Other examples include geometrically abrupt changes in marsh-edge trends and Lake Formation.

# Chapter 2. Lake Borgne Study Area/Geologic Framework

## *2.1 Louisiana Faults*

The BRFS is part of a larger, generally down-to-the-south Cenozoic fault network that spans the entire southern part of Louisiana (Fig. 3). The network of faults generally trend in the east west direction and consist of down–to-the-south normal faults. Most of the faults within the BRFS are growth faults, whereas the others are non-growth normal faults. Growth faults are distinct from other normal faults, inasmuch that they contain thicker stratigraphic units on the down-thrown side compared to time equivalent units on the up-thrown fault block (Ocamb, 1961). This fault system (Fig. 3) originated when high sedimentation rates created an overburden large enough to cause a detachment décollement along a weak layer such as salt or shale (Peel et al. 1995). It is thought that faults within this system undergo times of quiescence and then become active again during sedimentary loading (McCulloh et al., 2012).

### 2.1.1 Baton Rouge Fault System

Faults of the BRFS were first recognized by aerial photography (e.g. Fisk, 1944) and Murray (1961) suggested that the Baton Rouge system faults were originally active in the Eocene and reactivated in the Quaternary based on sedimentary thickening. This fault system extends west ward where it is known at the Tepetate system (Murray, 1961). East of Baton Rouge, Louisiana the fault system trends across Lake Pontchartrain (Lopez, 1991) and the Pearl River (Yeager et al., 2012). Further to the east this fault system continues into Lake Borgne, where its trend is unknown. Lopez (1991) used seismic data to map faults that transverse Lake Pontchartrain as well as photographs that capture elevation offset on the highway 11 bridge, which is evidence of fault motion. Other studies of the Lake Pontchartrain faults have used shallow high-resolution seismic data (Roth, 1999; Yeager et al., 2012), Lidar (Dokka 2011), and

habitat changes (Haggar, 2014) to map faults in the area. To the south (8mi) (12.8km) fault traces have elsewhere within south central Louisiana fault traces have been mapped using direct overhead and oblique aerial photography to identify scarps within marsh platforms that may indicate vertical offset as well as shallow seismic to confirm the existence of faults (Kuecher et al. 2001, Gagliano et al. 2003, and Martin, 2005)

### 2.1.2 Fault Slip Rates

Studies examining rates of fault motion along this system have suggested that pre Holocene slip (0.01-0.024in/decade) (0.025-0.06cm/decade) was slower than the modern rates (2-4in/decade) (5-10cm/decade), (Smith and Kazmann, 1978; Roland et al., 1981). Yeager et al. (2012) reported rates of fault slip in the lower Pearl River area at 0.05in/yr (1.2mm/yr) during the last 1,300 years and 0.008in/yr (0.2mm/yr) during the last 3,700 years.


**Figure 1.** Map showing generalized distribution of faults within Cenozoic strata of southern Louisiana (originally from Murray, 1961, modified by McCulloh, 2001).

## *2.2 Lake Borgne and Lake Pontchartrain*

Lakes Maurepas, Pontchartrain and Borgne are located in the Lake Pontchartrain drainage basin. This basin covers ~17000mi$^2$ (44,000 km$^2$) and extends from northern Mississippi to the Gulf of Mexico (Flocks et al., 2009a). Lake Pontchartrain is the largest of the lakes within the drainage basin with an area of 770mi$^2$ (2,000 km$^2$) (Flocks et al., 2009a). Within the basin there are eight main waterways that supply fresh water to Lakes Maurepas, Pontchartrain and Borgne. These include the Natalbany, Tickfaw, Tangipahoa, Blind, Amite, and Tchefuncte rivers and bayous Lacombe and Bonfouca. Tidal passes in the basin are the Rigolets, Chef Menteur Pass, North Pass, and Pass Manchac. The Rigolets and Chef Menteur Pass connect Lake Pontchartrain to Lake Borgne and the Gulf of Mexico, whereas North Pass and Pass Manchac connect Lake Pontchartrain to Lake Maurepas (Fig. 4).

Lake Pontchartrain and Lake Borgne are both shallow estuaries with a maximum depth of 16.5ft (5m) and 10ft (3m) respectively (NOAA, 1996). Lake Pontchartrain has a maximum length of 42mi (67km) and a maximum width of 33mi (37km), whereas Lake Borgne has a maximum length of 17mi (28km) and a maximum width of 23mi (38km). The salinities within Lake Pontchartrain average approximately 5ppt (Sikora et al., 1981), whereas the salinities in Lake Borgne range between 2 and 15ppt (USACE, 1984). Most of the water that is supplied to the lakes is fresh water and comes from either Lake Maurepas, supplied fresh water by the Blind River, Tickfaw River, and Amite River, or the Pearl River (Roth, 1999).

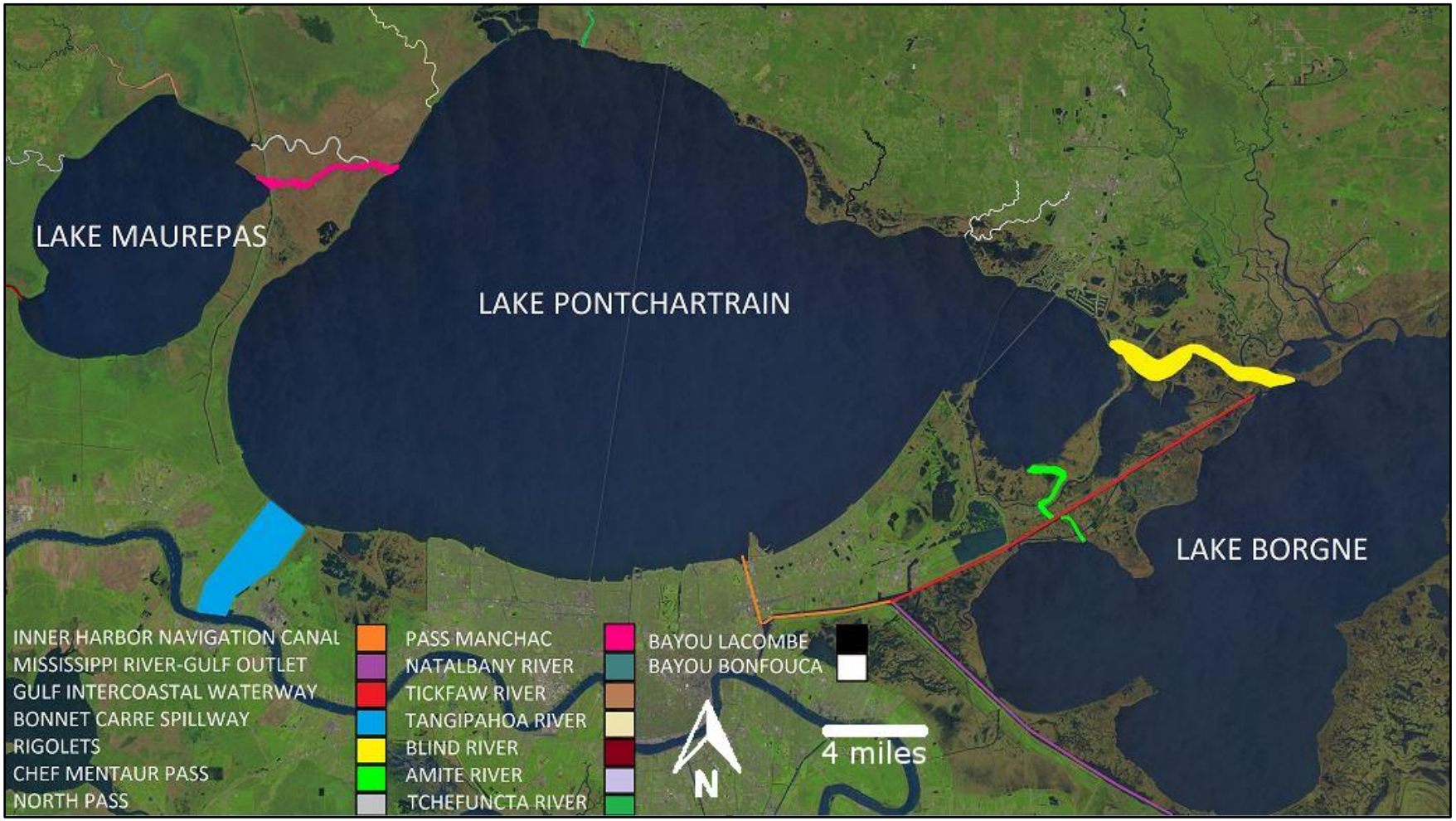


**Figure 4.** Base map depicting the water ways that exist within the Pontchartrain basin and between Lakes Maurepas, Pontchartrain, and Borgne (base image from USGS *Landsat Look Viewer March 27, 2015).*

### 2.2.1 Lake Pontchartrain and Lake Borgne Formation

Two different models of formation have been proposed for Lake Pontchartrain. The first by Otvos (1978) suggested the lake formed in two phases, the first phase began approximately 4.8ka when a barrier system (Pine Island Barrier) partially blocked off the Gulf of Mexico (Otvos, 1978). Stapor and Stone (2004) suggested an inner shelf sand source for the Pine Island Barrier and that sediment transport to the barrier system occurred with a brief sea-level fall approximately 4.1ka (Stapor and Stone, 2004). A second phase of lake formation began 3.9ka when the St. Bernard delta complex prograded closing off more of the open connection to the Gulf of Mexico and thus forming Lake Pontchartrain (Otvos, 1978). The St. Bernard complex was active for approximately 2,000 years before becoming abandoned (Kolb, 1975) (Fig. 5).

The second model for the formation of Lake Pontchartrain also explains the formation of Lake Borgne and is more tectonically driven compared to the previous model. The Lopez (1991) model suggests that Lake Pontchartrain and Lake Borgne began as a delta plain that subsided with down-to-the-south motion along the Baton Rogue-Denham Springs and Lake Borgne fault systems. Lopez (1991) compared width to depth ratios (collected by Price, 1974) of other broad, shallow lakes in southern Louisiana to Lakes Borgne and Pontchartrain and concluded that Lakes Borgne and Pontchartrain did not form from transgression like other lakes of Louisiana.

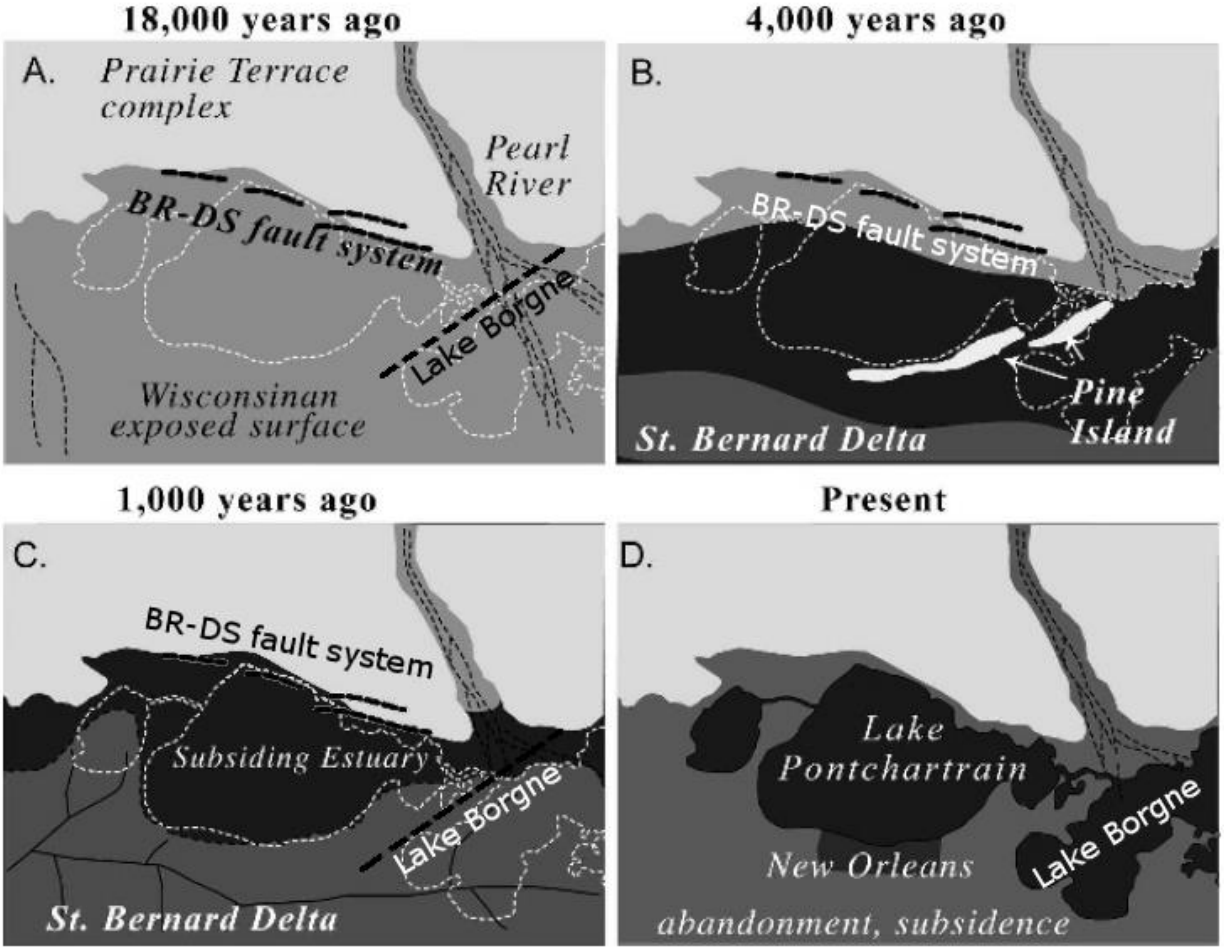


**Figure 5.** Chronological series of figures showing the formation of Lake Pontchartrain and Lake Borgne (modified from Flocks et al., 2009).

### 2.2.2 Lake Geologic Framework

During the mid to late 90's (1994, 1995, 1996, 1997, and 1998) the USGS conducted a study of Lakes Borgne and Pontchartrain. This project included the acquisition of 2-D, high-resolution seismic data (Fig. 7) and shallow (< 20ft) (6m) cores throughout the lake (Fig. 6 and Appendix A). Most of the seismic profiles were collected along west-trending directions, perpendicular to the ideal orientation (north tending) for imaging west-trending faults. Additionally, the seismic data is of poor character in Lake Borgne and of little use to this study. The shallow cores on the other hand provide a sedimentary framework of Lake Borgne Holocene strata. The average depth of penetration for the cores was 5ft (1.5m) with a maximum of 18ft (5.4m). On the basis of these cores the near-surface sediments of Lake Borgne are approximately 25% sand.

Lake Pontchartrain and Lake Borgne are low-energy environments with ~70% of Holocene sediments within the lake consisting of a grain size less than 63μm, which also suggests limited sediment input (Flocks et al., 2009b). The Holocene strata primarily consist of soft gray to dark-gray silty muds with few sand burrows (Flocks et al., 2009b); silt lenses and shell lags are present locally (Flocks et al., 2009b). In some locations a lithologically distinct Holocene stratum is as much as 27-in (70-cm) thick and consists of a heavily bioturbated, brownish-gray mud with sand-filled burrows and shell lags. Flocks et al. (2009b) suggested that the brown coloration is a result of oxidation that is promoted by bioturbation, dredging, and waves that stir up sediments. Shell lags within the unit are acoustic layer that shows up on high-resolution seismic surveys (Flocks et al., 2009b). Pleistocene sediments, below the unconformable Pleistocene-Holocene contact (Saucier, 1994); consist of stiff, olive-gray, silty clays with oxidized organic material and sand-filled burrows (Flocks et al., 2009b).

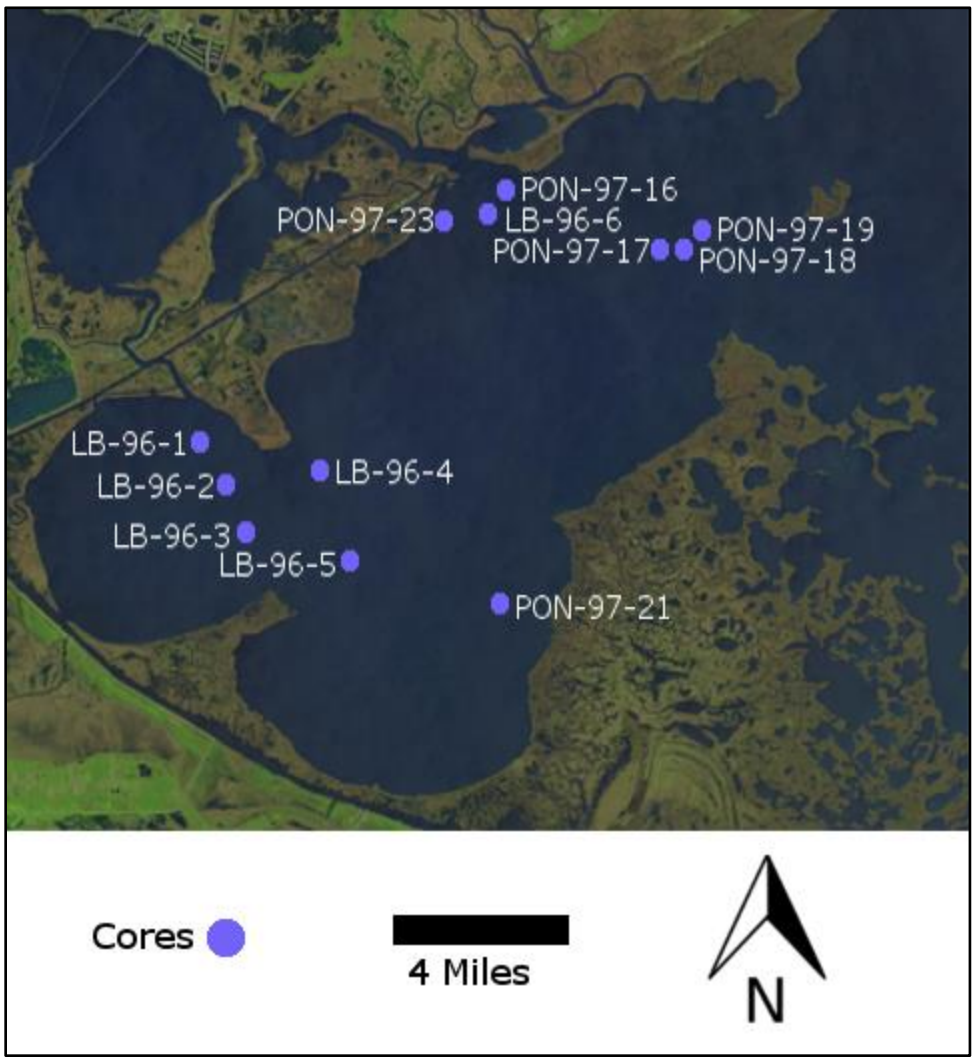


**Figure 6.** Base map showing the locations of USGS cores (base map from USGS *Landsat Look Viewer March 27, 2015, core locations from USGS (1998).*

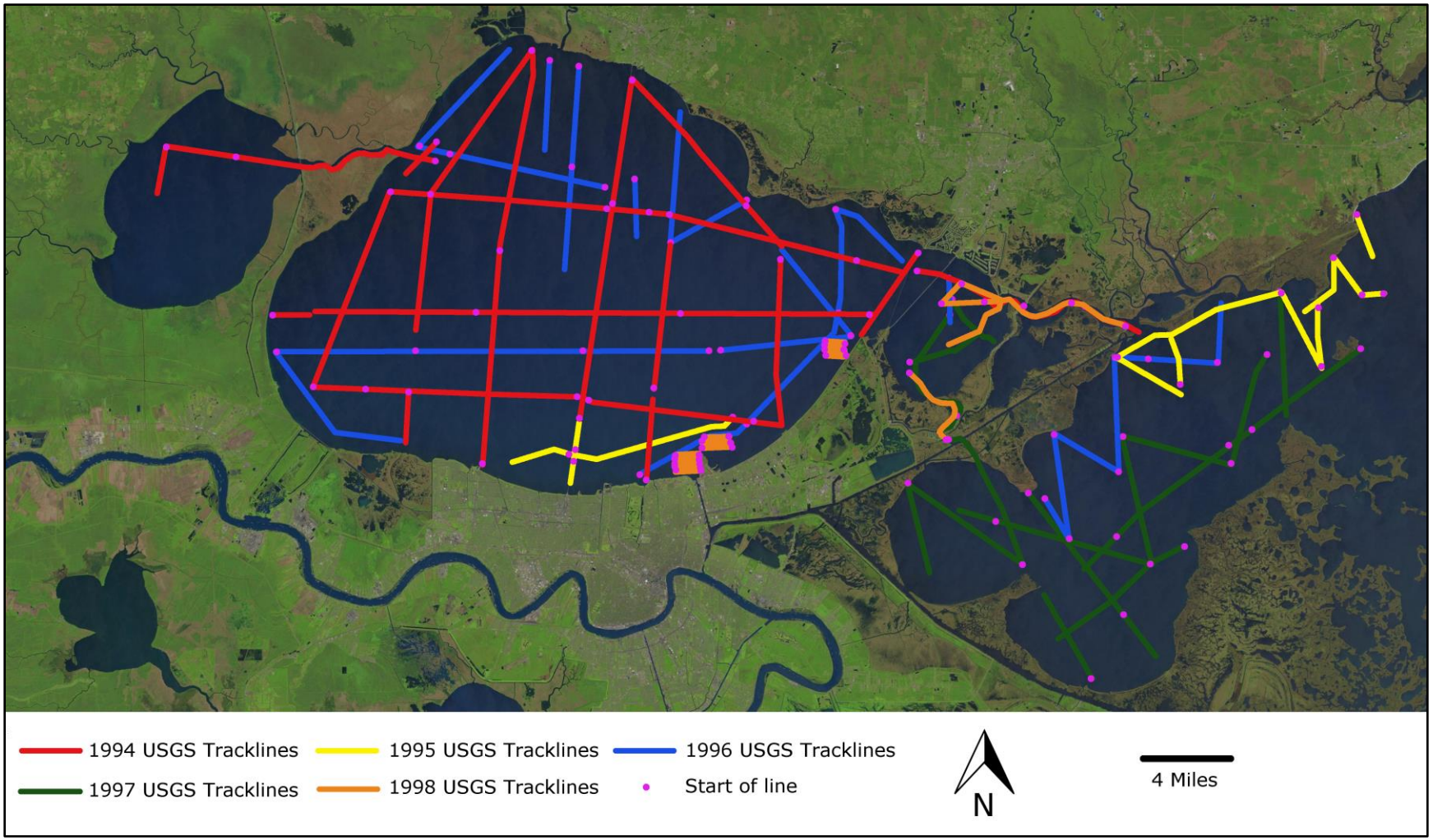


**Figure 7.** 2-D seismic lines acquired during a 1994-1998 USGS study with the starting point of each line denoted with a pink dot (image from USGS *Landsat Look Viewer March 27, 2015).*

# Chapter 3. Methods: Seismic Data and Aerial Photography

## *3.13-D Methodology*

### 3.1.13-D Seismic Data

Locations of deep-seated faults within Lake Borgne were mapped using two, donated 3-D industry seismic surveys, collected by WesternGeco. One survey covered part of west Lake Borgne (142mi$^2$, 367km$^2$), whereas the other covered 190 mi$^2$ (492 km$^2$) of east Lake Borgne (Fig. 8). The sample rate for both seismic surveys was 4ms and both seismic surveys were time migrated. The western survey is the deeper of the two extending to a two-way travel time of 6s, whereas the eastern survey is clipped at a two-way travel time of 1.5s.

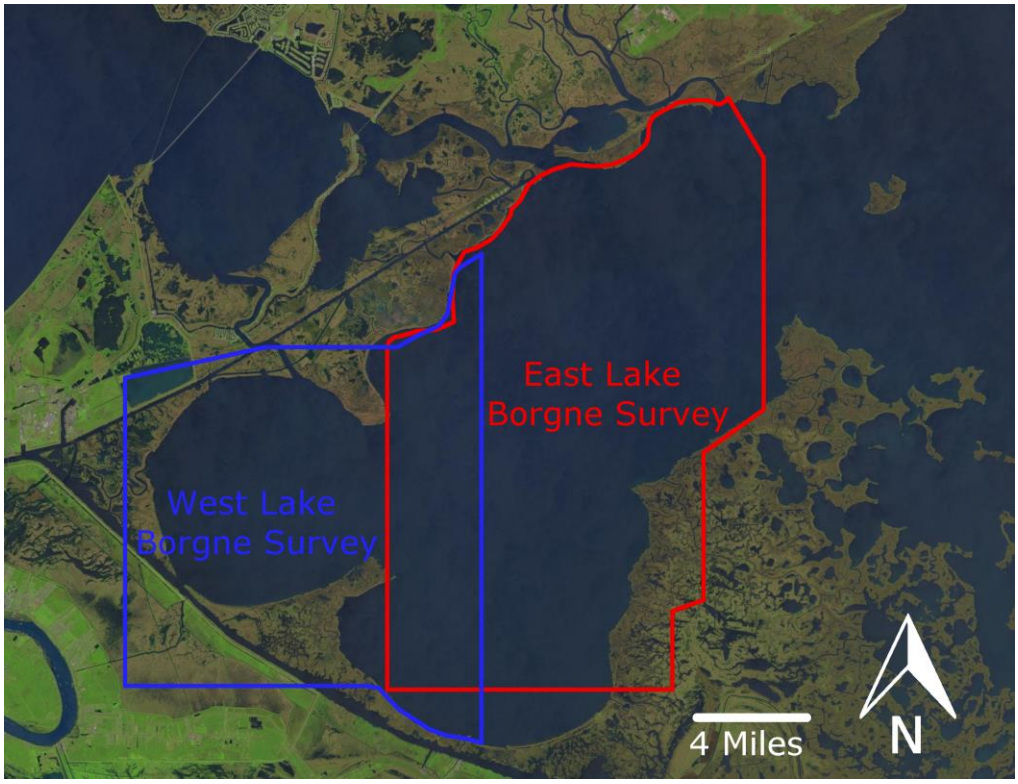


**Figure 8.** Base map displaying the extent of the east and west 3-D seismic surveys (image from USGS *Landsat Look Viewer March 27, 2015).*

Vertical resolution of both surveys was calculated using a method in (Avseth et al. 2010), where the wavelength is determined by dividing the average velocity by the dominant frequency (Fig. 9). The wavelength for each survey was then divided by four to determine the resolution of the seismic data; resulting in a 201ft (61m) vertical resolution for the western survey and 58ft (18m) for the eastern survey because of the different dominant frequency of each survey.

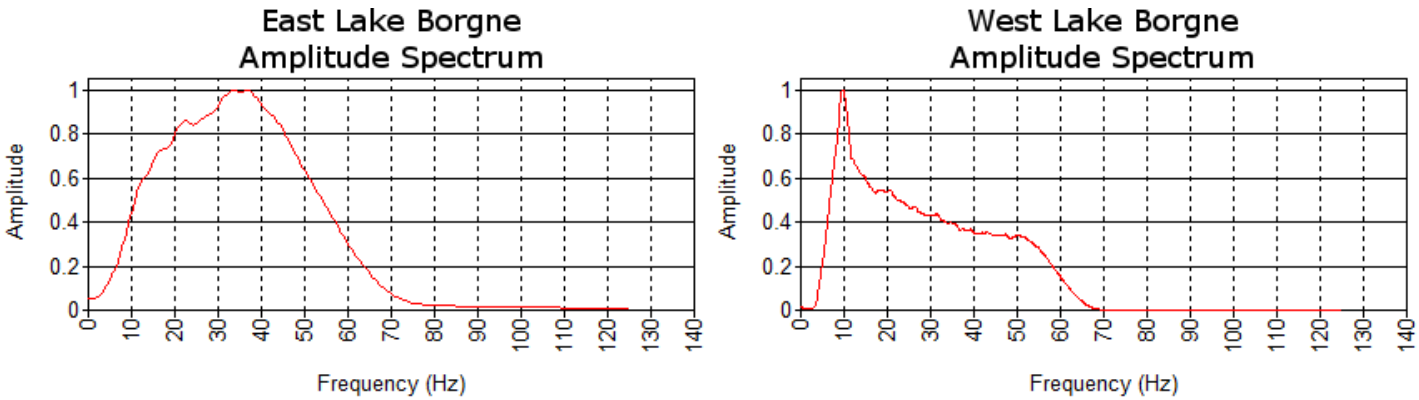


**Figure 9.** Plots of the amplitude survey spectrums for the east and west surveys. The dominant frequency for each of the surveys is the amplitude peak. In this project the eastern survey had a dominant frequency of 35Hz, whereas the survey to the west was 10Hz.

### 3.1.2 Synthetic Seismogram

There was no readily available time-depth data for the Lake Borgne and Lake Pontchartrain area so one had to be created for the purpose of tying wells into the seismic data. An accurate way of creating a time-depth chart is to construct a synthetic seismogram. The inputs required to construct a synthetic seismogram using *Synpack* (an *IHS Kingdom* extension) are digitized sonic and density well logs. There were recent (2008) well logs in the Lake Borgne area that contained the required logs, but they were in a TIF format, that is not recognized by *IHS Kingdom*. To digitize the well logsinto a suitable format an extension of the *IHS Kingdom suite*, called raster log editor, was used. The raster log editor extension allows one to import non-digital well log files and allows the user to define well log tracks, as well as calibrate the depth. Both

the density and sonic logs were manually digitized by tracing the log lines of the 10,420ft (3176m) deep Devon Energy Corporation state lease 19241 well number 1. After the proper well logs were digitized a synthetic seismogram was created (Fig. 10) and fit to the actual seismic trace. Once the synthetic seismogram was aligned with the actual seismic trace (peaks with peaks and troughs with troughs) a time-depth chart was created and since the Devon Energy well was one of the only wells in the area with both sonic and density logs it was feasible to apply this time-depth chart to all of the other wells in the area.

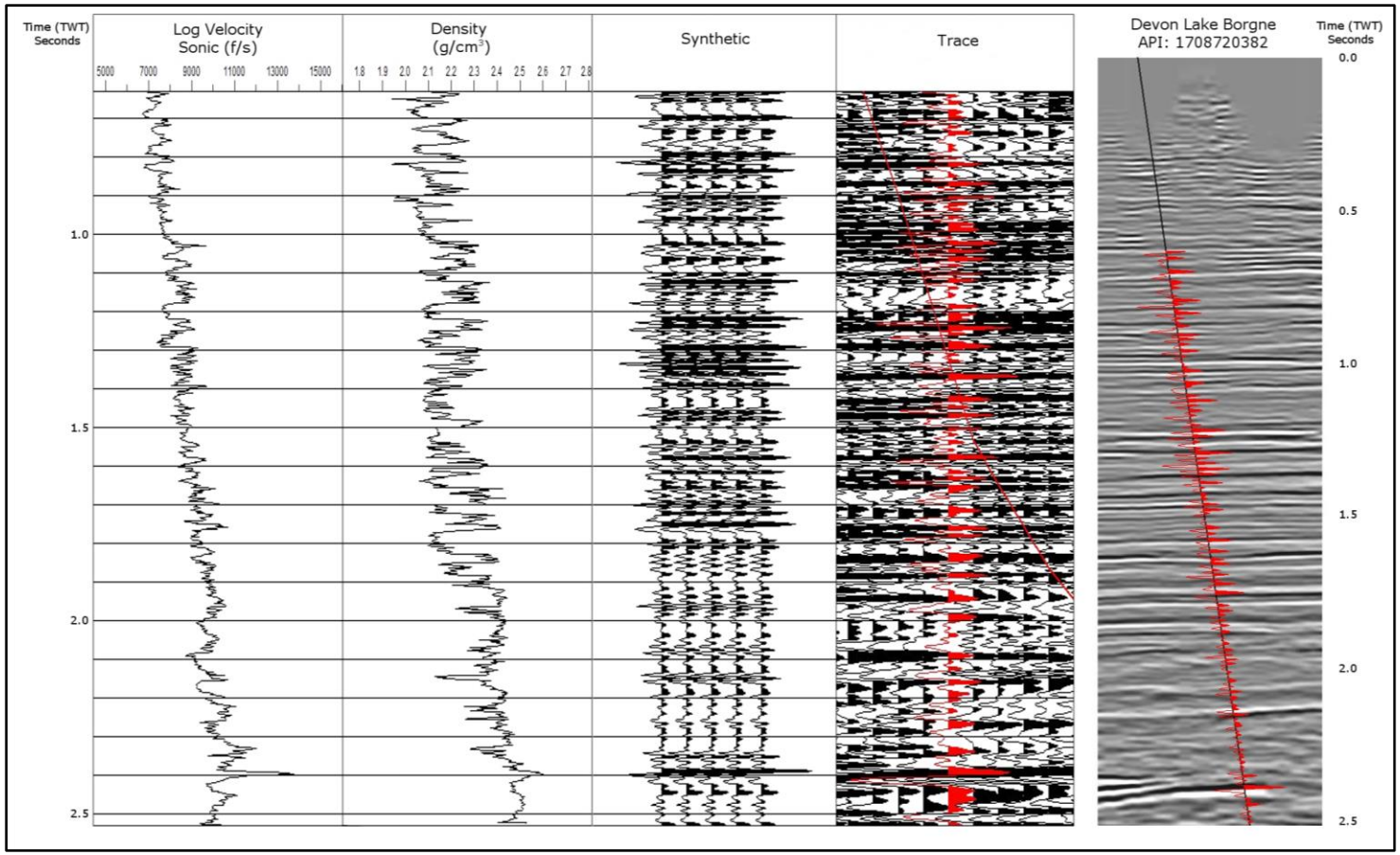


**Figure 10.** Left part of the figure shows the sonic and density well log inputs for the synthetic seismogram. Middle part of the figure shows the synthetic trace individually and overlain with the actual seismic trace. The right side shows the resulting synthetic on the Devon Energy API: 1708720382 well and how well it ties in with the amplitudes.

### 3.1.3 Well Logs

Well logs are abundant in Lake Borgne (Fig. 11) and Lake Pontchartrain (Fig. 12) area because 1960s through 1970s hydrocarbon exploration. All well logs of this study (n= 27) were obtained through the Louisiana Department of Natural Resources (sonris.com) and uploaded into *IHS Kingdom* using the raster, log-editor extension. Most of the well logs in this area only contain spontaneous potential (SP) and resistivity, primarily because it was not common practice to use gamma ray logging tools when these wells were drilled. The SP log shows the electrical potential between the rock layers and the borehole tool and porous strata (sand) are represented on a SP curve differently than non-porous strata (shale). For example the SP of a porous stratum will yield a curve that has a lower value relative to the SP curve of a non-porous stratum. Resistivity curves show the electrical resistivity of pore fluids within the strata and units with saltwater filled pores will create a signature that is distinctly different from strata with hydrocarbons.

Well logs of this study were used to establish age-depth relationships within the industry seismic reflection data. Logs within the Lake St. Catherine (Fig. 12) oil field indicate sand bodies at depth, age constrained with foraminifera *Textularia stapperi that* can be lithologically as well as chronostratigraphically correlated to well logs from Lake St. Catherine to Lake Borgne.

Three wells in Lake St. Catherine were correlated 2.8mi (4.5km) to the first well in Lake Borgne using SP and resistivity logs (Fig. 13). Similarly to the 3-D seismic surveys the well logs located in Lake Pontchartrain were also used to provide an age constraint on the 2-D seismic lines. The difference is that on the 3-D seismic surveys well locations fell were located within the survey and wells were located in between the 2-D lines. This means that foraminifera picks needed to be extrapolated from the well to the seismic line.

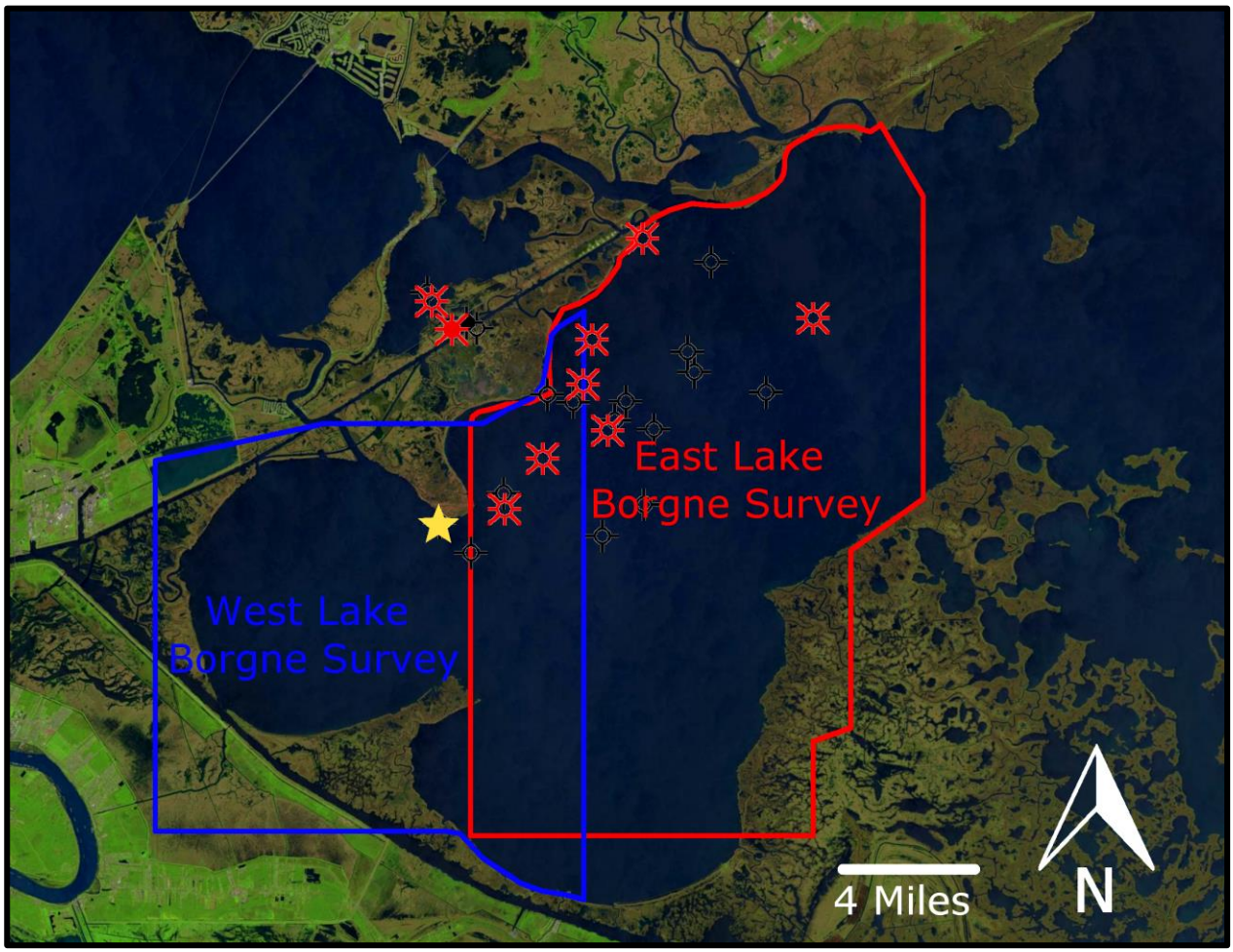


**Figure 11.** Map showing **w**ell locations in Lake Borgne. Black colored wells are oil wells, whereas red wells are gas wells. A solid well center indicates a productive hydrocarbon well. The well indicated by the star is the Devon Energy well used for the synthetic seismogram (background image from USGS *Landsat Look Viewer March 27, 2015).*


**Figure 12.** Well locations in Lake Pontchartrain. Black colored wells are oil wells, whereas red well are gas wells. Solid well center indicates a productive hydrocarbon well (image from USGS *Landsat Look Viewer March 27, 2015)*


**Figure 13.** Map showing the cross section line across the five wells that were correlated from Lake St. Catherine to Lake Borgne in figure 13 (image from USGS *Landsat Look Viewer March 27, 2015).*

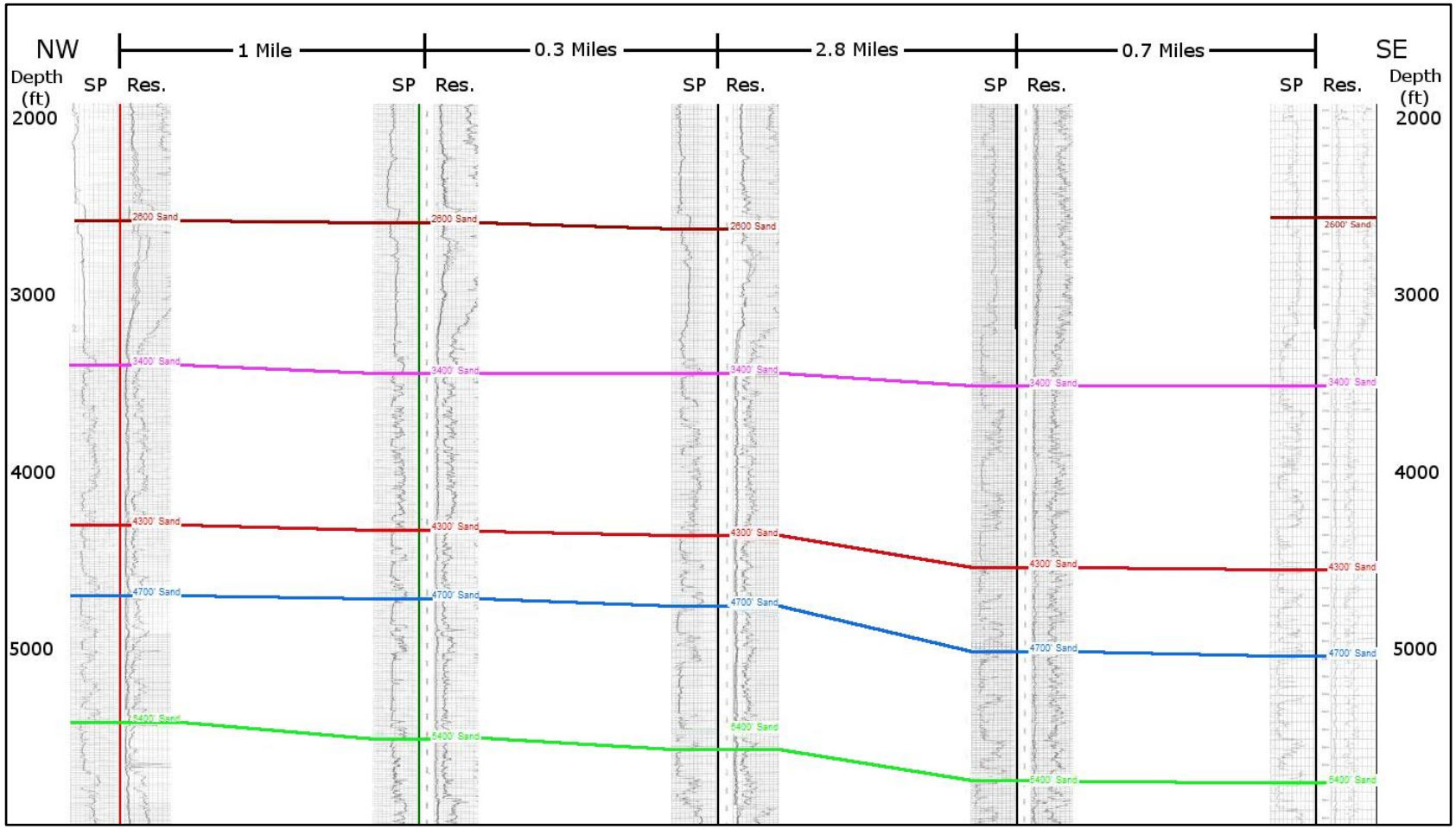


**Figure 14.** Two well logs located in Lake St. Catherine were correlated into Lake Borgne. The 4300' sand (red) was dated as middle Miocene on the basis of foraminifera control, specifically *Textularia stapperi* (well logs obtained from sonrise.com, foraminifera age from Bureau of Ocean Energy Management, 2003; trend of cross section is shown on figure 13).

### 3.1.4 Fault Interpretation

A focus of this project was to interpret the seismic surveys and determine whether any deep-seated faults are present at depth in the study area. To facilitate this, a seismic attribute known in *IHS Kingdom* as dip of maximum similarity (sometimes called a discontinuity attribute) was used. Discontinuity attributes scan all of the traces in the seismic survey and measures how dissimilar the amplitudes of adjacent traces are to each other. The result of this style of analysis is a new seismic volume within which white areas are similar (e.g. laterally continuous strata) and black areas are dissimilar, which can be faults, processing artifacts, and changes in dip (Fig. 15).

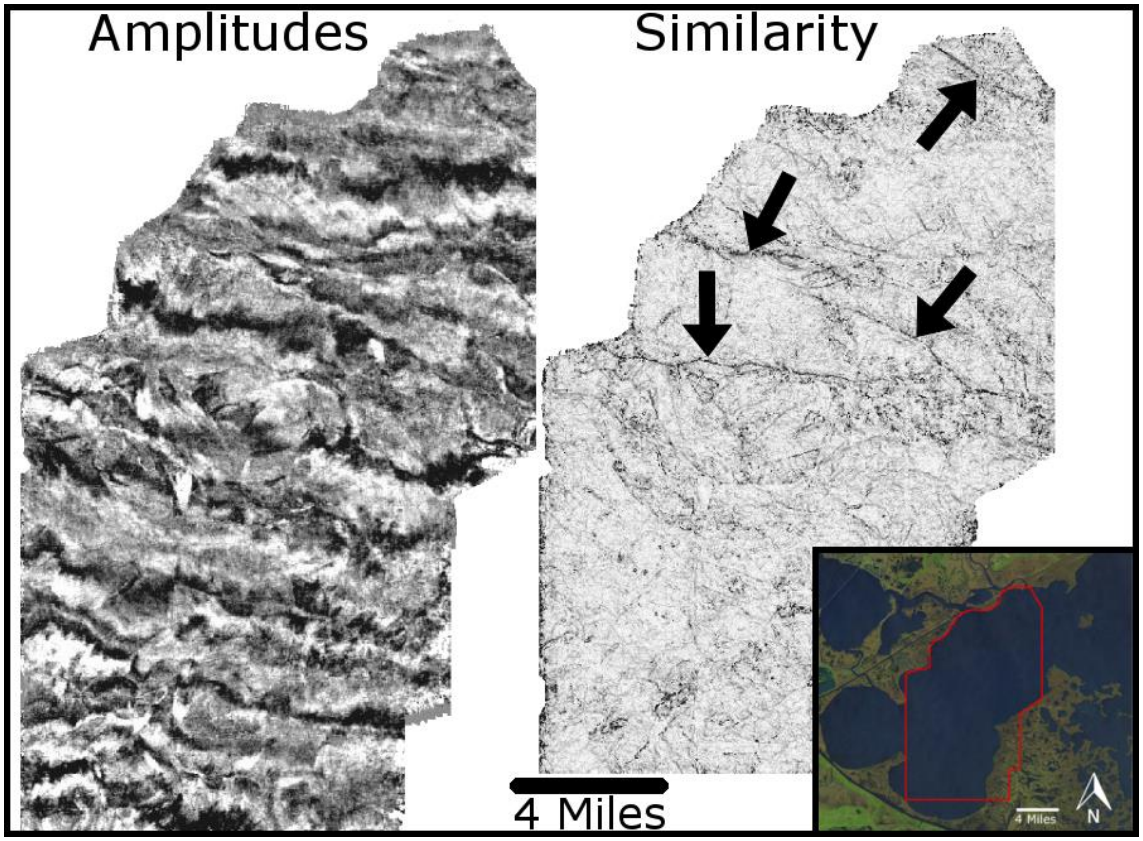


**Figure 15.** Time slices at a two-way travel time of 1s. Image on the left is amplitudes and image on the right is dip of maximum similarity with the location of faults indicated by arrows (inset map (image from USGS *Landsat Look Viewer March 27, 2015).*

Faults identified in the data set were mapped on the smallest interval possible (110ft) (33.5m) in the survey grid to get the most accurate representation of the fault plane. To ensure that most of the faults were found within the dataset strong seismic reflectors were mapped throughout the entire survey, while mapping the reflector any offset was marked as a potential fault. A strong reflector in seismic data exists when there is a drastic change in the velocity at which the acoustic waves travel through the strata, which indicates a change in lithology or pore content. The eastern seismic survey (Fig. 16) only becomes resolvable at a two-way travel time of approximately 0.4s due to lack of processing; this makes it unclear if the faults mapped in the survey extend into the near surface (1600ft)(487m) sediment. Faults were projected to the top of the seismic volume (0s two-way travel time) by extrapolating the at-depth fault angle stratigraphically upward (Fig. 17). This assumes that the magnitude of fault dip is constant from depth into more shallow strata but on the basis of there is no observable change in the curvature of the fault plane this is justified. Other studies (Kuecher et al. 2001 and Lopez, 1990) have shown that listric geometries of faults are typically observed at 2.5s to 2.0s which is similar to the faults observed in the western Lake Borgne survey. The result of this effort was the creation of a map showing the expected intersection of the at depth fault traces with the surface (Fig. 18). This map provided the fundamental basis for determining where near surface investigations should take place to assess whether deep–seated faults have impacted the surface or near surface stratigraphy; a starting point for the Chirp seismic collection.

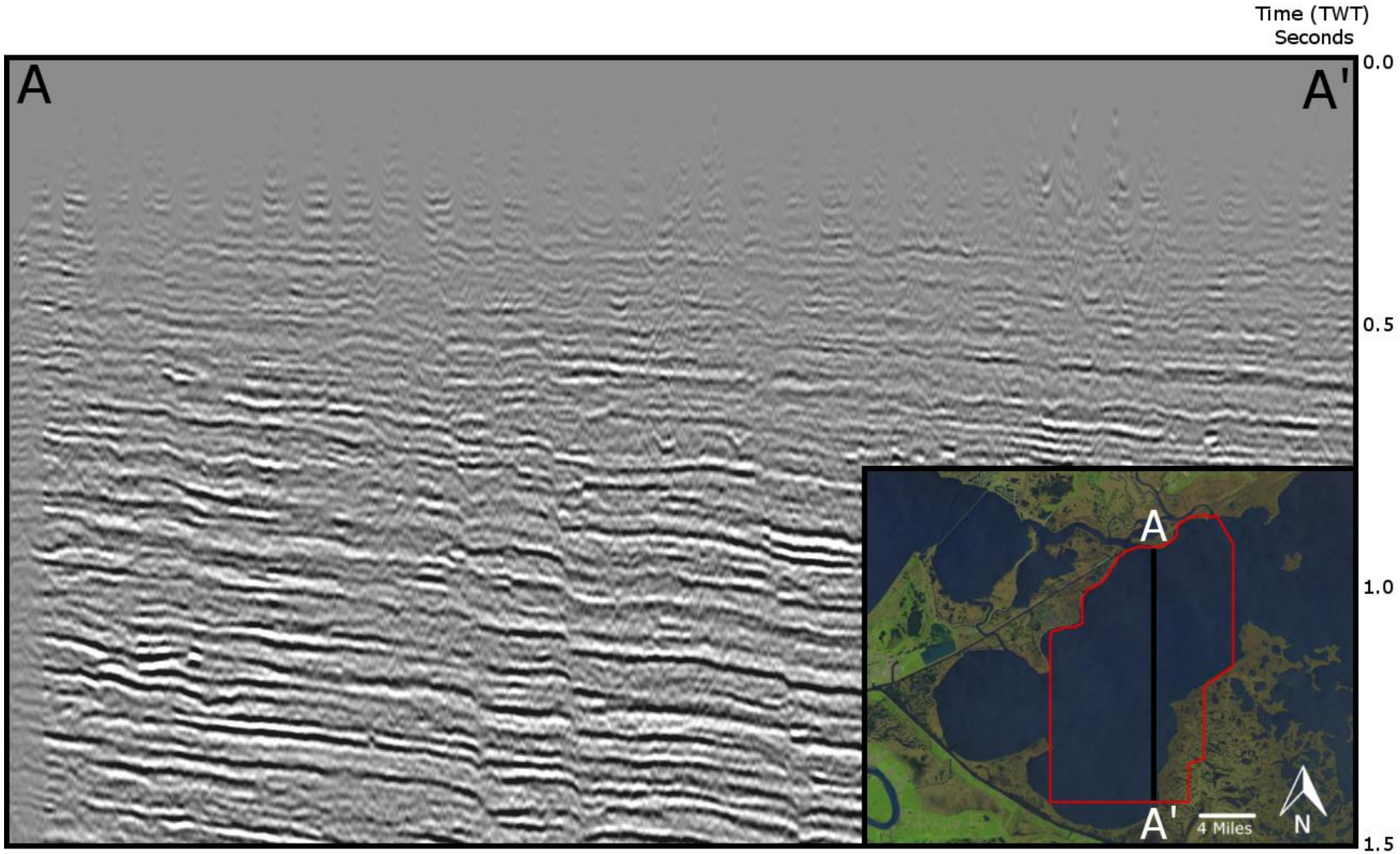


**Figure 16.** Uninterpreted seismic line A-A’ within the east Lake Borgne survey (inset map background from USGS *Landsat Look Viewer March 27, 2015).*

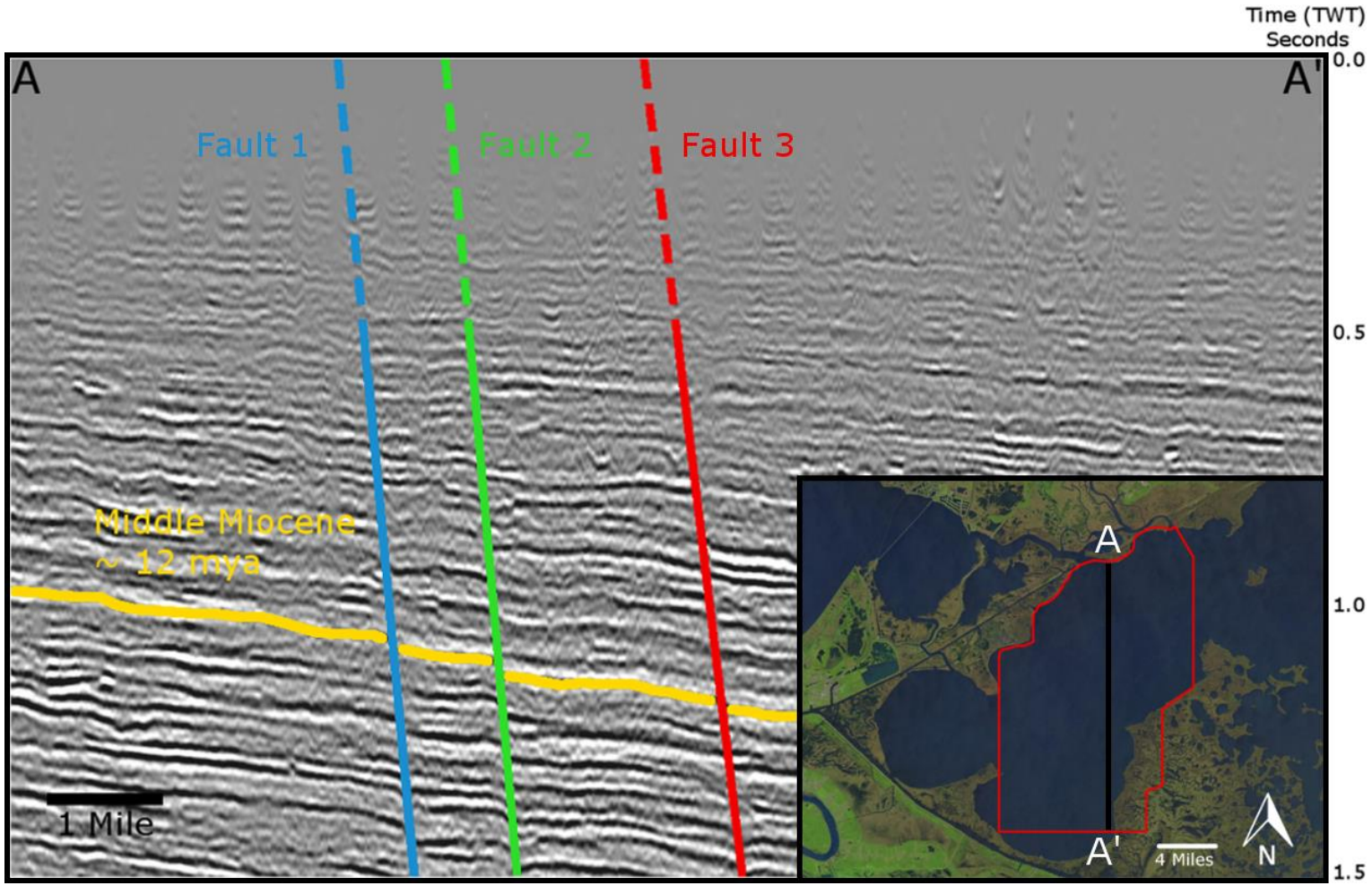


**Figure 17.** Seismic line A-A' showing the attitude of the three faults that are the primary focus of this study. The dashed portion of the faults represents the intervals that were projected stratigraphically upward. Yellow horizon is Middle Miocene in age determined from wells that were projected into the survey. From now on faults will be labeled as such fault 1 (blue), fault 2 (green), and fault 3 (red) (inset map background from USGS *Landsat Look Viewer March 27, 2015).*

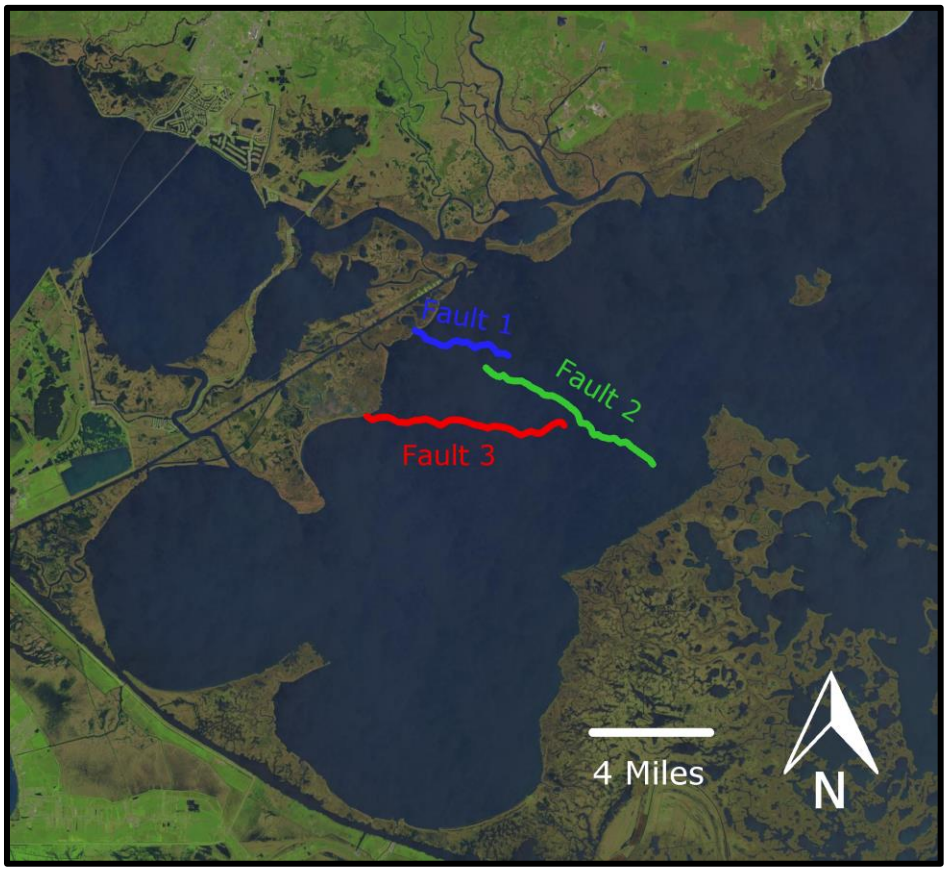


**Figure 18.** Projected fault traces at surface (0s two-way travel time). Three faults are present fault 1(blue), fault 2 (green), and fault 3 (red) (background image from USGS *Landsat Look Viewer March 27, 2015).*

## *3.2 Chirp Methodology*

### 3.2.1 Chirp System

Chirp seismic has been used in a wide array of studies focused on geohazards, pipeline routes, and marine archaeological investigations (Dyer, 2011; Tian, 2008; Bull et al. 1998) with success partially because of the system's ability to image the subsurface with excellent vertical resolution. The Chirp system used for this study was an *Edgetech* SB-216 system, which consists of a tow fish and a 3100-p topside processor. The *Edgetech* SB-216 tow fish contains a singular transducer for emitting the acoustic signal and two receiver arrays. The system operates in the frequency range of 2-16 kHz providing penetration depths of as much as 300ft (91m) depending on the sediment characteristics. Sand-rich strata are likely to be on the shallow end of penetrating depths (20ft) (6m) whereas mud-rich strata result in penetration depths of 300ft (91m). The vertical resolution for this system ranges between 2.3in (5.8cm) to 3.9in (9.9cm), which means this system could capture potential offsets in the Holocene as small as 3.9in (9.9cm). The topside unit is a real-time processor that converts the raw seismic data into transit waveforms. More specifications of the *Edgetech* SB-216 system are contained in table 1.

| SB-216S | |
|---|---|
| Frequency Range | 2-16 KHz |
| Pulse Bandwidth | 2-15 KHz 2-12 KHz 2-10 KHz |
| Vertical Resolution | 2.3in 3.1in 3.9in |
| Penetration in Sand | 20ft |
| Penetration in Clay | 260ft |
| Beam Width | 17 20 24 |
| Transmitters | 1 |
| Receiver Arrays | 2 |
| Input Power | 112 Watts |
| Dimensions | |
| Length | 41 in |
| Width | 31 in |
| Height | 18 in |
| Weight | 160 lb |
| Depth Rating | 984 ft |

**Table 1.** Specifications of the *Edgetech* SB-216 sub bottom profiler system that was used in this study to collect Chirp seismic data (from *Edgetech* Hardware Manual, 2014).

### 3.2.2 Data Collection

Two days of Chirp surveys were conducted during calm marine weather during which 30 survey lines were collected providing coverage along 32mi (51km). The sample rate of collection was 46 microseconds which means that data was collected every 46 microseconds.

A *Trimble* DGPS was linked during the surveys to a laptop running *Hypack Hydrographic Survey* software which was used for navigation.The Trimble DGPS was offset from the Edgetech tow fish by approximately 10ft (3m) there by providing a high degree of geographic positional accuracy. The planned survey lines (Fig. 19) were created using *Hypack* and when connected to the *Trimble* DGPS, *Hypack* provides line guidance (left right indication) during data collection. The other laptop (*Panasonic* Toughbook) provided storage and a real time look at the Chirp data as it was collected using *Edgetech Discover* software. The *Trimble* DGPS was also fed into this computer to provide locations for the shot points along the survey lines. The Chirp was able to penetrate to an average depth of approximately 15ft (4.5m).

### 3.2.3 Chirp Data Set

*Edgetech Discover* software collects data as: 1) standard Society of Exploration Geophysicists (SEG-Y 3200 byte header) and 2) JSF (proprietary *Edgetech* format). Since the 3-D industry survey was already loaded into *IHS Kingdom* as SEG-Y, it was logical to record Chirp in SEG-Y format so that data could be loaded into 3D seismic project. The loading procedure for the Chirp seismic data is different from the industry seismic because firstly the type of data (2-D vs. 3-D) and the geodetic projection in which the data was collected. To load the Chirp seismic data into the *IHS Kingdom* project required a conversion of the projection system from latitude and longitude WGS 1984 to state plane NAD 1927 (U.S. survey ft.). This required extracting the header data from SEGY Explore (an *IHS Kingdom* extension) into an Excel spreadsheet. The data on the spreadsheet is then converted into the desired format (NAD 1297 state plane) using the National Oceanic and Atmospheric Administration's (NOAA) *VDatum* software, the result is a spreadsheet with the converted locations of every shot point recorded on that specific line. The shot point coordinates were then loaded into *IHS Kingdom* for each Chirp line. Once the shot point locations were loaded, the amplitudes of individual shot points could be loaded.

### 3.2.4 Chirp Interpretation

The objective of collecting the Chirp images was to determine whether there existed any shallow signs of stratigraphic fault offset or stratigraphic disruption that could be the result of fault motion. Fault-induced deformation may be difficult to identify in the shallow stratigraphy and might not appear as clear stratigraphic offset because of the high water content of the substrate (Yeager et al. 2012), which could lead to ductile deformation rather than brittle deformation. In the area that the Chirp was collected and with the relatively shallow depths of

penetration it was to be expected that any signs of faulting would be ductile deformation because the sediments are unconsolidated.

### 3.2.5 Holocene/Pleistocene Boundary

The inferred Holocene/Pleistocene boundary was also interpreted on the Chirp lines to give an age perspective on how far the chirp was able to penetrate. To determine the approximate depth of the Holocene-Pleistocene stratigraphic contact in the study area an isopach map of the Holocene thickness (Kulp et al. 2002) was used. This depth was then converted into time using the average velocity of sound through unconsolidated sediment (3921f/s) (1500m/s) (Kulp et al. 2002; Suter, 1986; Kindinger, 1988; Sydrow and Roberts, 1996).

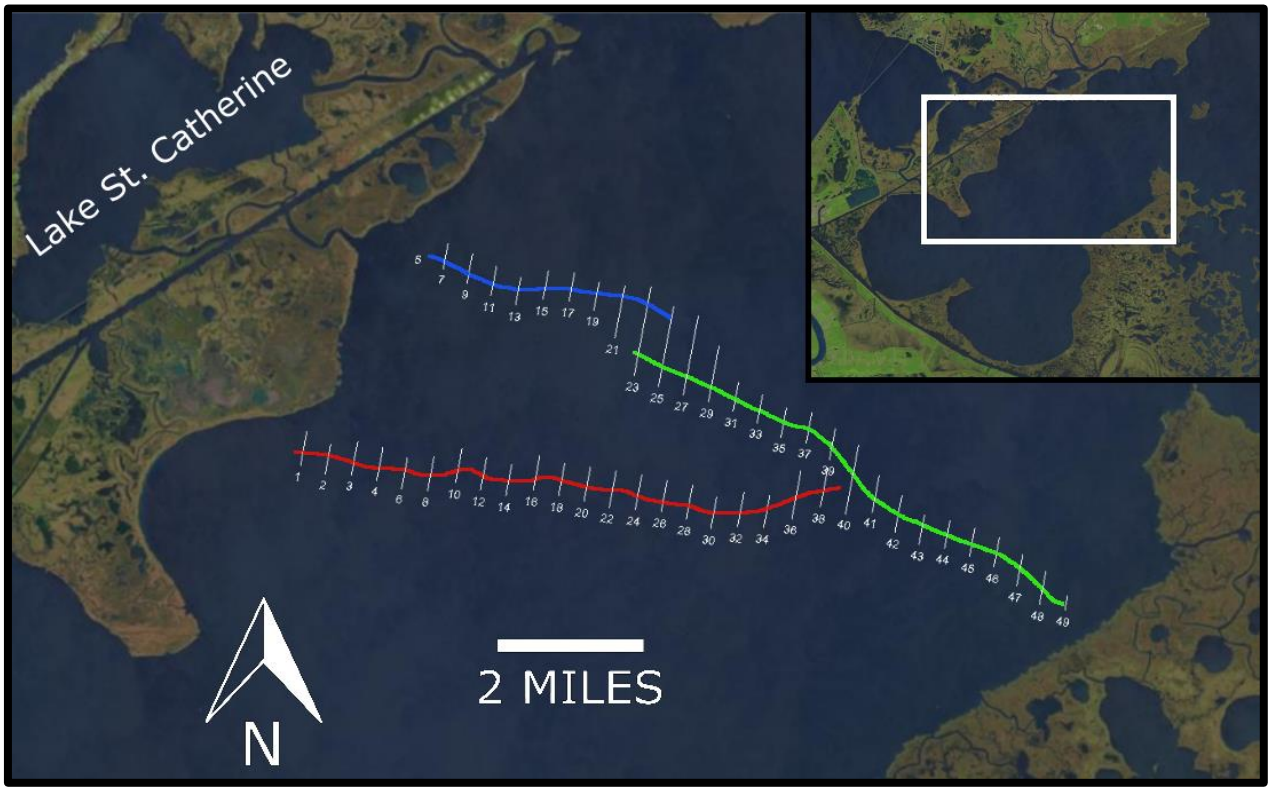


**Figure 19.** The 49 Chirp seismic lines that were planned to be collected in the middle of Lake Borgne where deeper industry imaged faults were projected to the surface. Short lines are ~1mi (1.6km) long, whereas the longest lines are ~ 2mi (3.2km) (image from USGS *Landsat Look Viewer March 27, 2015).*

## *3.3 2-D Lake Pontchartrain Methodology*

### 3.3.1 Data Set

The Lake Pontchartrain data set consists of 18, 2-dimensional seismic lines that cover the entirety of the lake (Fig.20) for a total distance of 382mi (614km). The seismic data was collected in 1985 by WesternGeco using a *DigiSeis* airgun. The sample rate for the data collection was 4ms and is time migrated. The calculated vertical resolution of the data is 201ft (61m) with a dominant frequency of 10Hz. The 2-D lines image a two-way travel time of 6s which is approximately 24,300ft (7406m) based on an average velocity of 8,100ft/s (2468m/s) that was calculated from the time-depth chart created by the synthetic seismogram. Compared to the two 3-D seismic data the 2-D seismic data were processed to a more shallow depth (400ft, 122m vs. 1620ft, 493m), which allows deep faults to be imaged closer to the lake bottom. The purpose of using the Lake Pontchartrain 2-D seismic lines was to determine whether faults of Lake Borgne are along-strike continuous into Lake Pontchartrain.

### 3.3.2 2-D Interpretation

Fault interpretation is different on 2-D seismic lines, compared to 3-D seismic volumes, because of are large distances between each seismic line (4mi) (6.4km). This makes fault interpretation a challenge because it is difficult to establish which faults are the same on adjacent 2-D lines. Horizon mapping on 2-D is similar to 3-D, the 2-D lines cross each other which allows the transfer of horizons from line to line. There are 7 wells that contain paleo-data within Lake Pontchartrain that helped constrain age relationships of amplitude horizons (Fig. 12).

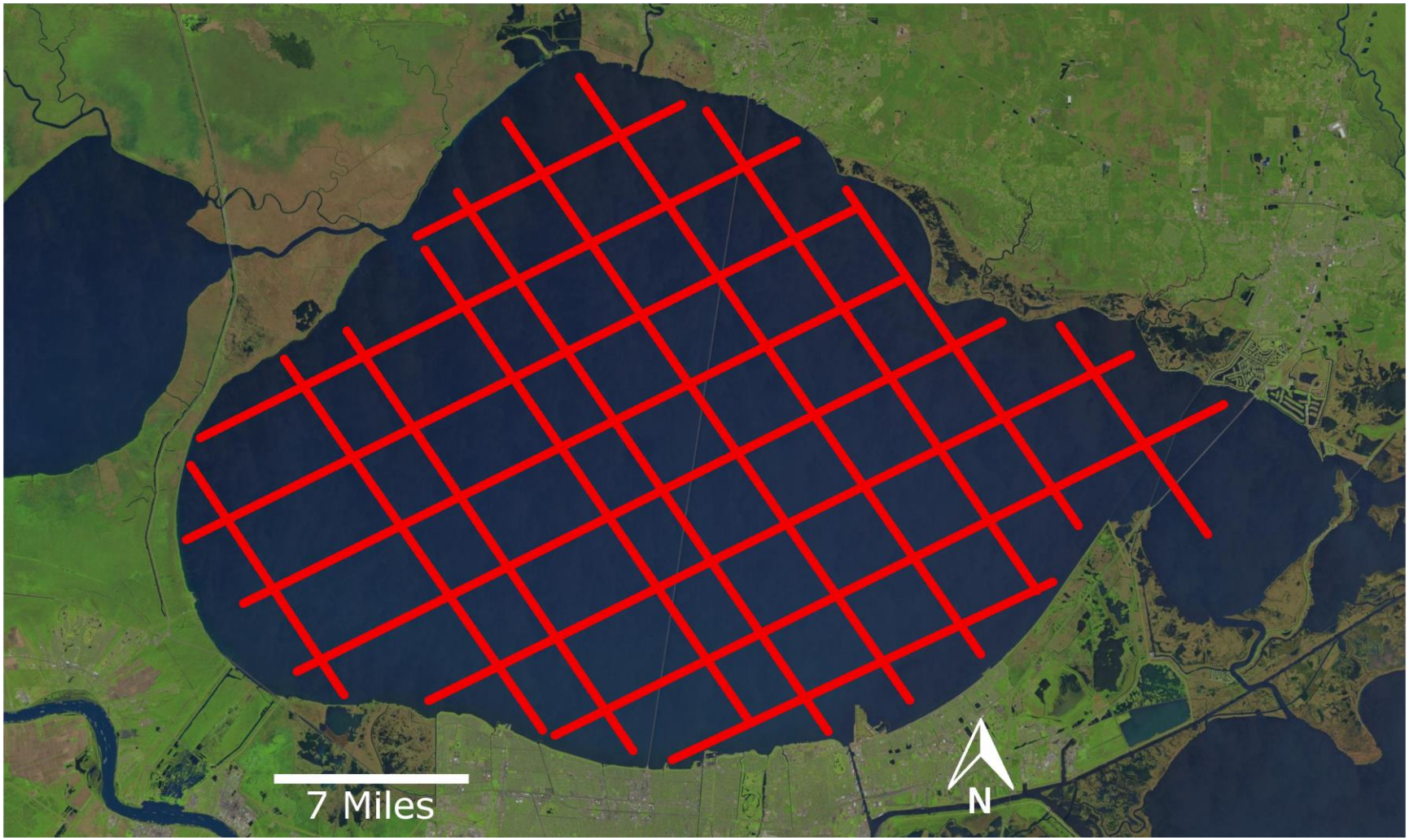


**Figure 20.** Base map showing the 2-D seismic lines in Lake Pontchartrain (image from USGS *Landsat Look Viewer March 27, 2015).*

## *3.4 Marsh Imagery Methodology*

Satellite imagery was compiled for this study with the purpose of investigating changes in marsh morphology proximal to faults in Lakes Borgne and Pontchartrain. The imagery was collected by the USGS's *LandsatLook* program. The *Landsat* mission began in 1972 with a goal of collecting images for planetary observation. Since the beginning of the program 8 satellites have been put into orbit, two of which are presently capturing images. Images from the mission are searchable through the USGS interface *LandsatLook Viewer*. In this study satellites 4, 5, 7, and 8 were used to establish a time frame from July of 1982 to present day. From July of 1982 until present day there were a total of 989 images with <20% cloud coverage; these images were analyzed, which resulted in 62 images that contained full imagery coverage of the study area.

# Chapter 4. Results

## *4.1 3-D Seismic Faults*

An analysis of the 3-D seismic surveys led to the recognition of four major faults (>3.7mi fault trace) (6km) within Lake Borgne (Fig.15). While there are many smaller faults (< 3.7mi fault trace) (6km) in the area, the major faults whose extent reaches the vertical (depth) boundary of the east Lake Borgne seismic survey will be the focus for this study. All of the major faults identified within this study are east striking, similar to the larger regional-scale fault trends of the northern Gulf of Mexico basin (e.g.Murray, 1961). Emphasis will be placed on the three faults that are closely grouped together (faults 1, 2, and 3) (Fig. 18) because of the time restrictions of this study. Faults 1 (blue), 2 (green), and 3 (red) have trace distances of approximately 4mi (6.4km), 7mi (11.2km), and 7.7mi (12.4km) respectively. Fault offsets are greater at depth and gradually decrease as the fault approaches the lake bottom. Calculated slip rate from Lower Miocene (~20mya) of fault number 3 is .1in/100yr (2.5cm/100yr). The largest offsets occur on fault 3 (1,061ft) (323m) (red) with the mildest offsets occurring on fault 1 (minimal) (blue). The dip of the fault scarp is uniform with a near vertical value of 68° for the three faults, but the eastern survey limits the ability to determine if the dip angle changes with depth. Since the angle is relatively constant the confidence levelis increasedin the upward projection of the fault location. Faults were mapped using the smallest interval possible on *IHS Kingdom* to ensure the most accurate depiction of the faults. 3-D representations were created of each fault (Fig. 21) by transforming the individual fault picks into a single grid (plane) using a flex algorithm tool in *IHS Kingdom*. The western seismic survey on the other hand is unclipped and images to a depth of 6s (~24,000ft) (7315m). At this depth the listric nature of the faults is revealed (Fig. 22).

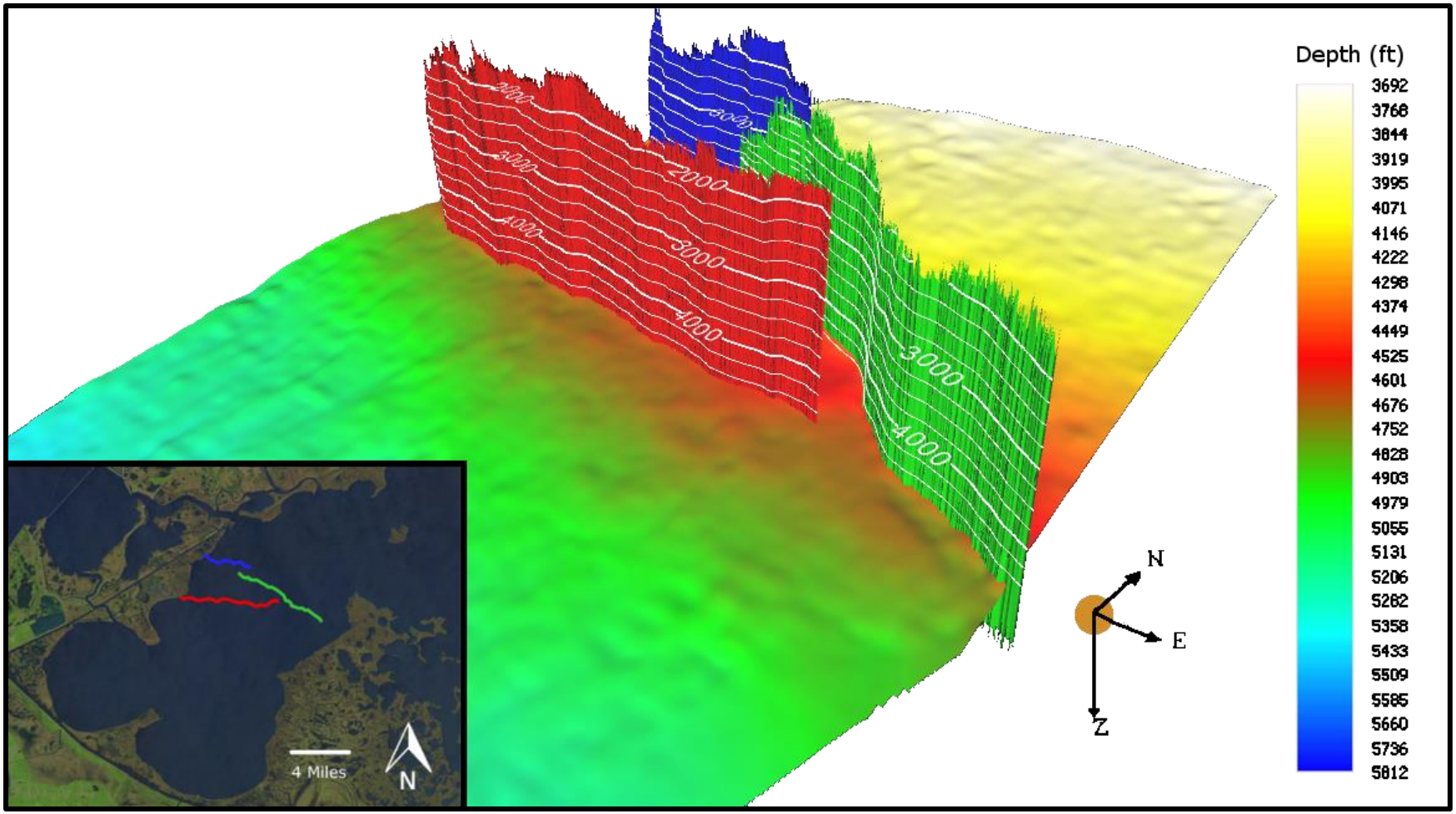


**Figure 21.** 3-D fault scarp representation with depth contours for each fault shown in white lines. The mapped basal surface represents the middle Miocene (~12ma) horizon with coloration depicting depth of the horizon below the surface (inset map from USGS *Landsat Look Viewer March 27, 2015).*

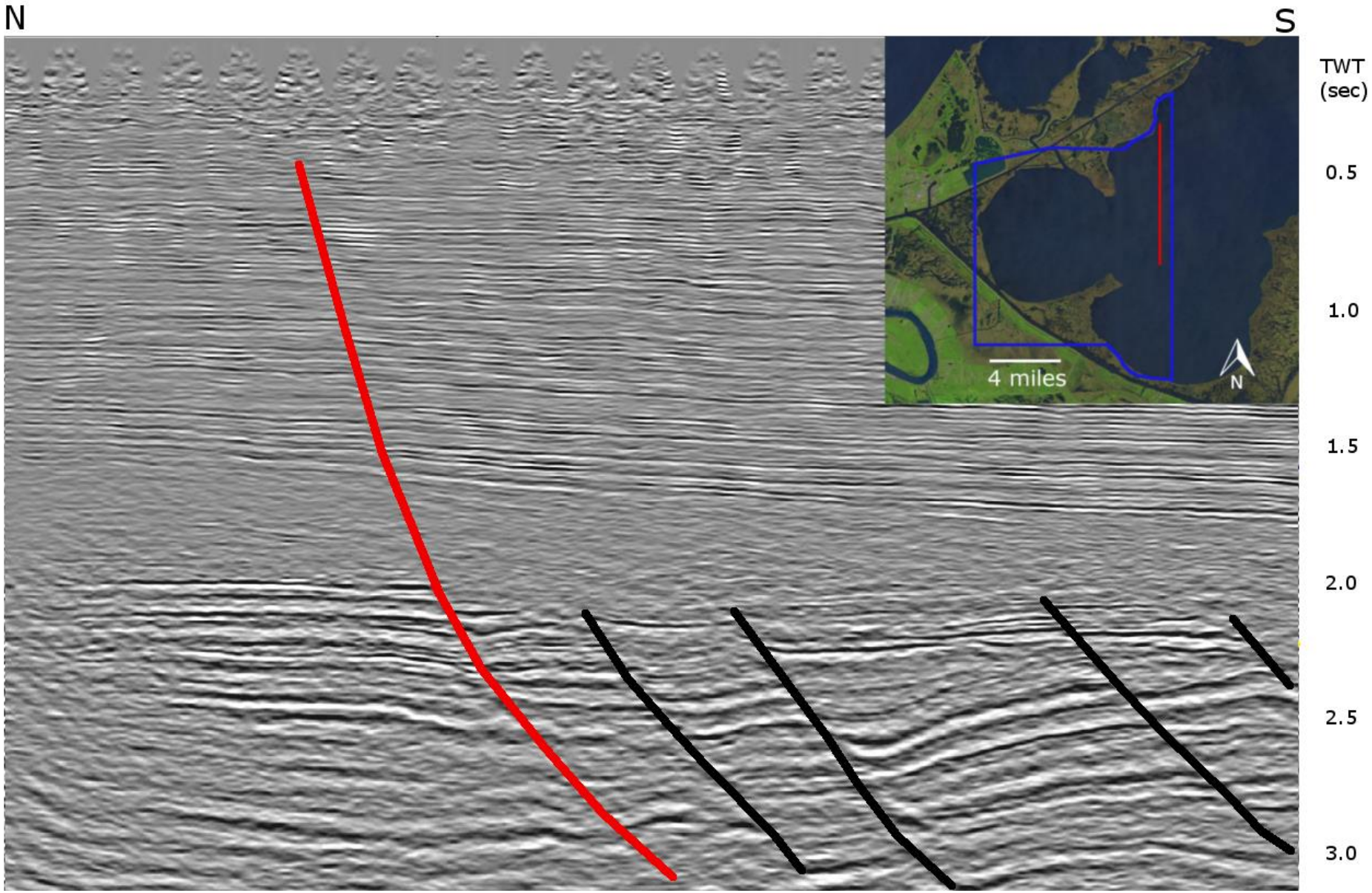


**Figure 22**. Interpreted north-trending seismic line of the west Lake Borgne survey. The red fault shown here is the same red fault on the eastern survey (eg. figure 17 and 31) (inset map from USGS *Landsat Look Viewer March 27, 2015).*

## *4.2 Chirp Seismic Faults*

When interpreting the Chirp seismic data there was not any clear evidence of brittle or ductile fault induced deformation. However there was a channel found on 11 out of the 30 total Chirp lines (Fig. 23). A number of Chirp lines cross the channel in a cross stream direction (Fig. 24), this allows for a measurement of channel width to be determined (500ft) (152m). The total depth of the channel was converted from 7ms TWT to a depth of 17ft (5.2m). Resolution in the Chirp data is high enough to be able to see individual migration surfaces (Fig. 25) that show the meandering of the channel throughout time. A number of Chirp lines capture a velocity pull up at the base of the channel; this is a material with a higher acoustic velocity (eg. shells or gravel). The channel closely follows fault number 3 for approximately 4mi (6.4km) then it meanders off of the data collection area. Since the data was only collected for 2,000ft (609m) on either side of the fault the channel gets lost when it doesn't parallel the fault. Since the location of the channel can only be located where Chirp seismic lines were collected inferences have to be made about the channel location between lines.

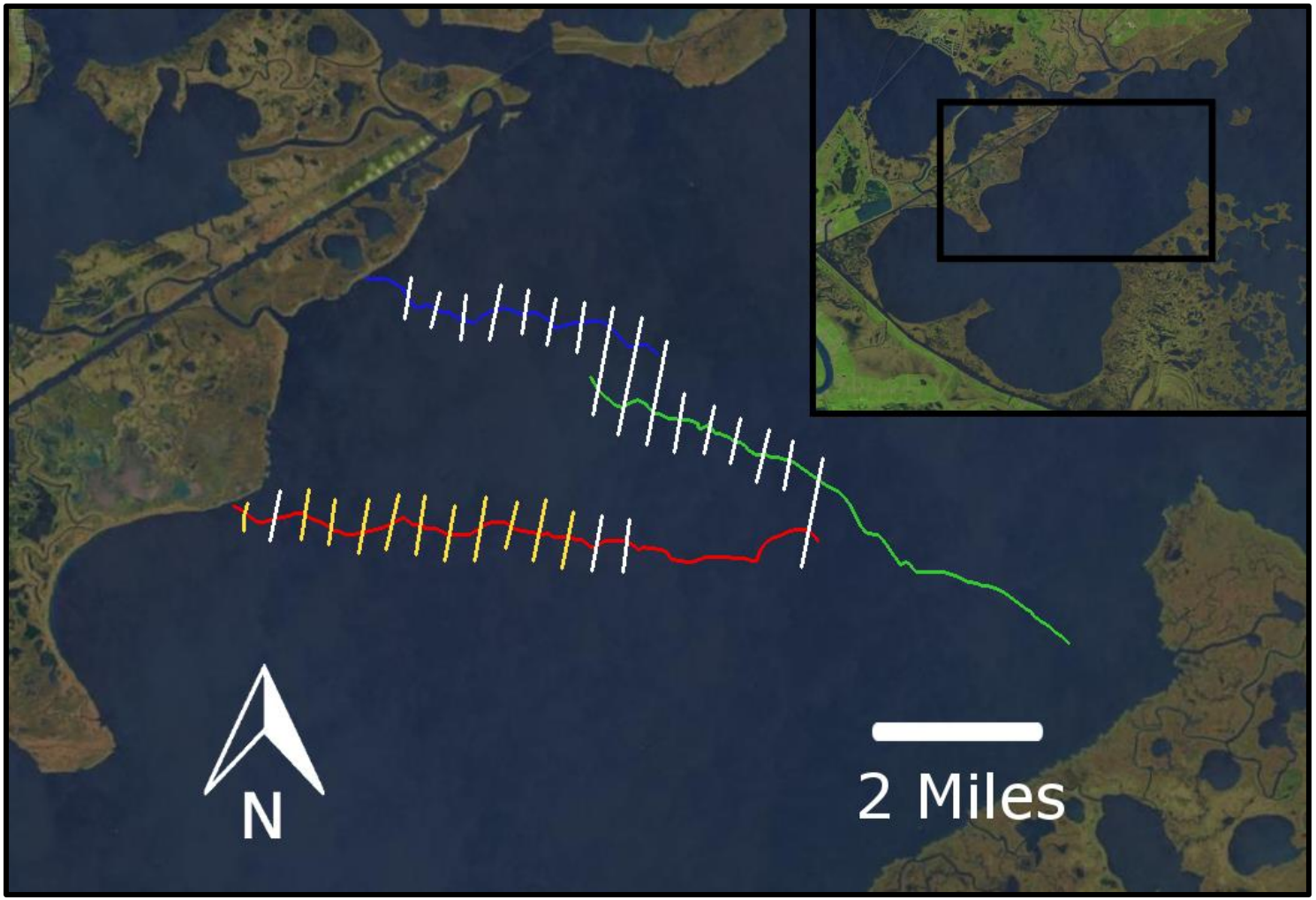


**Figure 23.** Base map showing Chirp seismic lines collected. White lines represent collected lines that do not intersect a channel, whereas yellow lines represent collected lines that do intersect a channel (base map from USGS *Landsat Look Viewer March 27, 2015).*

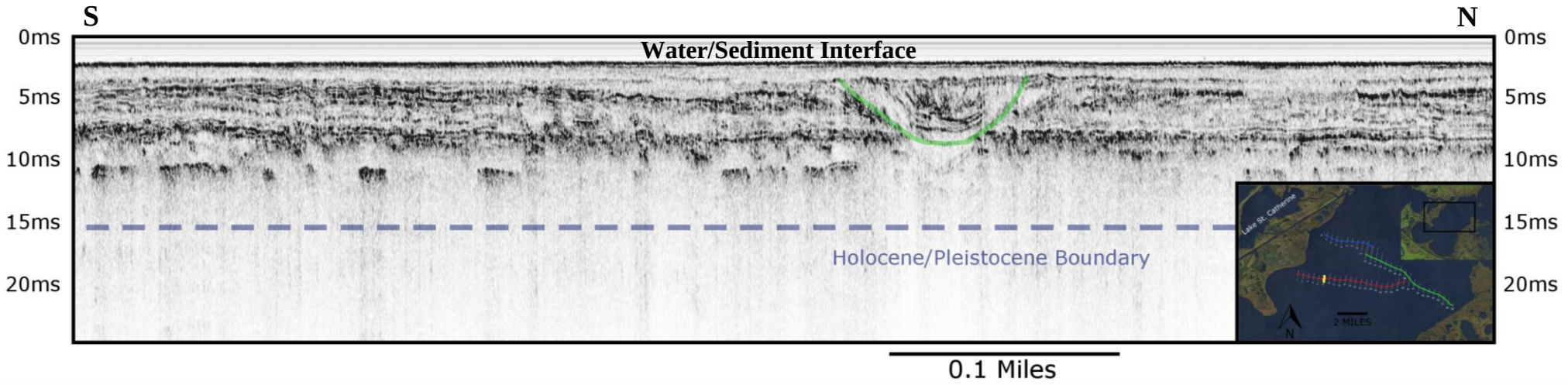


**Figure 24.** Chirp seismic line #8. This line intersects the channel (green) perpendicular to flow. The dashed blue line represents where the approximate Holocene/Pleistocene age boundary is based on an isopach map from Kulp et al. (2002) (inset map from USGS *Landsat Look Viewer March 27, 2015).*

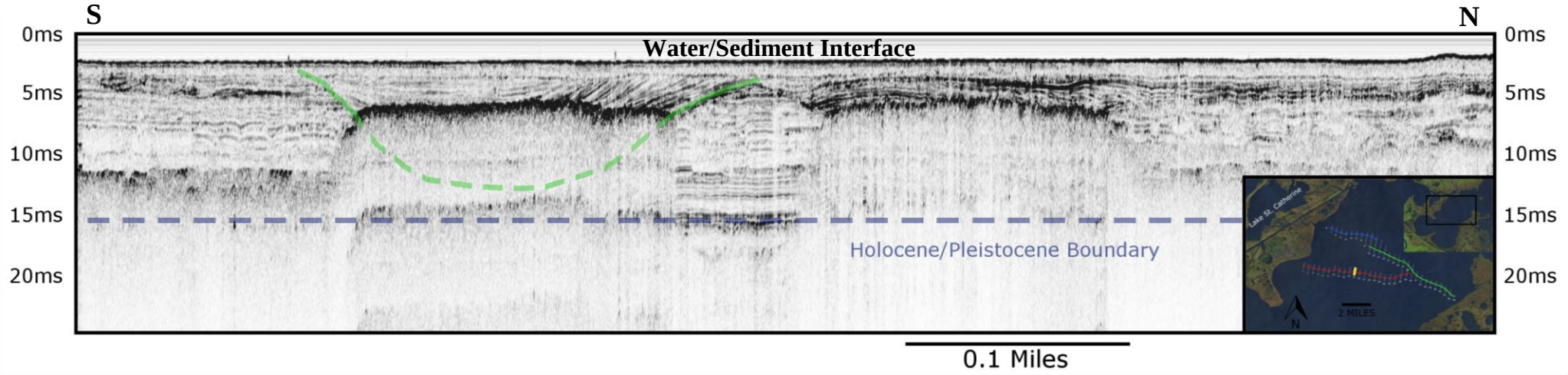


**Figure 25.** Chirp seismic line #18. This line intersects the channel at an oblique angle causing the channel (green) to appear wider than it actually is, point bar meanders are present.The dashed blue line represents where the approximate Holocene/Pleistoceneage boundary is based on an isopach map from Kulp et al. (2002) (inset map from USGS *Landsat Look Viewer March 27, 2015).*

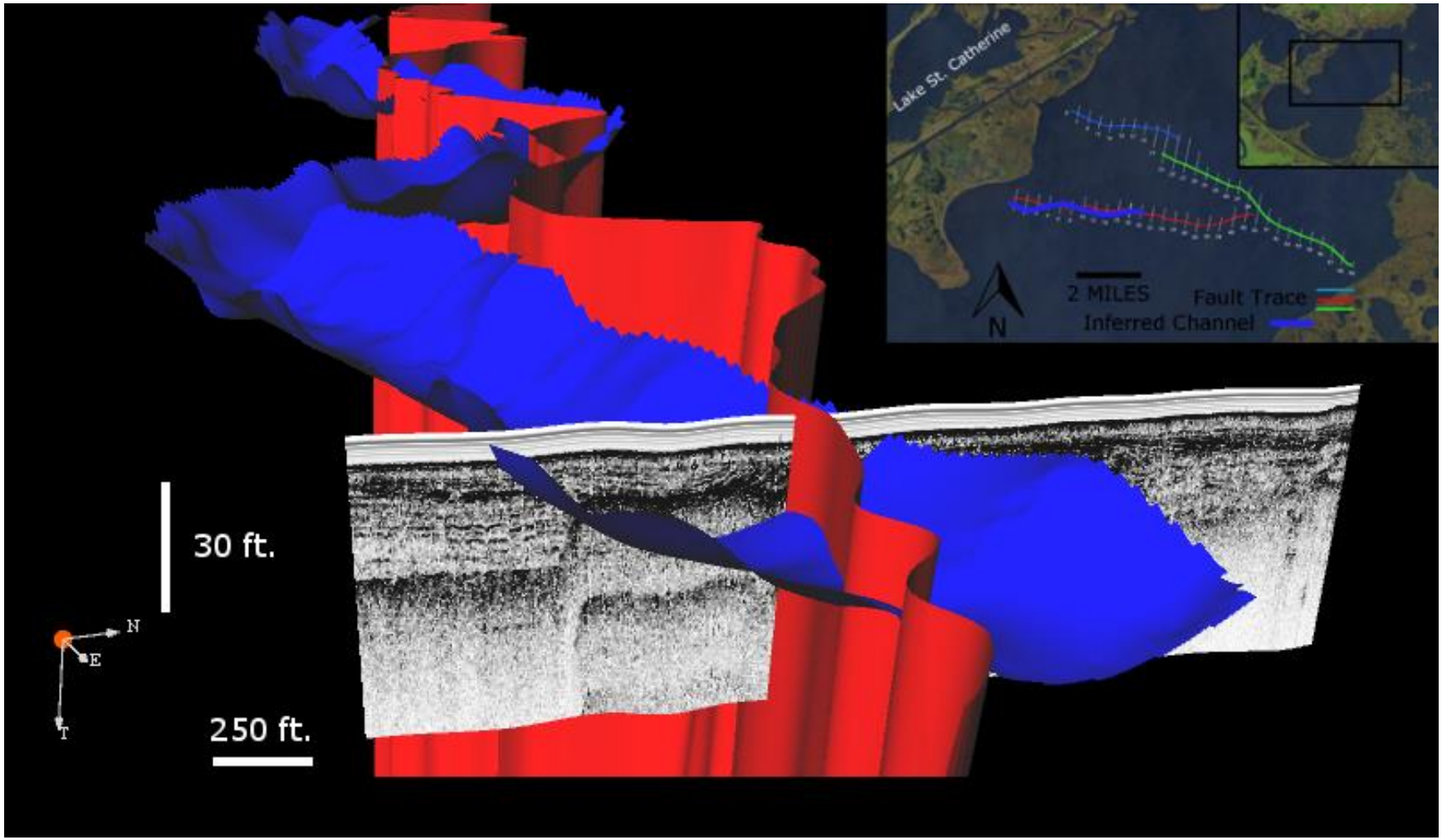


**Figure 26.** 3-D representation of the interaction between the interpreted river channel (blue) and fault #3 (red). Chirp seismic line 18 is also shown intersecting the fluvial channel. The inset map shows the length of the fluvial channel (blue) within the available data (inset map from USGS *Landsat Look Viewer March 27, 2015*).

### *4.3 2-D Seismic Faults*

The northern section of Lake Pontchartrain contains multiple normal down- to-the-south faults. The faults extend up to 1,000ft (304m) from a depth of approximately 14,000ft (4267m) before they become unresolvable. Previous studies (Lopez, 1991; Roth, 1999) in this area help provide some guidance for the interpolation between areas of no data coverage. These faults strike similarly to the faults found in Lake Borgne and dip at an angle of approximately 65°. A favorable connection is made by extending the fault traces to the east where they come into contact with the Lake Borgne faults. This suggests that these faults are one in the same. The offsets for these faults are largest (Approximately 900ft (274m)) at depth (12,000ft) (3657m) and become smaller at more shallow depths. Faults in the southern part of Lake Pontchartrain (Figs. 28 and 30) are similar to the northern faults but are resolvable at deeper depths (14,000ft) (4267m), providing a true perspective on their listric nature. After interpreting the faults on the 2-D seismic data set in Lake Pontchartrain and projecting the fault traces eastward, two of the mapped faults in Lake Pontchartrain appear to continue into Lake Borgne (Fig. 32).

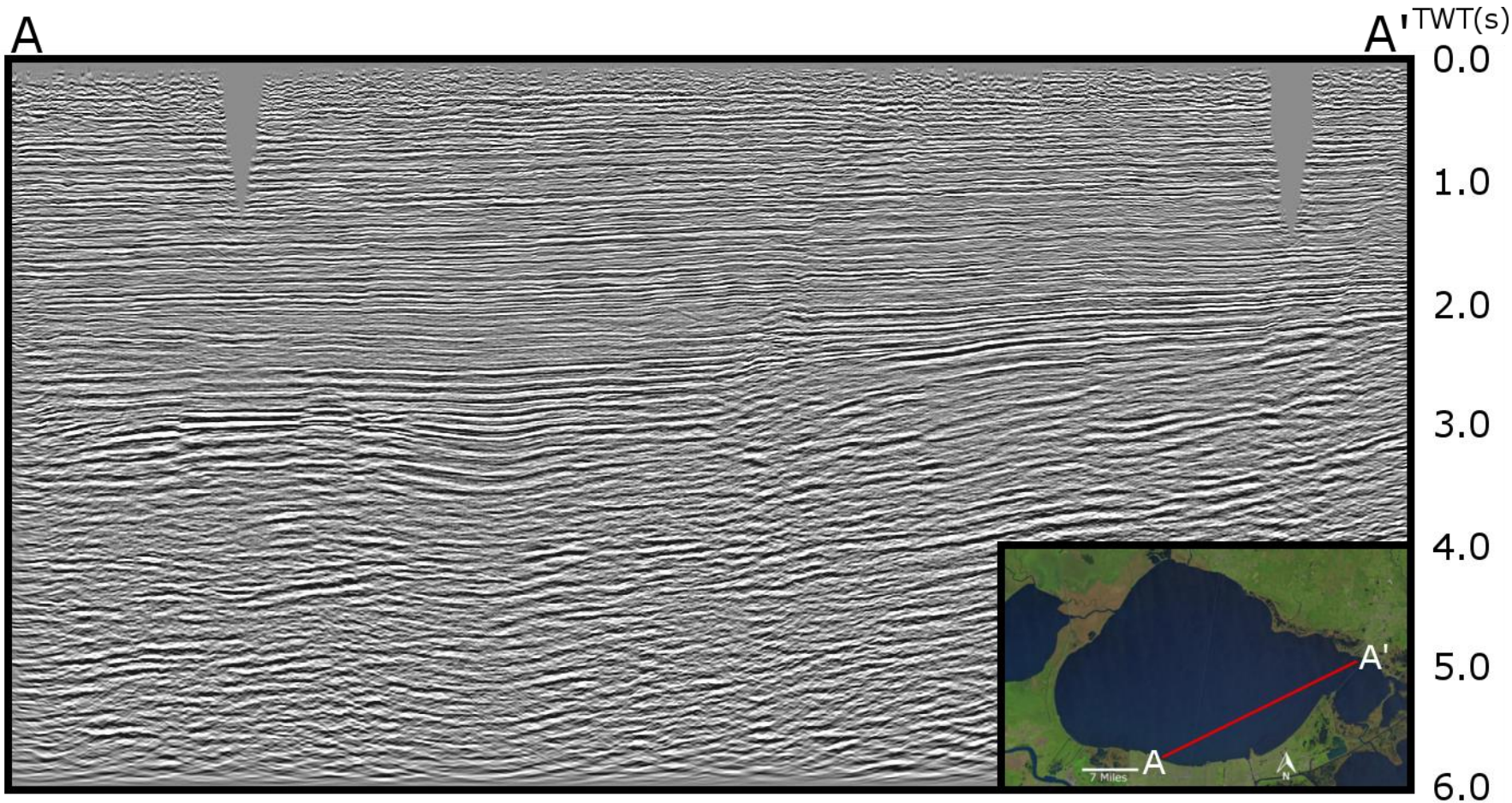


**Figure 27. U**ninterpreted 2-D seismic line 85-14 within Lake Pontchartrain (inset map from USGS *Landsat Look Viewer March 27, 2015).*

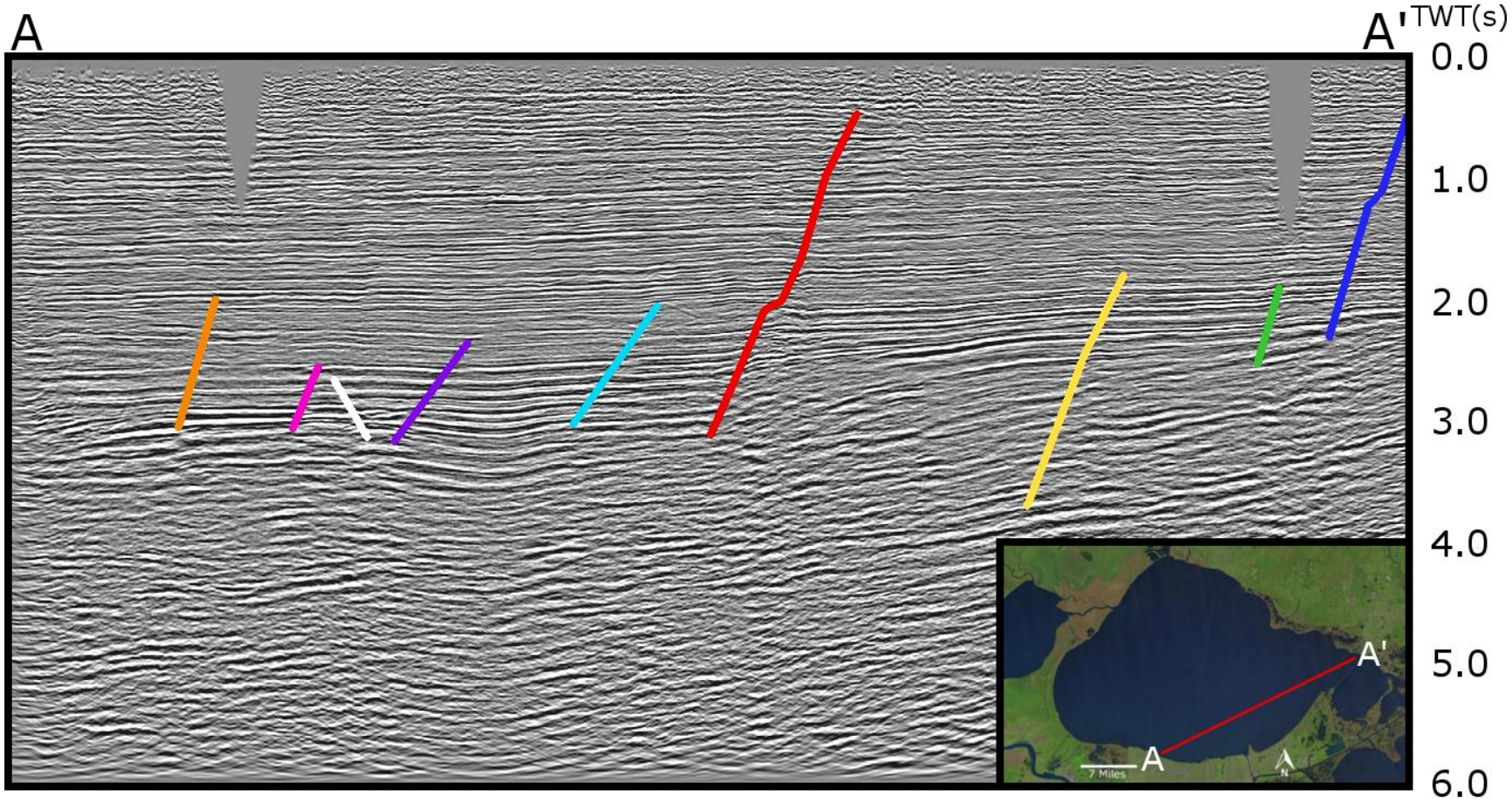


**Figure 28.** Interpreted 2-D seismic line 85-14. Faults shown here are down-to-the-south normal faults. The blue and red faults shown here are thought to be the same faults mapped in blue and red mapped in Lake Borgne (e.g. Fig. 32) (inset map from USGS *Landsat Look Viewer March 27, 2015).*

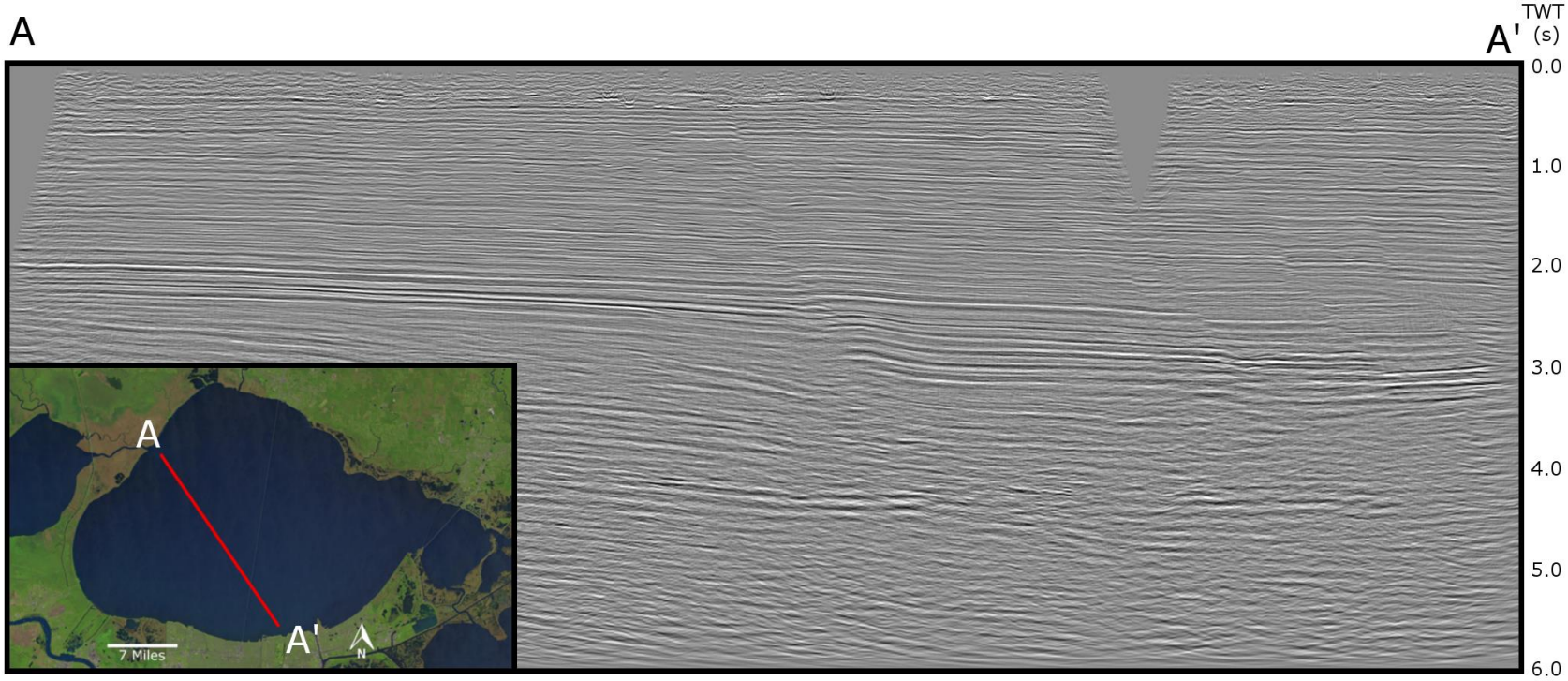


**Figure 29.** Uninterpreted 2-D seismic line 85-09 within Lake Pontchartrain (inset map from USGS *Landsat Look Viewer March 27, 2015).*

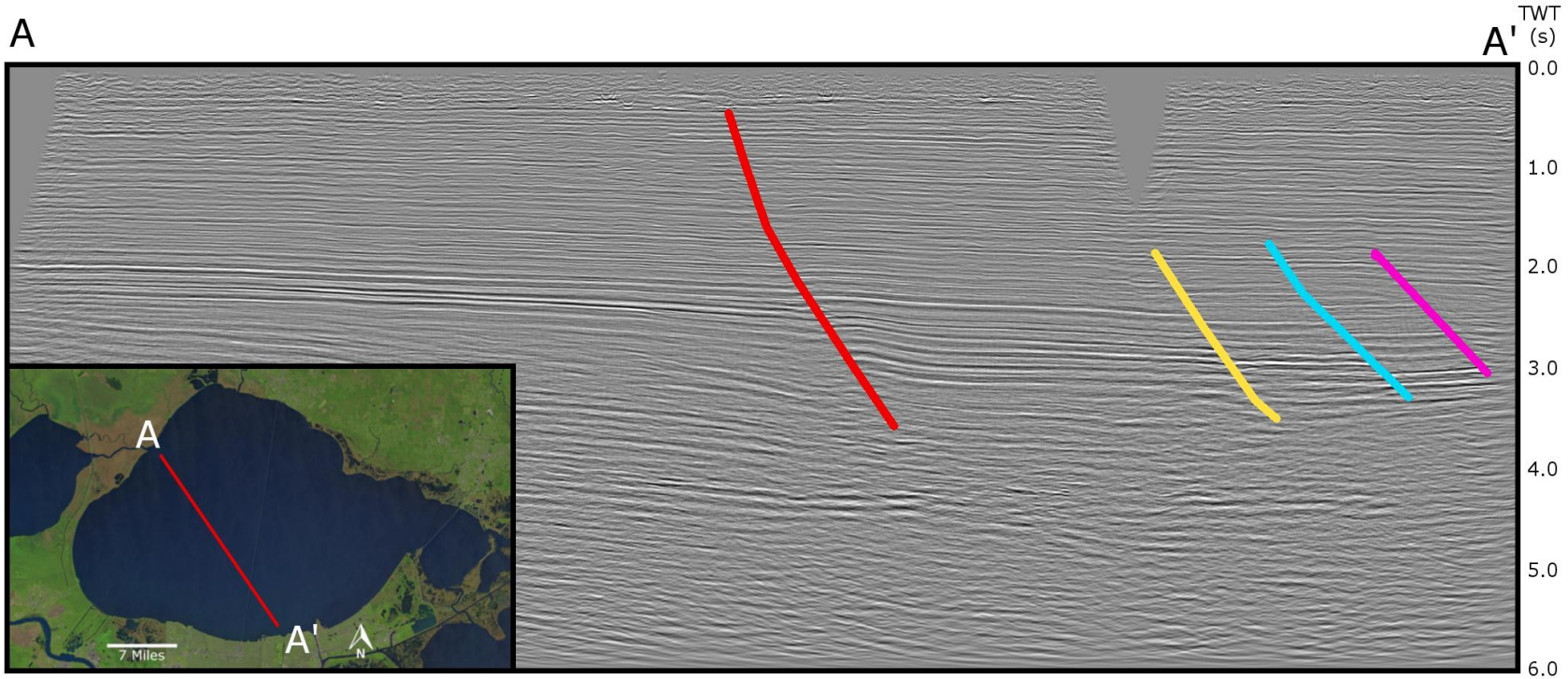


**Figure 30.** Interpreted 2-D seismic line 85-09. The red fault shown here is thought to be the same fault shown in figure 31 and extends into Lake Borgne (inset map from USGS *Landsat Look Viewer March 27, 2015).*

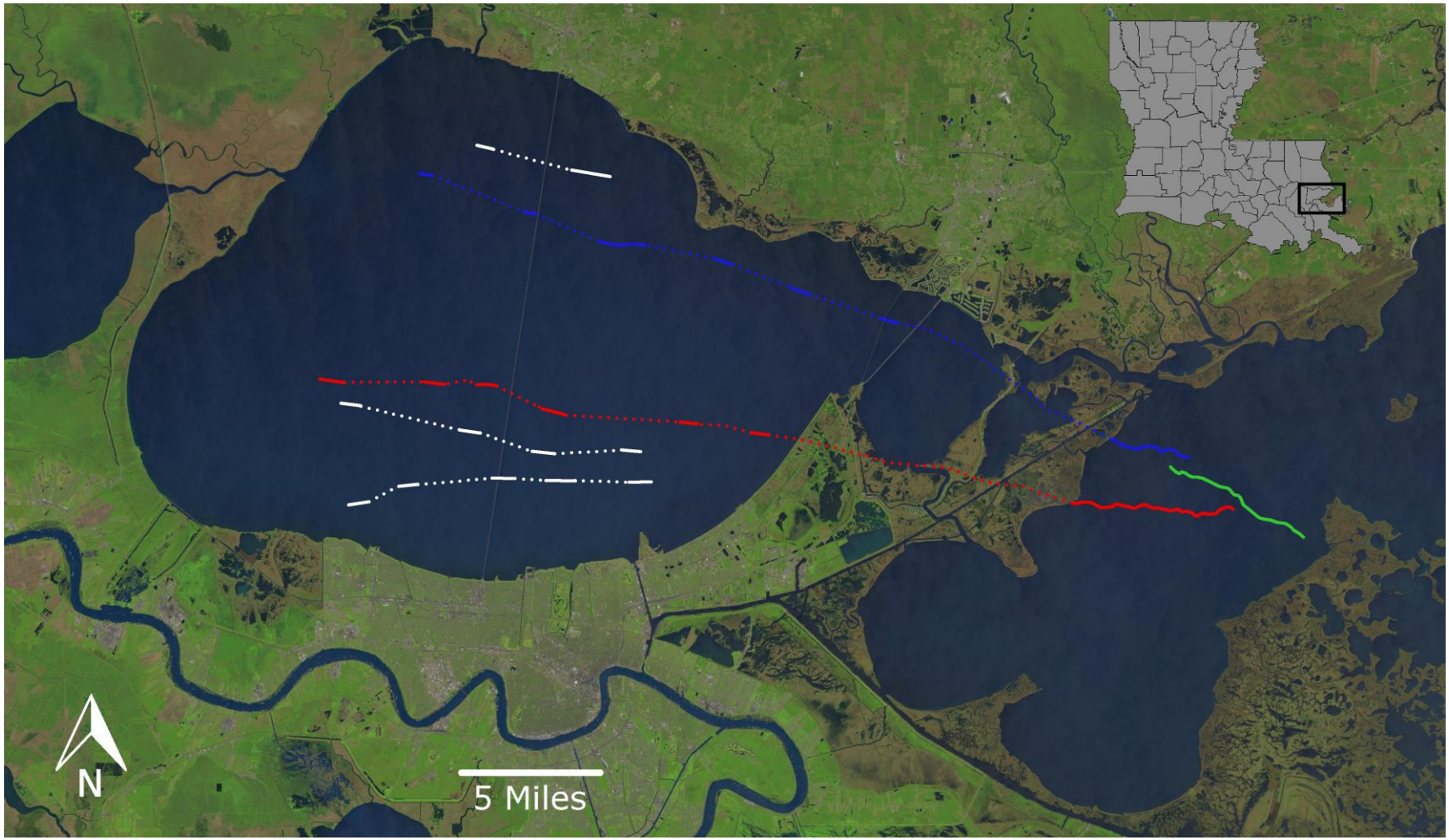


**Figure 31.** Traces of faults mapped in both the 2-D and 3-D surveys. Solid traces indicate confirmed fault traces within 3-D seismic whereas dotted lines indicate inferred fault traces between 2-D seismic transects.. The red and blue faults are correlated across the "Landbridge", an important connection between New Orleans and environments of the Pleistocene uplands to the north (image from USGS *Landsat Look Viewer March 27, 2015).* Within the land bridge note the alignment of fault traces to linear and rectilinear open-water and marsh edge relationships as well as the decrease in width of eastern Lake Pontchartrain and Lake St. Catherine.

## *4.4 Marsh Imagery*

The focal area of the satellite imagery is the "New Orleans Landbridge". This section of land lies in between both datasets (Lake Pontchartrain 2-D and Lake Borgne 3-D) and with faults correlated across the "Landbridge" it is the ideal location for fault expression at the surface. The imagery compiled for this study ranges in age from present day to 1982 with approximately one satellite image per year. A noticeable change in the marsh is present between the years of 2004 and 2005 with Hurricane Katrina occurring within this time period. Within the years following Hurricane Katrina (2006 and 2007) more marshland loss took place within this area, even more than the time period immediately following hurricane Katrina (Fig. 32). This land loss follows the linearity of fault 3, which is correlated through this section of the "Landbridge". This pattern of land loss continues from 2005 until 2013, then it appears that the marsh is able to reclaim some of the lost land in the present day (2016) (Fig. 33). This is the same fault (3) that is paralleled by the channel discovered in the Chirp seismic data.

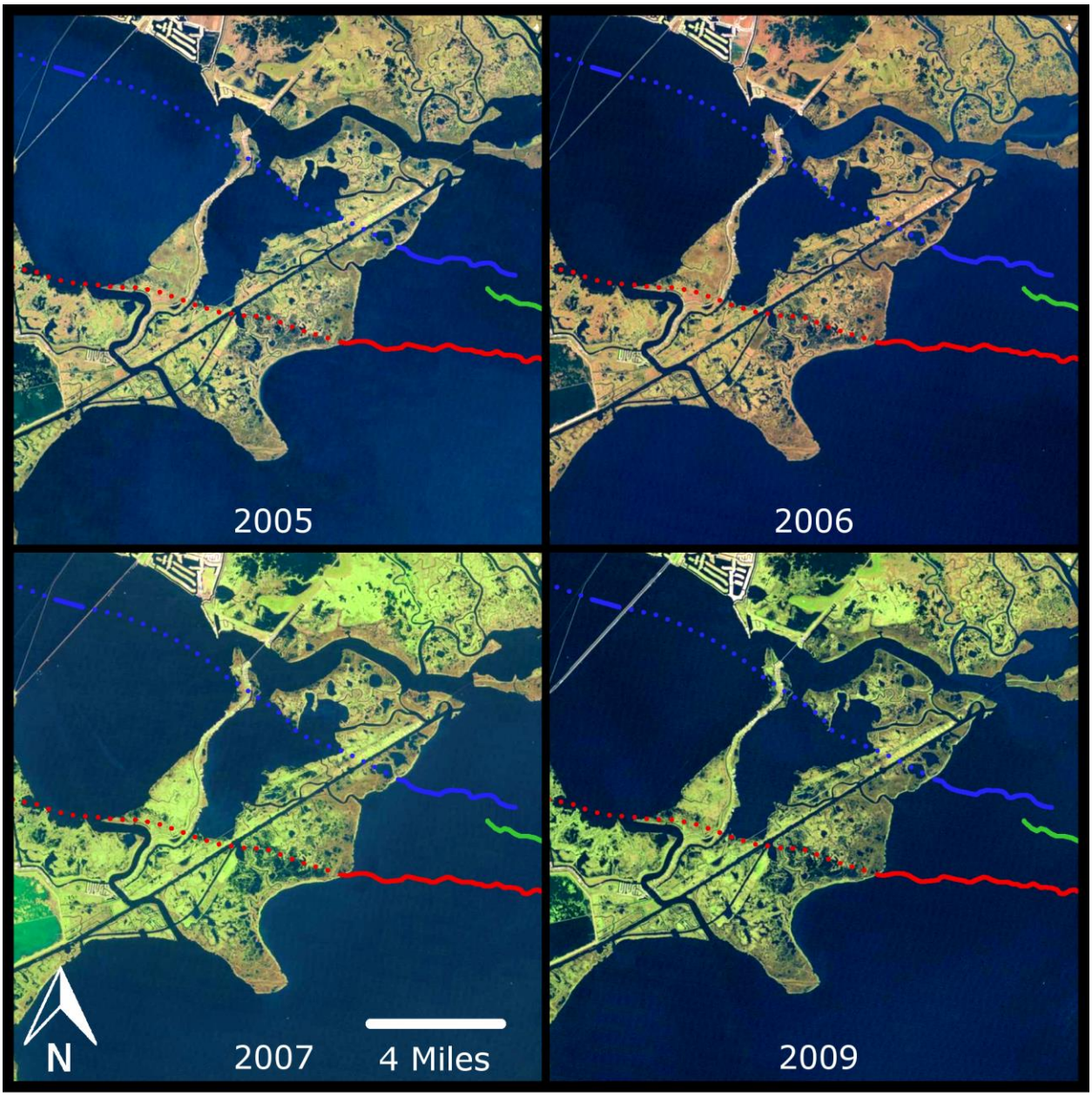


**Figure 32.** Satellite images from 4 different years, overlain with the fault trace (solid line) and projected fault trace (dotted line) (images from USGS *Landsat Look Viewer).*

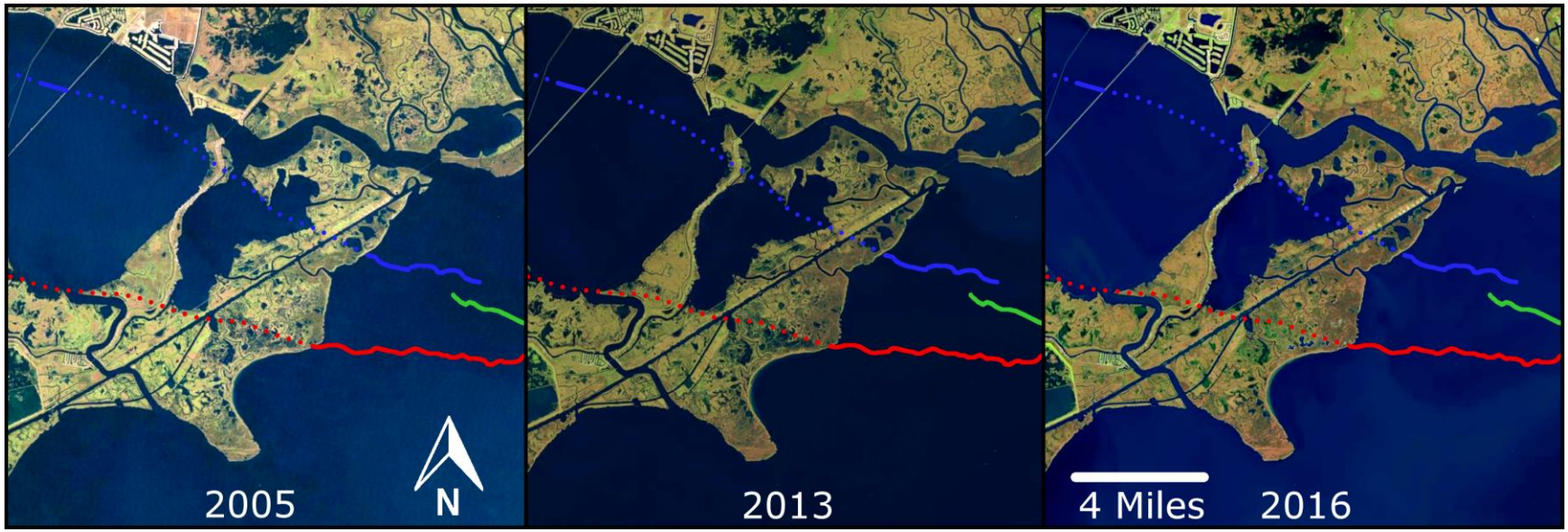

**Figure 33.** Satellite images from 3 different years, overlain with the fault trace (solid line) and projected fault trace (dotted line) (images from USGS *Landsat Look Viewer).*

# Chapter 5. Discussion

## *5.1 Fault Activity*

The interpretation of the industry seismic data sets revealed the locations of deep-seated faults in Lake Borgne. The Chirp data does not image any clear signs of offset within the stratigraphy in Lake Borgne; this could be caused by any of the following reasons.

1) The deep seated faults identified of this study are not active and have not affected Holocene strata (last ~10kyr).
2) There is no near surface fault motion within the stratigraphic depth that the Chirp is capable of imaging. The faults are present at depth but have not been active during the latest Quaternary and therefore have not affected Late Quaternary strata.
3) The faults are currently active, but due to wave activity the fault induced offset recorded in the stratigraphic record has been erased.
4) The resolution of the Chirp system is limiting the ability of fault induced offset in the stratigraphic record to be imaged.
5) The faults are not currently active, but were active earlier in the Holocene. The faulting has influenced the geomorphology of nearby rivers.

## *5.2 Inactive Faults*

There is the possibility is that these particular faults are not active and instead are in an inactive period. Loading by sediments has been shown to be a primary driving mechanism of fault motion (Nelson, 1991).The reason that they have become inactive could be due to a lack of sedimentation into Lake Borgne. The Mississippi River Delta switched lobes from the St. Bernard to the Lafourche approximately 1.5ka (Törnqvist et al., 1996) this would reduce the

sediment input into the Lake Borgne area substantially. This would allow the forces from differential loading to equalize and cease movement of faults.

## *5.3 Preservation of Stratigraphy*

The large surface area of the lake combined with water depths <10ft (3m) provide an ideal environment for waves that re-suspend lake-bottom sediments. The mean water depth for the chirp data collection was approximately 8ft (2.4m). A wave height of 2.5ft (0.75m) is sufficient to interact with the sediment interface and Troslcair (2013) found a 4-yr time frame (2008-2011) during which mean wave heights ranged 0.4ft (0.12m) to 0.5ft (0.15m) with maximum wave heightsof 4ft (1.23m) to 5.5ft (1.7m).The re-suspension of sediment has a chance to disturb artifacts left by faulting such as fault scarps. Altered fault scarps could easily blend in with the surrounding imperfections of the lake sub strata. Evidence of sediment re-suspension would be massive bedding, this occurs in the upper 2ft (0.5m) of some of the cores (Appx. A) collected in Lake Borgne. Even though the Chirp system is capable of imaging centimeter-scale offsets of strata, wave activity can erase the scarps leaving nothing to be imaged.

## *5.4 Chirp Data Resolution*

The ability to resolve small-scale (<3.9in) (<10cm) offset within near surface strata is dictated by the resolution of the techniques used to image strata. To gauge whether Chirp seismic could image recent stratigraphic offsets the slowest published Holocene slip rate was considered when calculating an estimate of Holocene throw (.05in/yr Yeager et al., 2012). For example assume the middle Holocene (stratigraphic depth of channel) is approximately 5kyr old and if the slip rate averaged .05in/ yr (1.2mm/yr), than the expected total throw would be approximately 20ft (6m). The manual for the *Edgetech SB-216* states that maximum resolution is

2.3in (5.8cm) for the settings (2-12 kHz) that were used for data collection of this study. This means assuming the faults were active from 5ka to present time that the Chirp system would have the capability to image the offset created by the faults.

### *5.5 River Channel Steering*

Before the invasive techniques used for oil, natural gas and water extraction existed the two main causes of subsidence in southern Louisiana were natural compaction and faulting. The channel occurs in the upper third of the Holocene strata within the progradational facies as outlined in Frazier (1967). With the depth and size of the channel (500ft wide) (152m) it is probable that this channel was a part of the St. Bernard delta complex when that delta lobe was active (1.3 – 3.5ka) (Törnqvist et al., 1996). Since channels and rivers direct themselves towards areas of maximum subsidence (Alexander and Leeder, 1987) and during this time in the development of the Mississippi river delta, faulting would have played a major role in subsidence.

The way that a channel or river responds when it encounters a fault depends on the width of the channel, the offset of the fault, and the orientation of the channel with respect to the fault. A study (Armstrong et al., 2014) using a 3-D seismic survey located in Breton Sound and Barataria Bay which is located approximately 12 miles south of Lake Borgne. This study investigated 54 different paleo-channels that crossed over Miocene growth faults. The study concluded that narrow channels (393- 492ft) (120-150m) are more likely to parallel the hanging wall after they encounter a fault while wider channels and channel belts tend to emerge perpendicular to the strike of a fault. Another factor that influences how the channel reacts after it crosses a fault is the displacement of the fault scarp. A river crossing a fault scarp with a higher

displacement is more likely to parallel the hanging wall than to come out perpendicular to the fault trace (Armstrong et al., 2014).

In the case of the channel that parallels fault #3 for 4mi (6.4km) it is difficult to tell the orientation of the channel before and after the fault because the Chirp seismic is only close to the projected fault. The channel is present on the western most Chirp line that is closest to the marsh and when moving eastward the channel is present for 11 lines and then disappears. The disappearance of the channel could indicate that it returns to its original orientation before it encountered the fault. If the channel was a part of the St. Bernard delta complex the termination of the channel would be expected to be further to the west. More Chirp seismic in the area would help locate the channel.

# Chapter 6. Conclusion

The analysis of well-log data, deep industry seismic surveys (~24,000ft) (7,300m), high-resolution seismic data, and aerial photography. These data were used to evaluate evidence of fault motion within the Holocene stratigraphy and geomorphology of the Lake Borgne region within the Pontchartrain Basin. Three down-to-the-south faults were found within the northern half of the industry seismic volumes, analysis within the southern section of the surveys was hampered by poorer quality data, and no significant fault trends vertically <328ft (100m) and horizontally <0.6mi (1km) were identified. This system is strike-aligned to the BRFS and industry seismic data within Lake Pontchartrain suggests a structural linkage that has created a predominantly down-to-the-basin, regionally extensive (>328ft) (>100m) fault trend. High-resolution Chirp seismic across the fault trends imaged Holocene channel patterns with the largest and most continuous of the channels strike-aligned to the trend of a fault that can be mapped to within 1600ft (487m) of the subsurface. The channel is continuous along the structural trend for 4mi (6.4km) mimicking the fault trace that entire distance.

Experimental and field studies of fluvial evolution have shown the pivotal role that land-surface elevation changes can lend to shifting fluvial patterns specifically toward zones of subsidence (Alexander and Leeder, 1987, Peakall et al., 2000, Kim et al., 2010). Besides controlling individual fluvial channels tectonic tilting has been experimentally shown to cause channel-belts to shift towards areas of increased subsidence (Mackey and Bridge, 1995). In addition to influencing the path of fluvial channels, faulting can also change the sinuosity and avulsion frequency of a channel as shown in a study by Maynard (2006).

The younger, landbridge geomorphology of the area lying between Lake Borgne and

Lake Pontchartrain provides additional evidence of recent elevation adjustments. Aerial imagery shows linear patterns in marshland along of the fault-strike extrapolated trace between Lake Borgne and Lake Pontchartrain. A clear indication of fault scarping in a fetch-limited interior marsh pond as well as the ongoing enlargement and creation of water bodies within the fault trend axis suggest a more recent slip than what controlled likely mid to late Holocene channels of the Mississippi River Delta.

The merger of deep seismic, shallow seismic and sequential aerial imagery has revealed that deep-seated faults are extending into the shallow stratigraphy of the Lake Borgne Area. As shown by Chirp imaging these faults influenced mid to late Holocene river channels as the Mississippi River Delta prograded across the study area. The indicative fault features shown in the aerial photography expose that the marsh within the Landbridge was and will be continually shaped by faulting.

# References

Alexander, J., Leeder, M.R., 1987, Active tectonic control on alluvial architecture. In: Ethridge, F.G., Flores, R.M., Harvey, M.D. (Eds.), Recent Developments in Fluvial Sedimentology: Contributions from the Third International Fluvial Sedimentology Conference Society of Economic Paleontologists and Mineralogists, Special Publication No. 39, p. 243–252.

Armstrong, C., Mohrig, D., Hess, T., George, T., & Straub, K. M., 2014, Influence of growth faults on coastal fluvial systems: examples from the late Miocene to Recent Mississippi River Delta. Sedimentary Geology, 301, p. 120-132.

Avseth, P., Mukerji, T., & Mavko, G., 2010, Quantitative seismic interpretation: Applying rock physics tools to reduce interpretation risk. Cambridge university press, p. 1-408.

Bray, R. B., & Hanor, J. S., 1990, Spatial variations in subsurface pore fluid properties in a portion of Southeast Louisiana; implications for regional fluid flow and solute transport. Transactions - Gulf Coast Association of Geological Societies, p. 4053-4064.

Bull J.M., Quinn R., Dix J.K., 1998, Reflection coefficient calculation from marine high-resolution seismic reflection (Chirp) data and application to an archaeological case study. Mar Geophys Res 20: p. 1–11.

Chew, D.L., 1987, Clam Shell Dredging in Lakes Pontchartrain and Maurepas, Louisiana. Red River Basin Coordinating Committee New Orleans LA, p. 1-395.

Dokka, R. K., 2006, Modern-day tectonic subsidence in coastal Louisiana. Geology 34, p. 281-284.

Dokka, R.K., 2011, the role of deep processes in late 20th century subsidence of New Orleans and coastal areas of southern Louisiana and Mississippi. Journal of Geophysical Research: Solid Earth 116.B6. p. 1-25.

Durham, C. O., Jr.and Peeples, E. M. III., 1956, Pleistocene Fault Zone in Southeastern Louisiana, Gulf Coast Assoc. Geol. Soc., Trans., v. 6, p. 65-66.

Dyer, J.M., 2011, Geohazard identification: the gap between the possible and reality in geophysical surveys for the engineering industry.Marine Geophysical Research 32.1-2: p. 37-47.

Fisk, H.N., 1944, Geological investigation of the alluvial valley of the lower Mississippi River.War Department, Corps of Engineers, p. 1-78.

Flocks, J., Kulp, M., Smith, J., & Williams, S. J., 2009a, Review of the geologic history of thePontchartrain Basin, Northern Gulf of Mexico. Journal of Coastal Research, p. 12-22.

Flocks, J., Kindinger, J., Marot, M., & Holmes, C., 2009b, Sediment characterization and dynamics in Lake Pontchartrain, Louisiana. Journal of Coastal Research, p. 113-126.

Frazier, D. E., 1967, Recent deltaic deposits of the Mississippi River: their development and chronology.Gulf Coast Association of Geological Societies Transactions
Vol. 17 (1967), p. 287-315.

Gagliano, S. M., Kemp III, E. B., Wicker, K. M., Wiltenmuth, K. S., & Sabate, R. W., 2003, Neo-tectonic framework of southeast Louisiana and applications to coastal restoration. Gulf Coast Association of Geological Societies Transactions, Vol. 53, p. 262-276

Haggar, K.S., 2014, Coastal Land Loss and Landscape Level Plant Community Succession: An Expected Result of Natural Tectonic Subsidence, Fault Movement, and Sea Level Rise. Gulf Coast Association of Geological Societies Transactions, Vol. 64, p. 139-159.

Heinrich, P. V., 2006, Pleistocene and Holocene fluvial systems of the lower Pearl River, Mississippi and Louisiana, USA: Gulf Coast Association of Geological Societies Transactions, v. 56, p. 267-278.

Kim, W., Sheets, B. A., and Paola, C., 2010, Steering of experimental channels by lateral basin tilting. Basin Research, 22(3), p. 286-301.

Kindinger, J.L., 1988, Seismic stratigraphy of the Mississippi-Alabama shelf and upper continental slope: Marine Geology, v. 83, p. 79–94.

Kolb, C. R., F. L. Smith, and R. C. Silva., 1975, Pleistocene sediments of the New Orleans-Lake Pontchartrain area.US Army Corps Technical Report, No. S-75-6, p.1-56.

Kuecher, G. J., Roberts, H. H., Thompson, M. D., & Matthews, I., 2001, Evidence for active growth faulting in the Terrebonne delta plain, south Louisiana: Implications for wetland loss and the vertical migration of petroleum. Environmental Geosciences, 8(2), p. 77-94.

Kulp, M.A., Howell P., Adiau S., Penland S., Kindinger J., Williams S.J, 2002, Latest Quaternary stratigraphic framework of the Mississippi delta region: Transactions ofThe Gulf Coast Association of Geological Societies, 52, p. 572–582.

Lopez, J.A., 1990, Structural styles of growth faults in the US Gulf Coast Basin. Geological Society, London, Special Publications 50.1 p. 203-219.

Lopez, J.A., 1991 Origin of Lake Pontchartrain and the 1987 Irish Bayou earthquake. Coastal Depositional Systems in the Gulf of Mexico: Quaternary Framework and Environmental Issues, Gulf Coast Section Publ. Vol. 9, p. 103-110.

Mackey, S. D., and Bridge, J. S., 1995, Three-dimensional model of alluvial stratigraphy: theory and application. Journal of Sedimentary Research, Vol. 65B, p. 7-31.

Martin, E., 2006, Fault induced subsidence near Empire and Bastian Bay, Louisiana [Master's Thesis]: New Orleans, Tulane University, p. 1-163.

McCulloh, R.P., and Heinrich, P.V., 2013, Surface faults of the south Louisiana growth-fault province." Geological Society of America Special Papers, p. 37-49.

McCulloh, R.P., 2001, Active Faults in East Baton Rouge Parish, Louisiana. Louisiana Geological Survey, p. 1-6

Murray, G.E., 1961 Geology of the Atlantic and Gulf coastal province of North America. Harper, p. 1-692

Nelson, T. H., 1991, Salt tectonics and listric-normal faulting, *in* Salvador, A., ed., The Gulf of Mexico Basin: Boulder, Colorado, Geological Society of America, the Geology of North America, v. J, p. 73-89.

National Oceanic and Atmospheric Administration, 1996, Nautical Chart no. 11369

Ocamb, R.D., 1961, Growth Faults of South Louisiana. Transactions - Gulf Coast Association of Geological Societies 11, p.139-175.

Otvos, E. G., 1978, New Orleans - south Hancock Holocene barrier trends and origins of Lake Ponchartrain: Transactions: Gulf Coast Association of Geological Societies, v. 28, p. 337-355.

Peakall, J., Leeder, M., Best, J., and Ashworth, P, 2000, River response to lateral ground tilting: a synthesis and some implications for the modelling of alluvial architecture in extensional basins. Basin Research, 12(3-4), p. 413-424.

Peel, F. J., Travis C.J., and Hossack, J.R., 1995, Genetic structural provinces and salt tectonics of the Cenozoic offshore US Gulf of Mexico: a preliminary analysis. in M. P. A. Jackson, D. G. Roberts, and S. Snelson, eds., Salt tectonics: a global perspective: AAPG Memoir 65, p. 153-175.

Penland, S., Andrew D.B., and Louis D.B. III., 2002, Geologic classification of coastal land loss between 1932 and 1990 in the Mississippi River Delta Plain, southeastern Louisiana. Gulf Coast Association of Geological Societies Transactions Vol. 52, p.799-807.

Price, W.A., 1947, Equilibrium of form and forces in tidal basins of coast of Texas and Louisiana." AAPG Bulletin 31.9 p. 1619-1663.

Roland, H. L., Hill, T. F., Autin, P., Durham Jr, C. O., & Smith, C. G., 1981, The Baton Rouge and Denham Springs-Scotlandville faults. Louisiana Geological Survey, Dept of natural Resources, p. 1-26.

Reid, R.L., 2013, Defending New Orleans, Civil Engineering, v. 83, no. 11, p. 48-83

Roth, M. L., 1999, Late Pleistocene to Recent subsurface geology of Lake Pontchartrain, Louisiana: integration of geophysical and geological techniques. [Master's Thesis]: New Orleans, University of New Orleans, p. 1-175.

Russell, R. J., 1940, Quaternary history of Louisiana. Geological Society of America Bulletin, 51(8), p. 1199-1233.

Saucier, R.T., 1994. Geomorphology and Quaternary Geologic History of the Lower Mississippi Valley. Vicksburg, Mississippi: U.S. ArmyCorps of Engineers, Waterways Experiment Station, volume 1, p. 1-361.

Shelton, J.W., 1984, Listric normal faults: an illustrated summary. AAPG Bulletin 68.7, p. 801-815.

Sheriff, R.E., and Lloyd P.G., 1995, Exploration seismology. Cambridge university press, p. 1-592.

Sikora, W. B., Sikora, J. P., & Prior, A. M., 1981, Environmental effects of hydraulic dredging for clam shells in Lake Pontchartrain, Louisiana (No. LSU-CEL-81-18). Louisiana State University, Baton Rouge Ecology Lab, p. 1-151.

Smith, C.G., and Raphael G.K., 1978, Subsidence in the Capital Area Ground Water Conservation District: An Update. Capital Area Ground Water Conservation Commission, p. 1-31.

Stapor, F.W., and Gregory W.S., 2004, a new depositional model for the buried 4000 yr BP New Orleans barrier: implications for sea-level fluctuations and onshore transport from a nearshore shelf source. Marine Geology 204.1, p. 215-234.

Stoessell, R. K., and Prochaska, L., 2005, Chemical evidence for migration of deep formation fluids into shallow aquifers in south Louisiana. Gulf Coast Association of Geological Societies Transactions Vol. 55, p. 794-808

Suter, J.R., 1986, Ancient fluvial systems and Holocene deposits, southwestern Louisiana Continental Shelf, in Berryhill, H.L., Jr.,ed., Late Quaternary facies and structure, northern Gulf of Mexico, American Association of Petroleum Geologists Studies in Geology 23, p. 81–130

Sydrow, J., and H.H. Roberts, 1996, Stratigraphic framework of a Late Pleistocene shelf-edge delta, northeast Gulf of Mexico: American Association of Petroleum Geologists Bulletin, v. 78, no. 8, p. 1276–1312.

Tian W-M., 2008, Integrated method for the detection and location of underwater pipelines. Appl Acoust 69(5), p. 387–398.

Tomaszewski, D.J., 1996, Distribution and movement of saltwater in aquifers in the Baton Rouge area, Louisiana, 1990-1992. Louisiana Department of Transportation and Development, p. 1-44.

Törnqvist, T. E., Kidder, T. R., Autin, W. J., andVan der Borg, K., 1996, A revised chronology for Mississippi River subdeltas. Science, 273(5282), p. 1693-1696.

Trosclair, K. J., 2013, Wave transformation at a saltmarsh edge and resulting marsh edge erosion: Observations and modeling. Diss. [Master's Thesis] New Orleans, University of New Orleans, p. 1-73.

U.S. Army Corps of Engineers, 1984, Mississippi and Louisiana estuarine areas: freshwater diversion to Lake Pontchartrain basin and Mississippi Sound. Feasibility Study. Vol. 1, Main report, environmental impact statement, p. 1-654.

U.S. Geological Survey, 1998, Environmental Geochemistry and Sediment Quality in Lake Pontchartrain: New Field Sampling Techniques and Data Description.

Yeager, K. M., Brunner, C. A., Kulp, M. A., Fischer, D., Feagin, R. A., Schindler, K. J., and Bera, G., 2012, Significance of active growth faulting on marsh accretion processes in the lower Pearl River, Louisiana. Geomorphology, 153, p. 127-143.

## APPENDIX A Cores

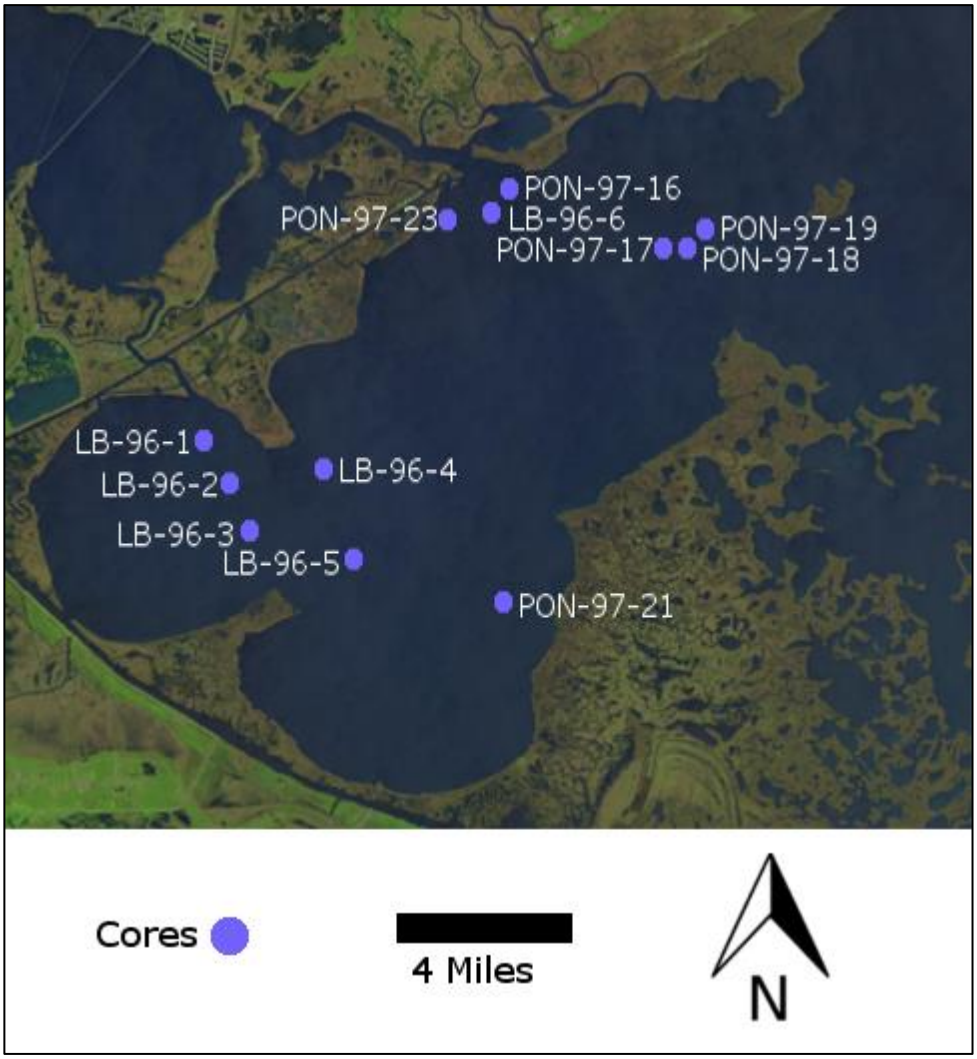


**Appendix A Figure 1.** Distribution of the vibracores within Lake Borgne.

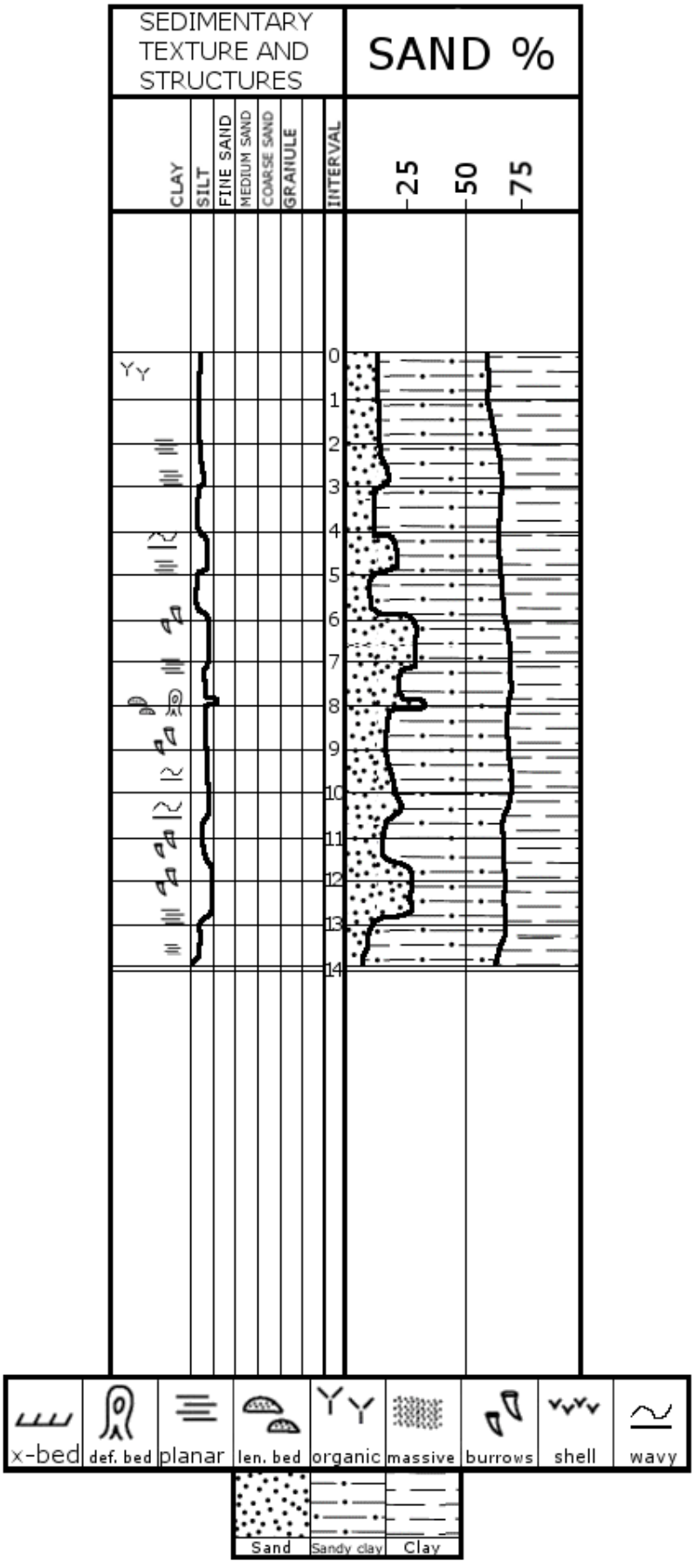


**Appendix A Figure 2.** Vibracore 96-1

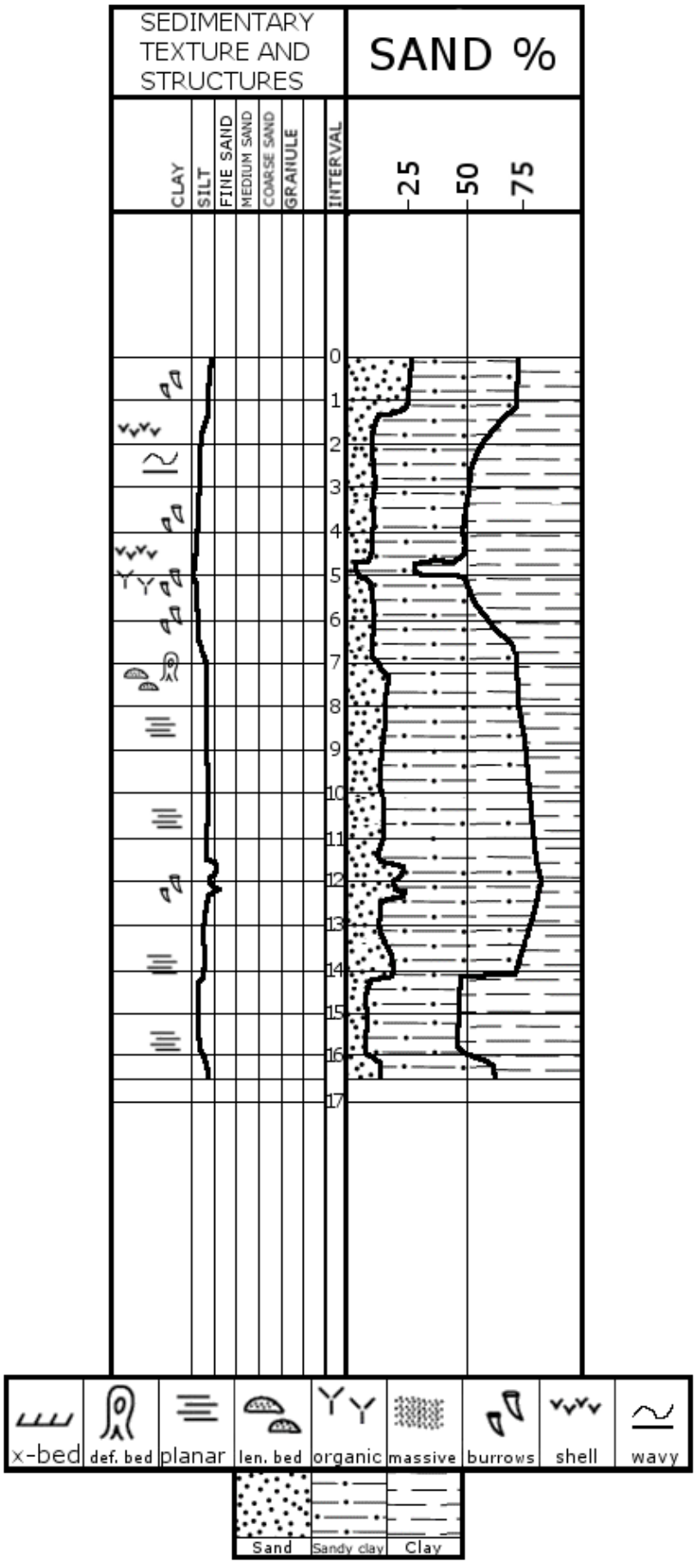


**Appendix A Figure 3.** Vibracore 96-2

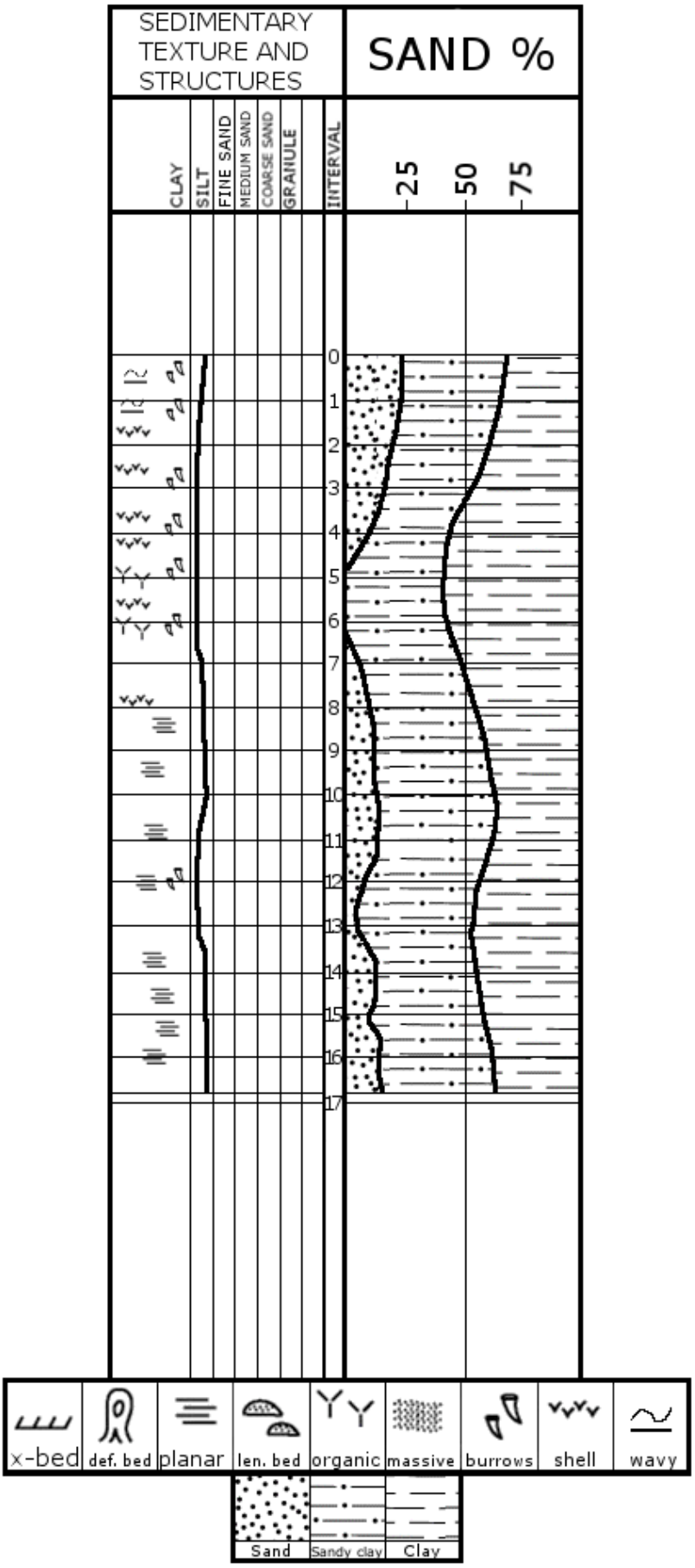


**Appendix A Figure 4.** Vibracore 96-3

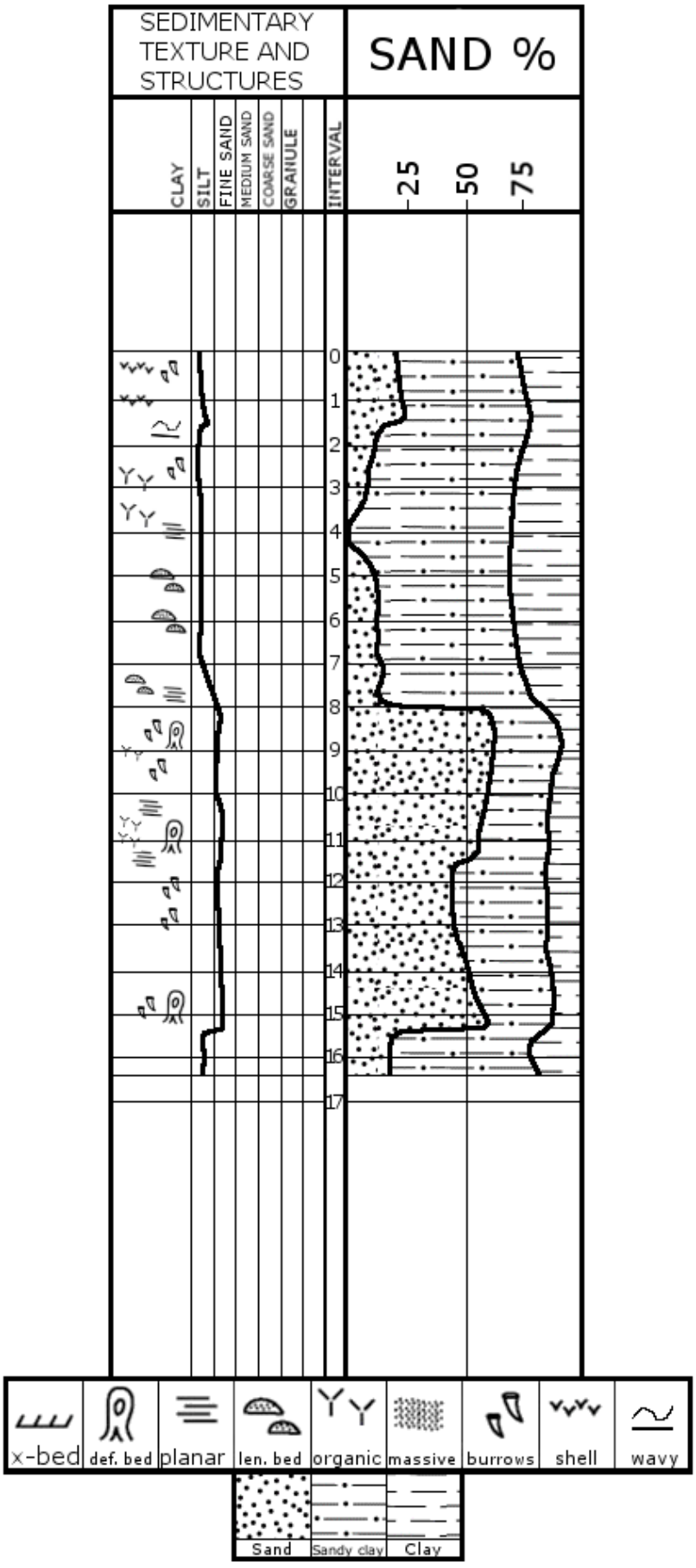


**Appendix A Figure 5.** Vibracore 96-4

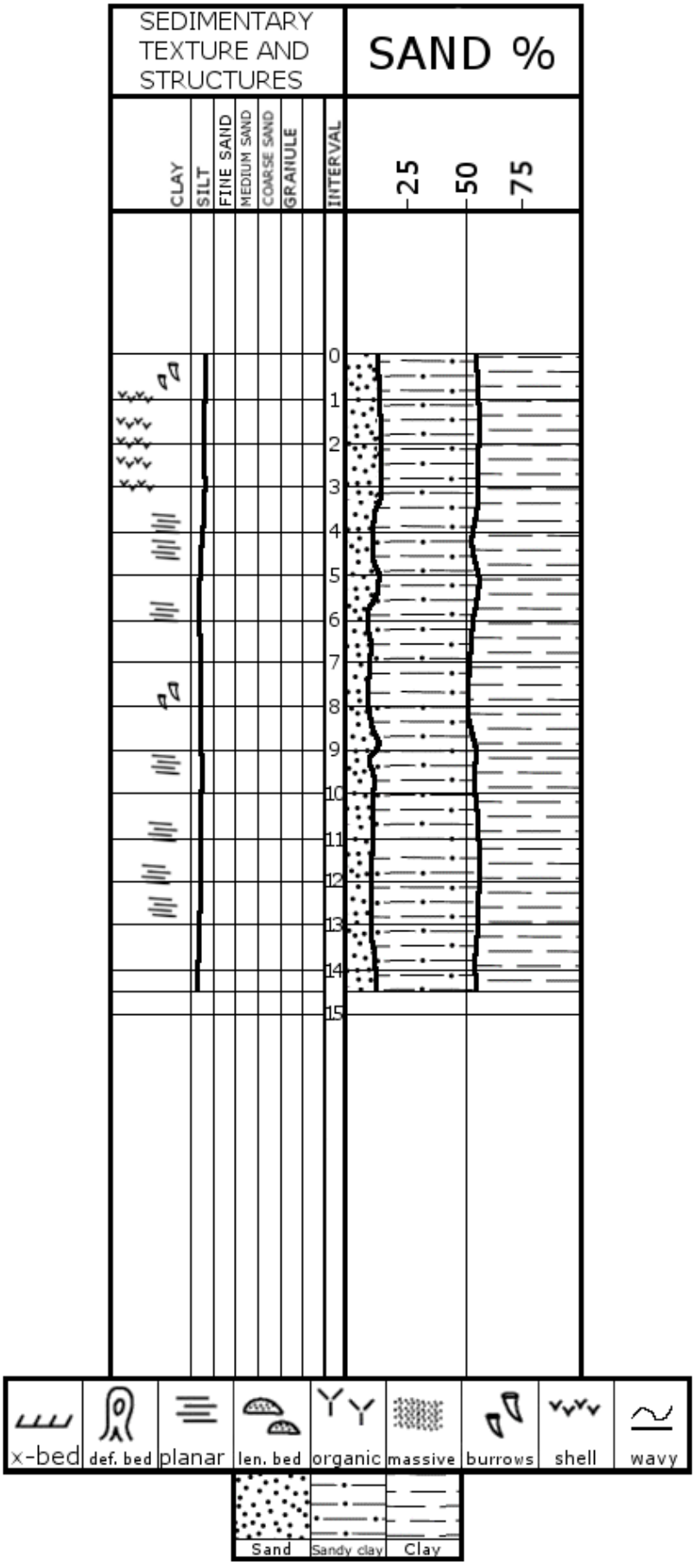


**Appendix A Figure 6.** Vibracore 96-5

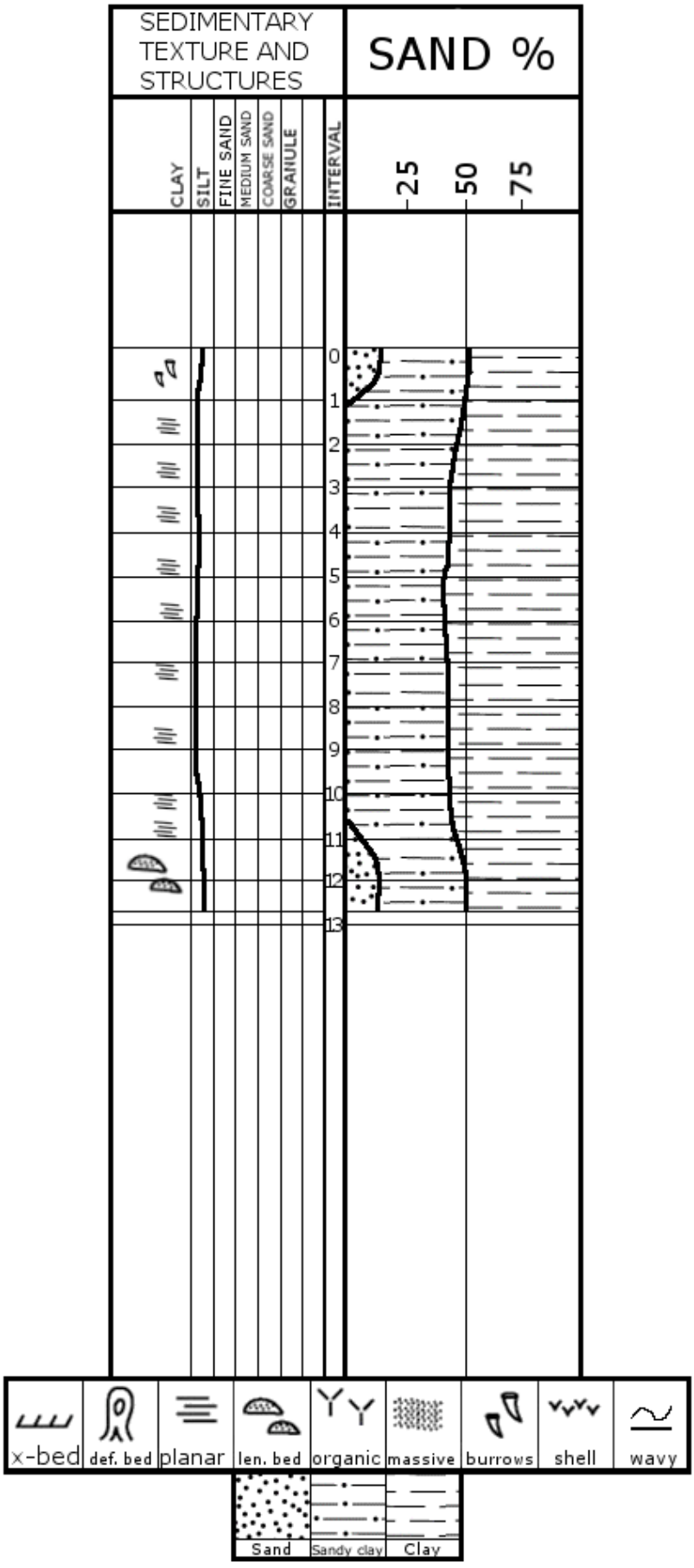


**Appendix A Figure 7.** Vibracore 97-16

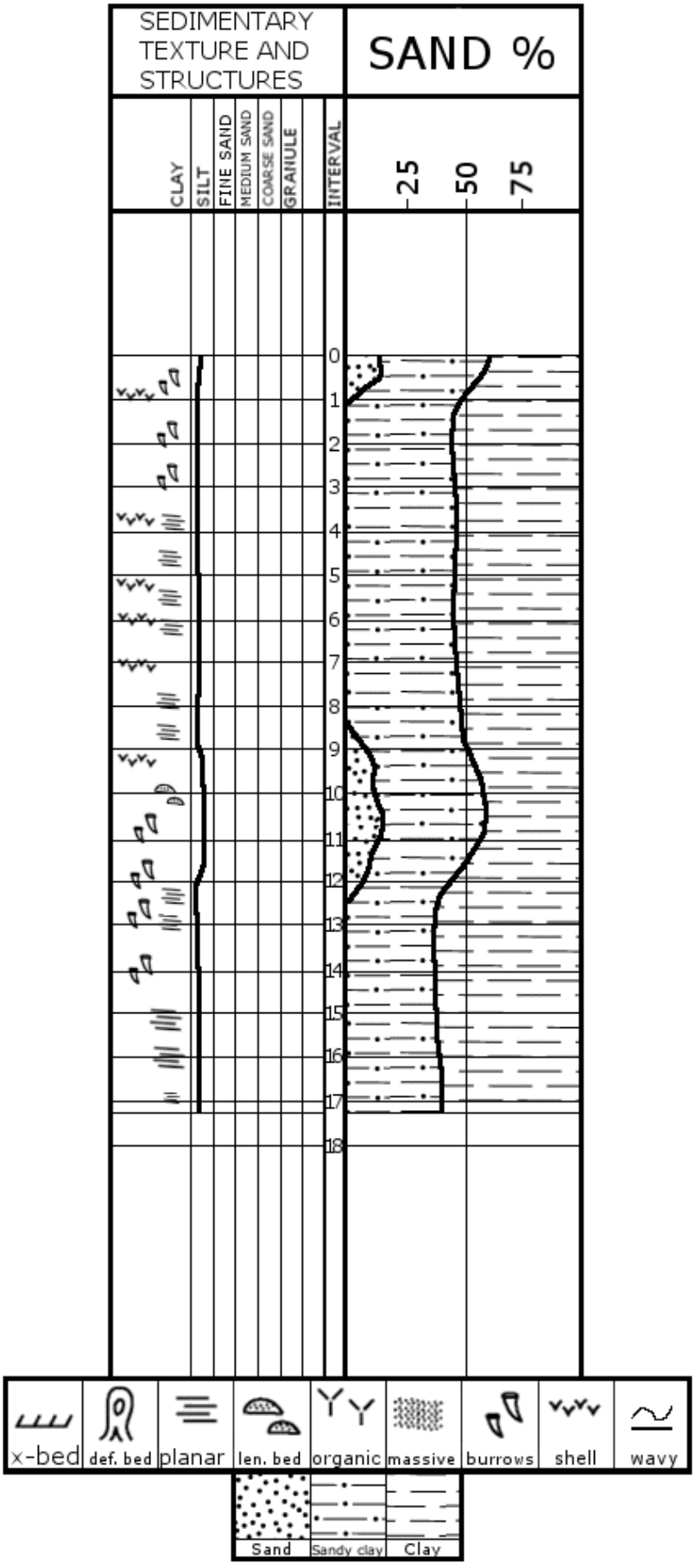


**Appendix A Figure 8.** Vibracore 97-17

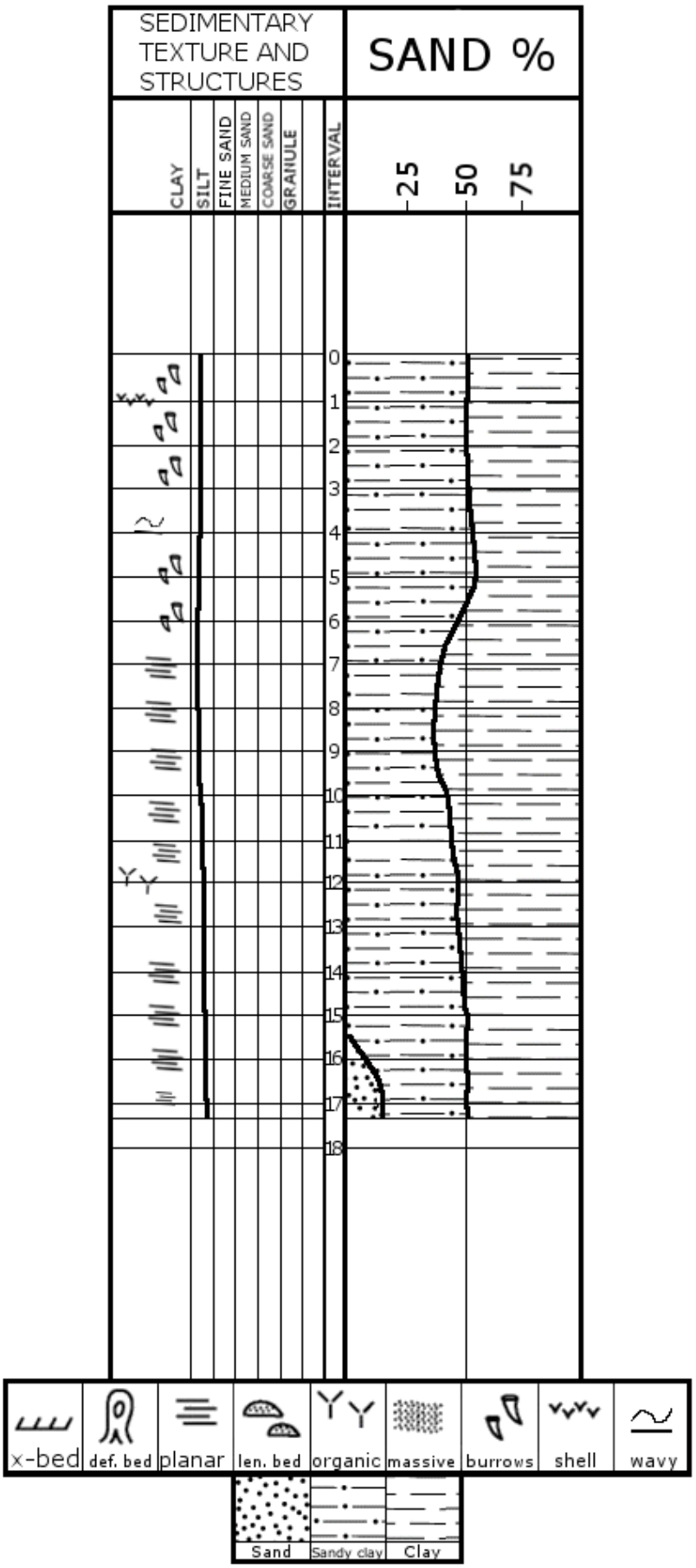


**Appendix A Figure 9.** Vibracore 97-18

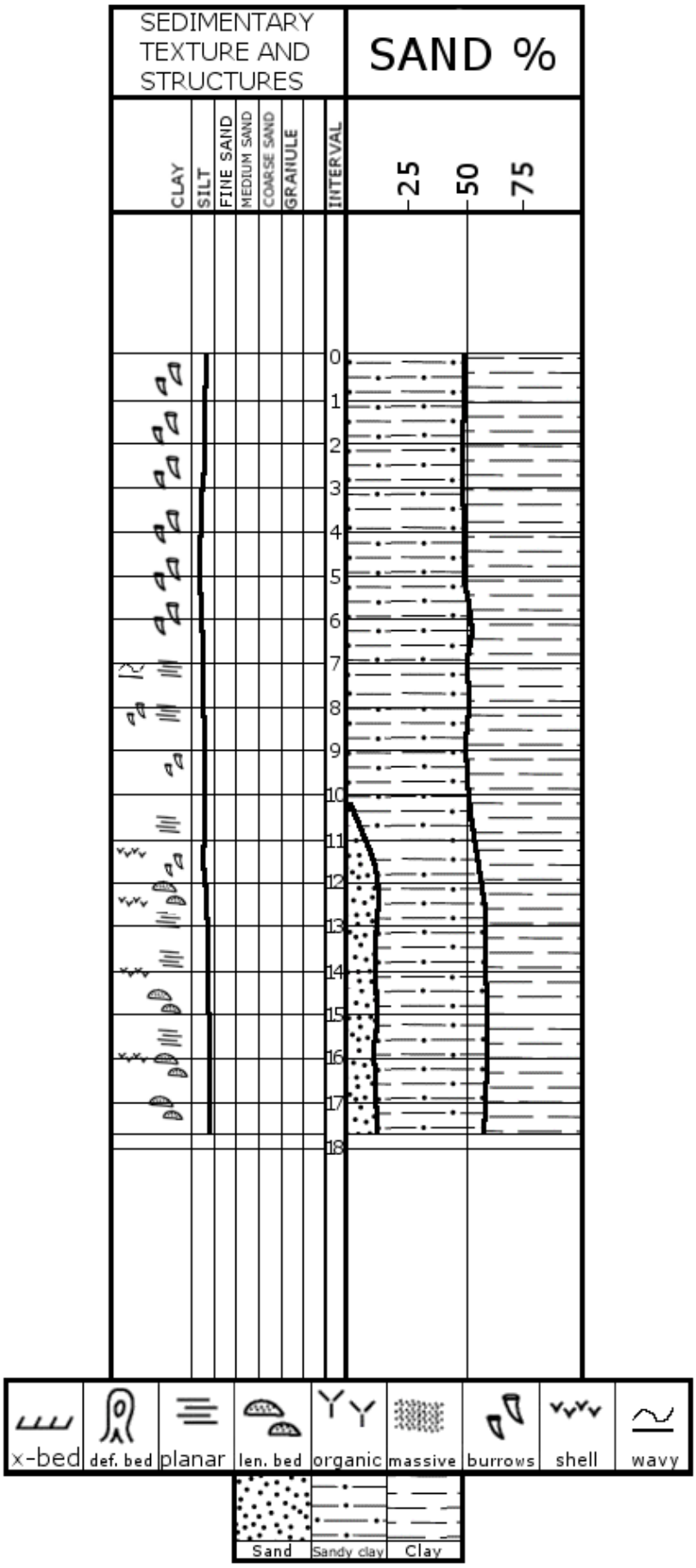


**Appendix A Figure 10.** Vibracore 97-19

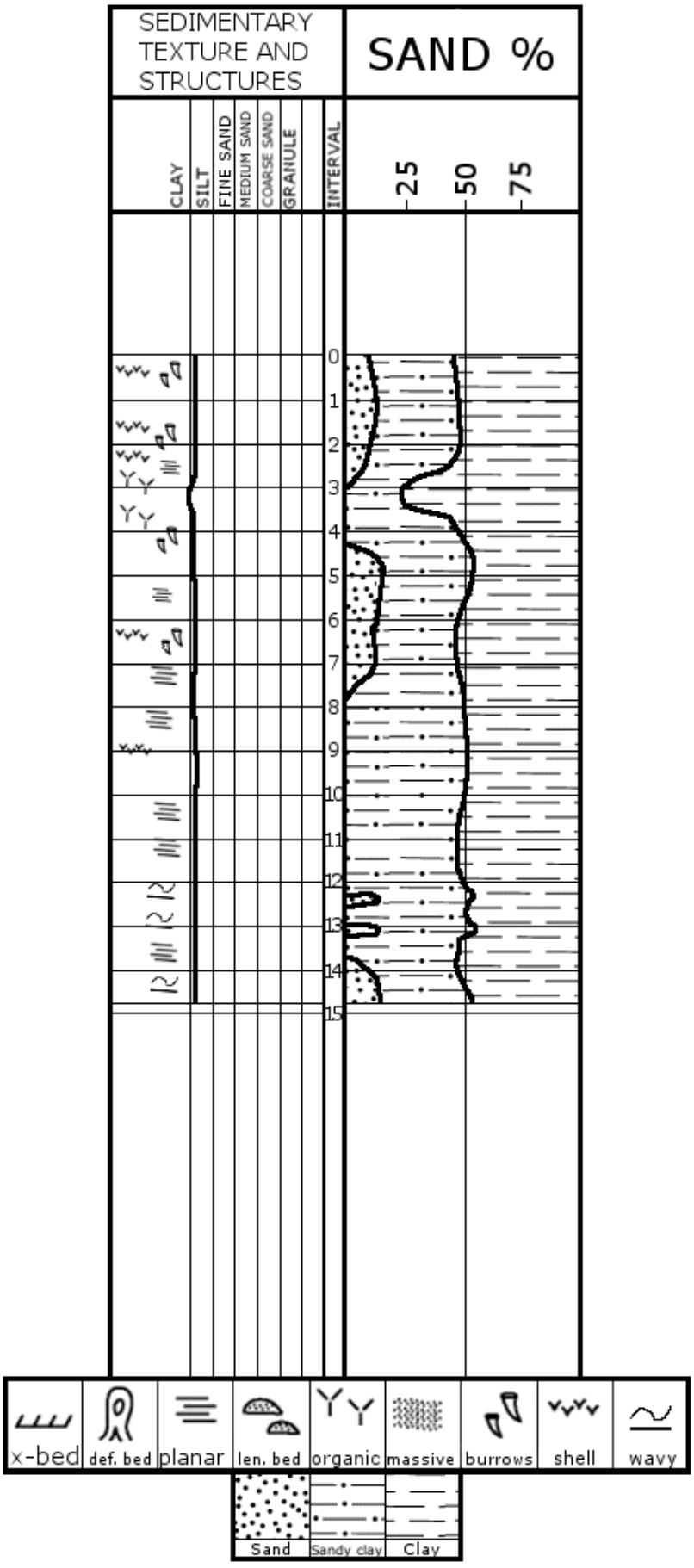


**Appendix A Figure 11.** Vibracore 97-21

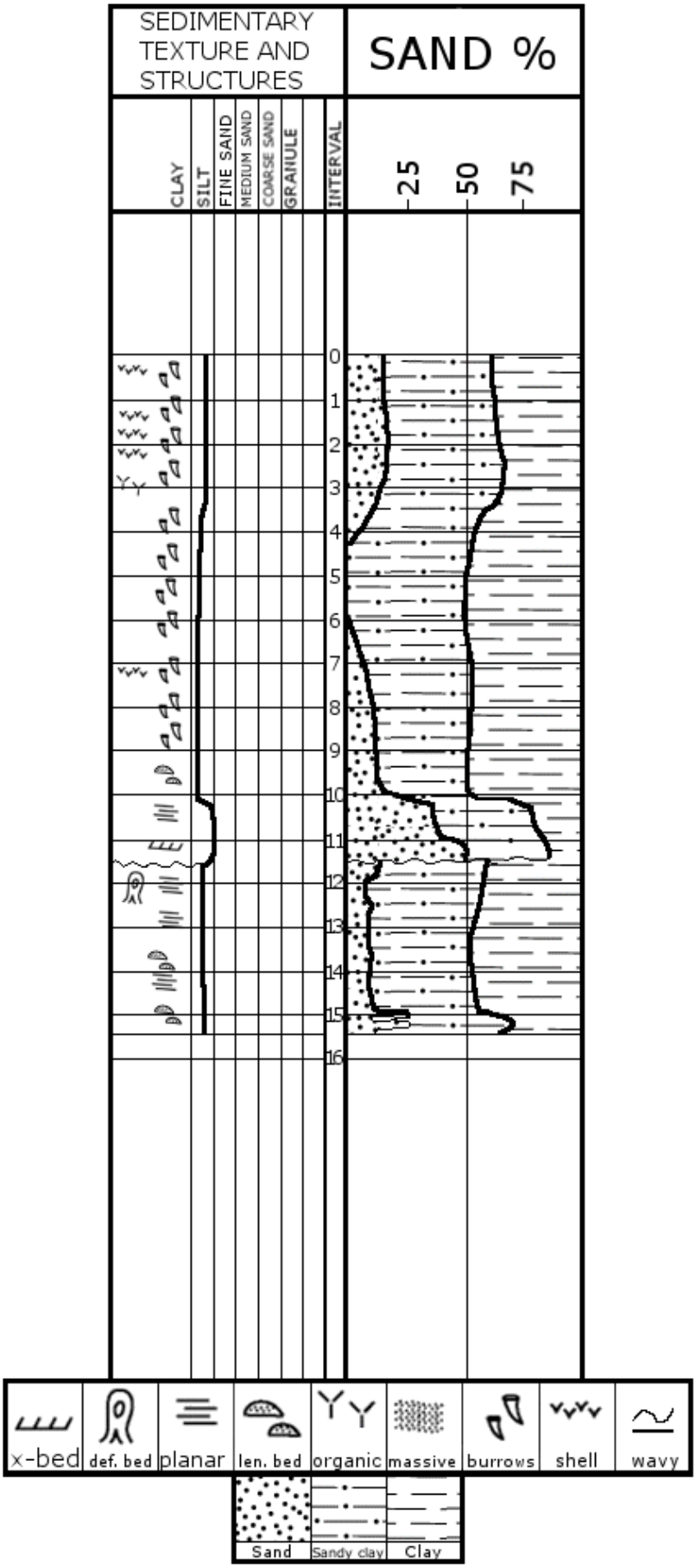


**Appendix A Figure 12.** Vibracore97-2

## Appendix B Chirp Collection Dates

| Date 07/18/2016 | Weather - Clear | Speed ~ 3.7 Knots | Seas < 1 foot | Frequency 2-12kHz |
|---|---|---|---|---|
| Line # | Start Time | End Time | Collection Direction | Notes |
| 36 | 10:20am | 10:27am | North | |
| 35 | 10:33am | 10:40am | South | |
| 33 | 10:46am | 10:55am | North | |
| 31 | 11:03am | 11:10am | South | |
| 29 | 11:15am | 11:24am | South | |
| 27 | 11:29am | 11:39am | North | Wind Speed Increased waves ~ 1 foot |
| 25 | 11:44am | 12:05pm | South | |
| 23 | 12:17pm | 12:35pm | North | |
| 21 | 12:41pm | 1:01pm | South | |
| 19 | 1:09pm | 1:17pm | South | |
| 17 | 1:23pm | 1:31pm | North | |
| 15 | 1:36pm | 1:44pm | South | |
| 13 | 1:50pm | 1:59pm | North | |
| 11 | 2:11pm | 2:18pm | South | |
| 9 | 2:39pm | 2:45pm | North | |
| Date 07/19/2016 | Morning - Storms | Speed ~ 4.0 Knots | Seas ~ 1 foot | Frequency 2-12kHz |
| Line # | Start Time | End Time | Collection Direction | Notes |
| 24 | 11:13am | 11:23am | North | |
| 22 | 11:28am | 11:36am | South | |
| 20 | 11:43am | 11:53am | North | |
| 18 | 11:57am | 12:06pm | South | |
| 16 | 12:13pm | 12:22pm | North | |
| 14 | 12:29pm | 12:37pm | South | |
| 12 | 12:45pm | 12:54pm | North | |
| 10 | 12:59pm | 1:08pm | South | |
| 8 | 1:15pm | 1:24pm | North | |
| 6 | 1:29pm | 1:37pm | South | |
| 4 | 1:43pm | 1:50pm | North | |
| 3 | 1:56pm | 2:04pm | South | |
| 2 | 2:08pm | 2:16pm | North | |
| 1 | 2:20pm | 2:28pm | South | Ended Day Due to Storms |

**Table 2.** Shows the collection starts and end times of each Chirp line that was collected as well as the azimuth along which the line was collected.

## APPENDIX CChirp Seismic Lines

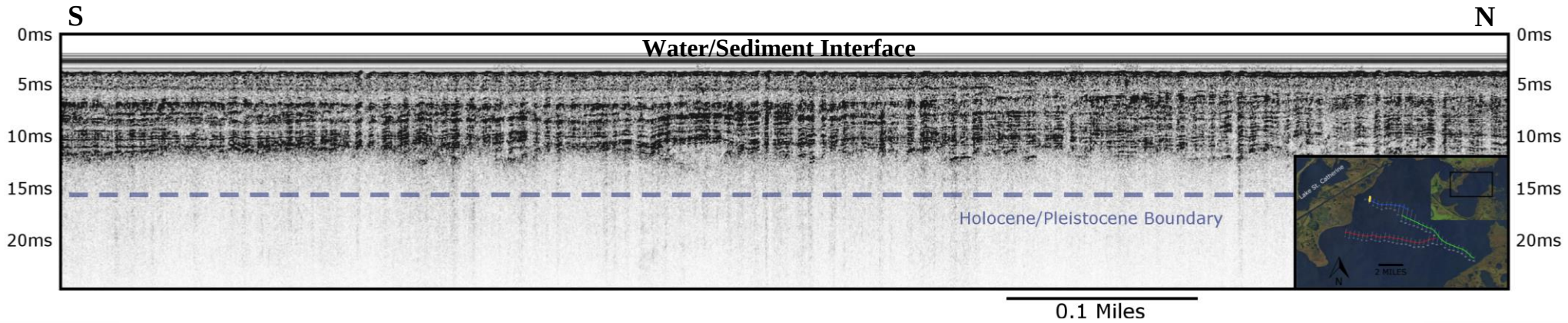


**Appendix C Figure 1.** Chirp seismic line #7. The dashed blue line represents where the approximate Holocene/Pleistocene age boundary is based on an isopach map from Kulp et al. (2002) (inset map from USGS *Landsat Look Viewer March 27, 2015).*

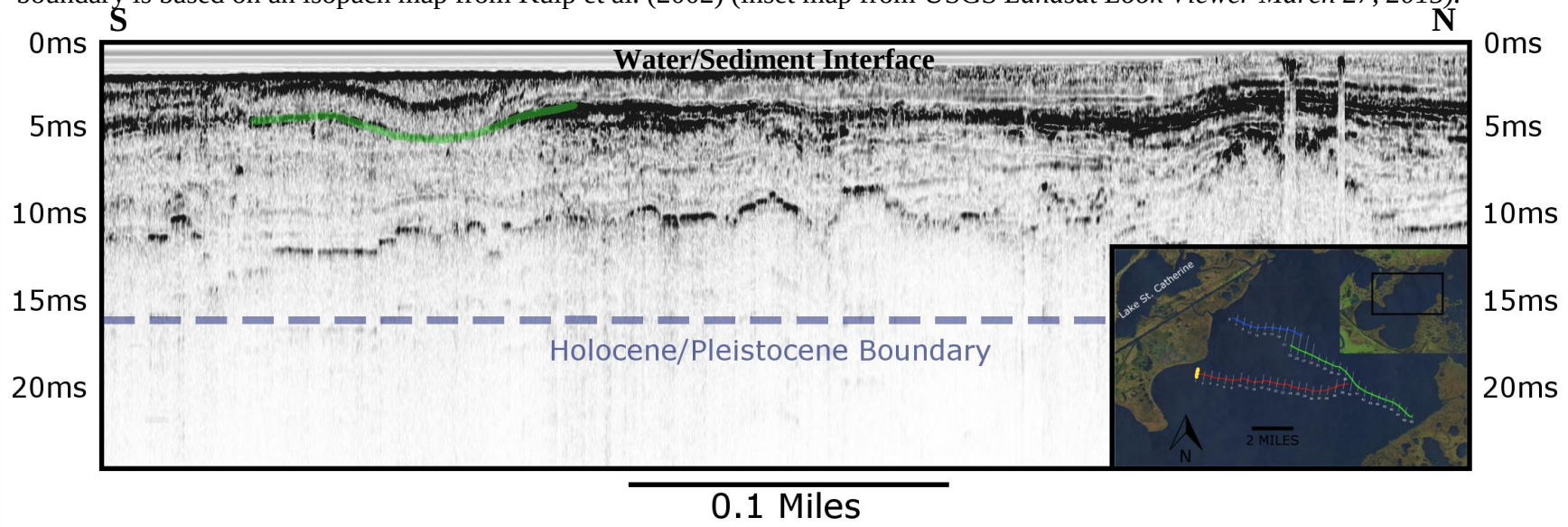


**Appendix C Figure 2.** Chirp seismic line #1. The green line represents the interpreted channel bottom and the dashed blue line represents where the approximate Holocene/Pleistocene age boundary is based on an isopach map from Kulp et al. (2002) (inset map from USGS *Landsat Look Viewer March 27, 2015).*

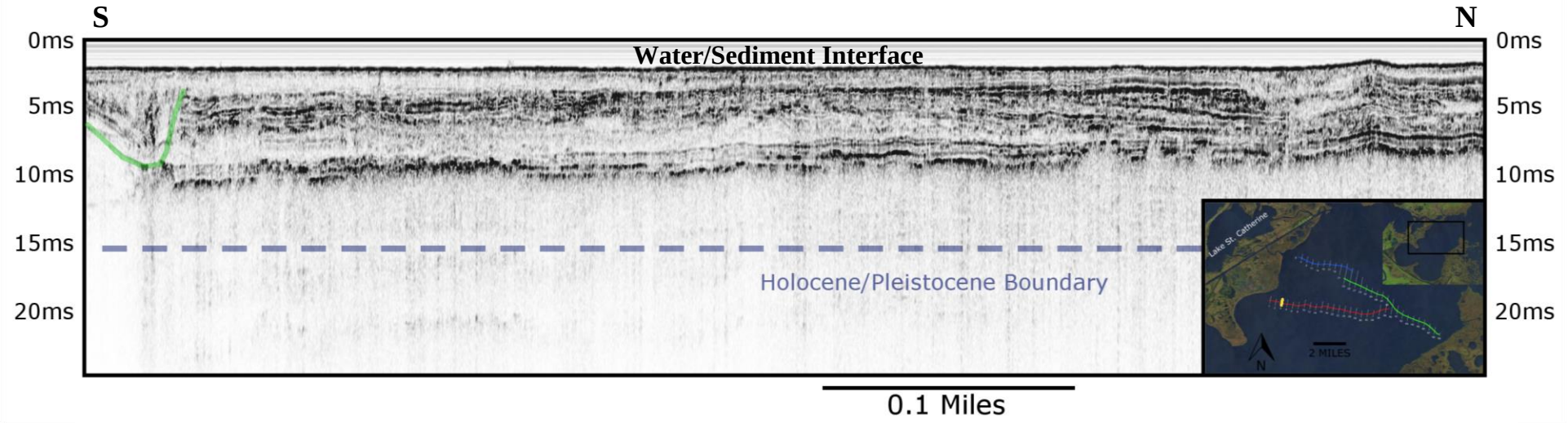


**Appendix C Figure 3.** Chirp seismic line #3. The green line represents the interpreted channel bottom and the dashed blue line represents where the approximate Holocene/Pleistocene age boundary is based on an isopach map from Kulp et al. (2002) (inset map from USGS *Landsat Look Viewer March 27, 2015).*

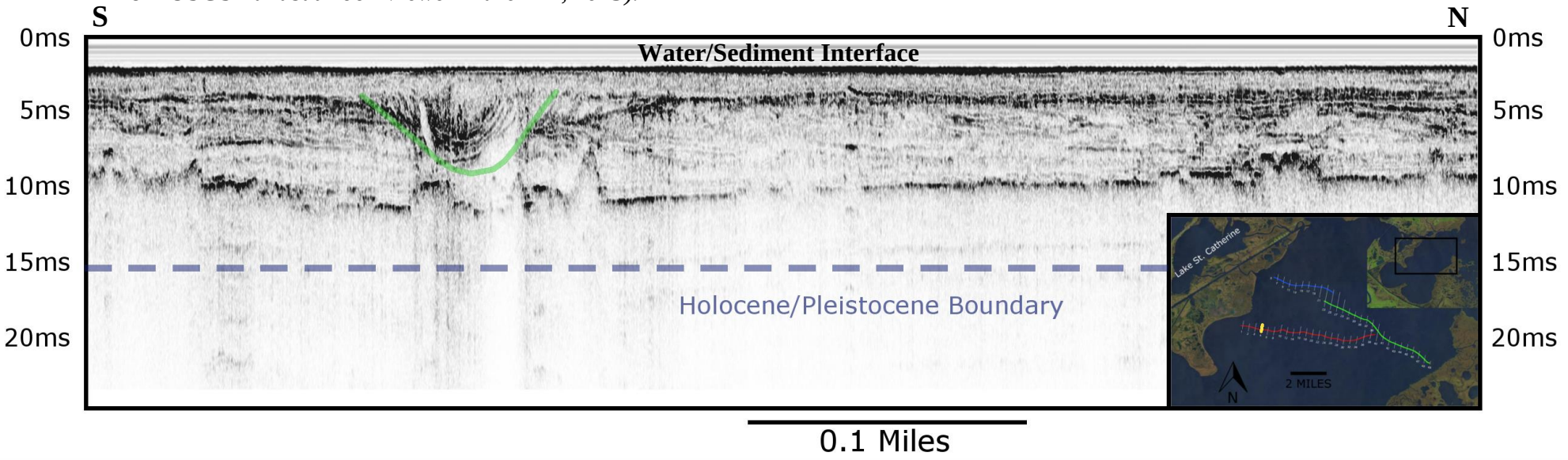


**Appendix C Figure 4.** Chirp seismic line #4. The green line represents the interpreted channel bottom and the dashed blue line represents where the approximate Holocene/Pleistocene age boundary is based on an isopach map from Kulp et al. (2002) (inset map from USGS *Landsat Look Viewer March 27, 2015).*

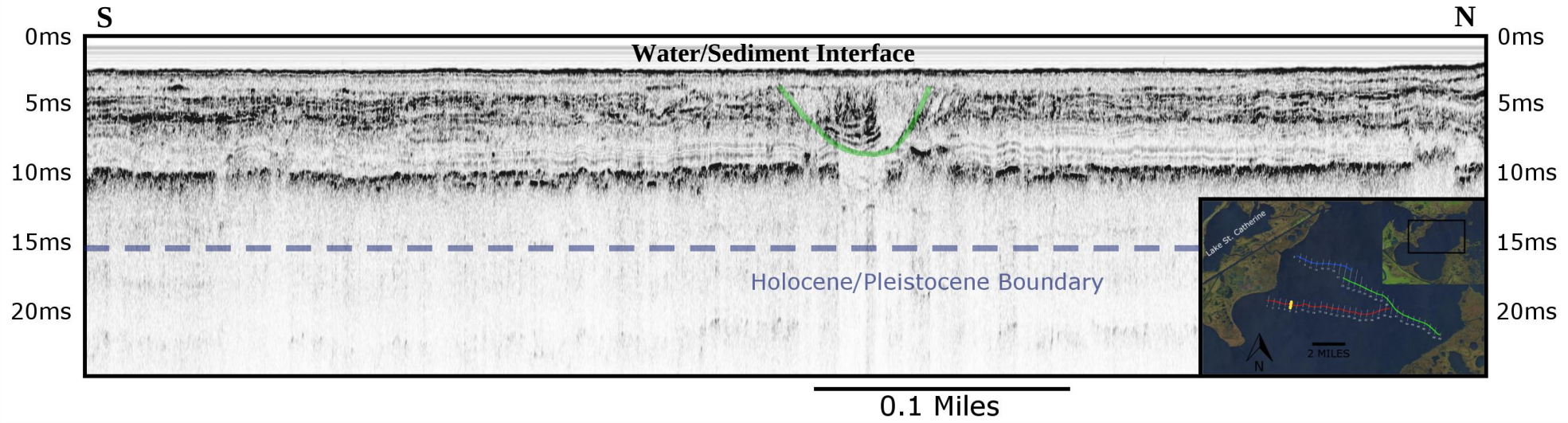


**Appendix C Figure 5.** Chirp seismic line #6. The green line represents the interpreted channel bottom and the dashed blue line represents where the approximate Holocene/Pleistocene age boundary is based on an isopach map from Kulp et al. (2002) (inset map from USGS *Landsat Look Viewer March 27, 2015).*

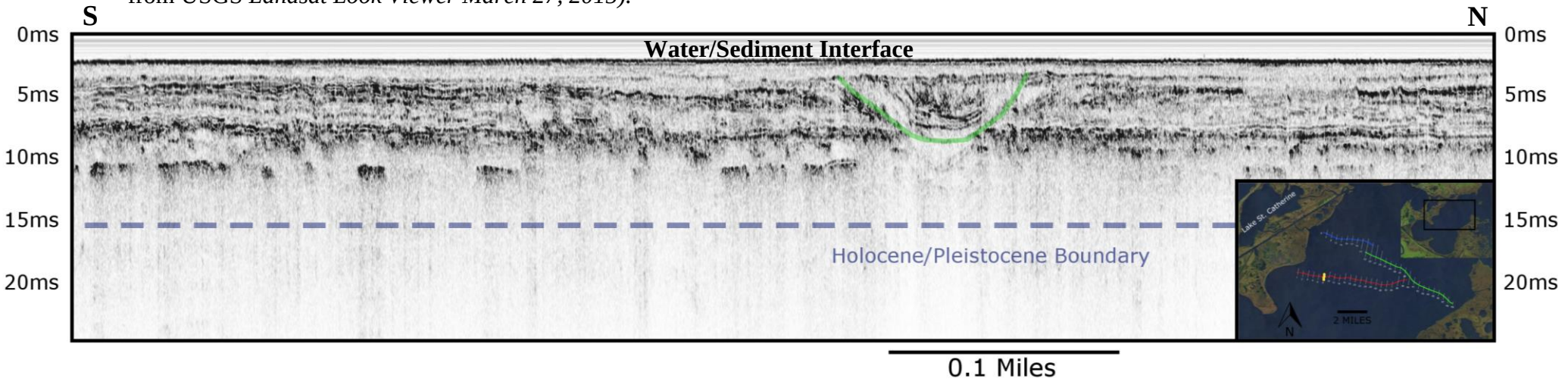


**Appendix C Figure 6.** Chirp seismic line #8. The green line represents the interpreted channel bottom and the dashed blue line represents where the approximate Holocene/Pleistocene age boundary is based on an isopach map from Kulp et al. (2002) (inset map from USGS *Landsat Look Viewer March 27, 2015).*

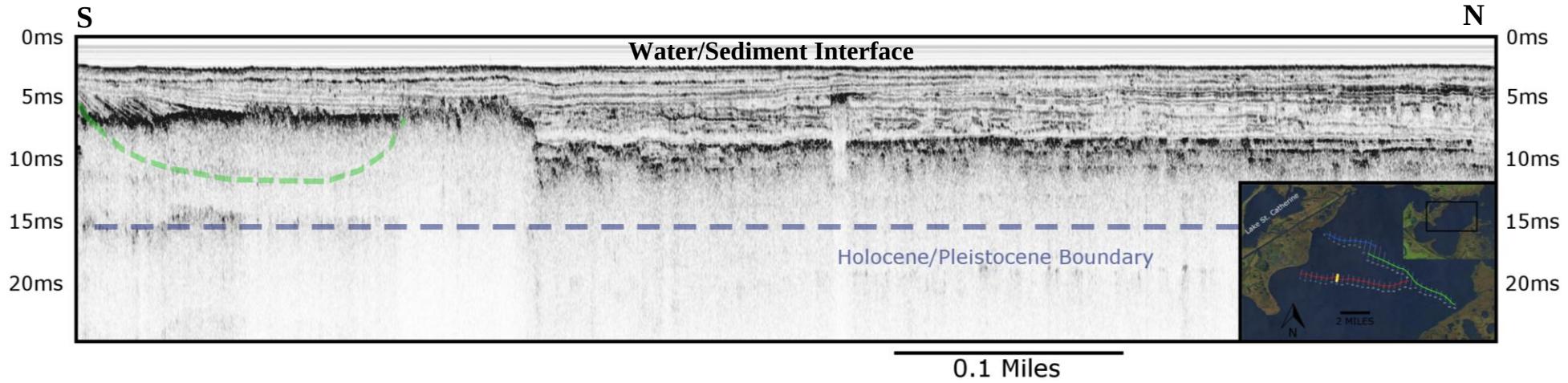


**Appendix C Figure 7.** Chirp seismic line #12. The green line represents the interpreted channel bottom and the dashed blue line represents where the approximate Holocene/Pleistocene age boundary is based on an isopach map from Kulp et al. (2002) (inset map from USGS *Landsat Look Viewer March 27, 2015*).

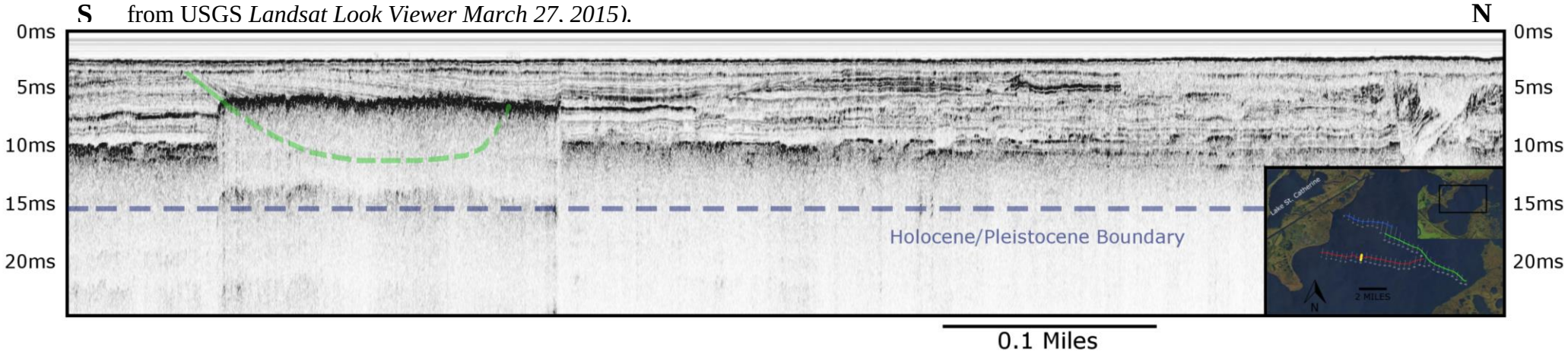


**Appendix C Figure 8.** Chirp seismic line #14. The green line represents the interpreted channel bottom and the dashed blue line represents where the approximate Holocene/Pleistocene age boundary is based on an isopach map from Kulp et al. (2002) (inset map from USGS *Landsat Look Viewer March 27, 2015).*

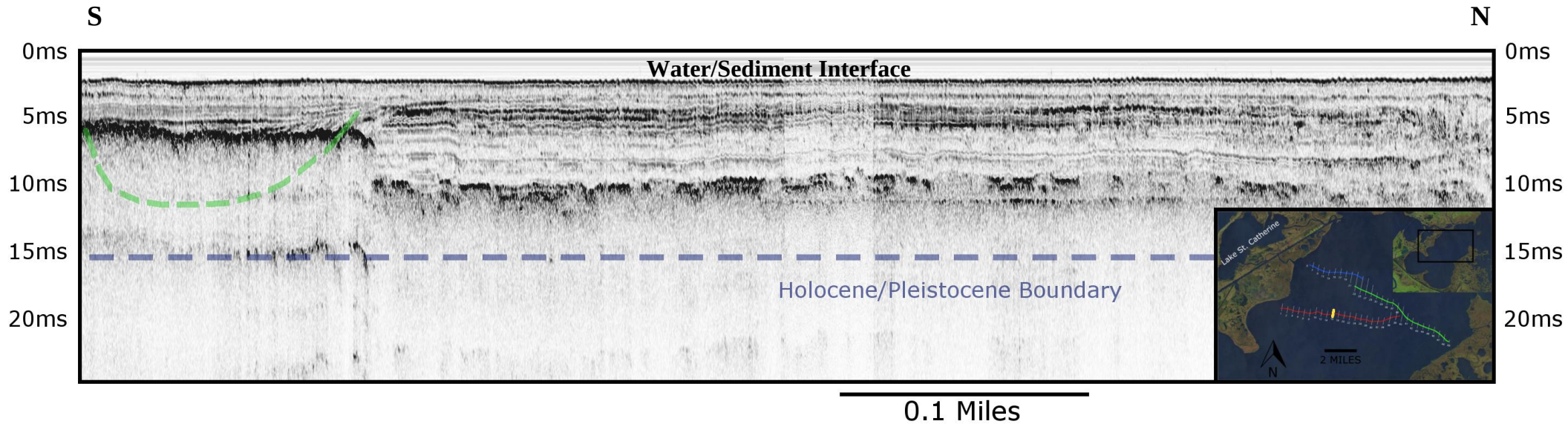


**Appendix C Figure 9.** Chirp seismic line #16. The green line represents the interpreted channel bottom and the dashed blue line represents where the approximate Holocene/Pleistocene age boundary is based on an isopach map from Kulp et al. (2002) (inset map from USGS *Landsat Look Viewer March 27, 2015).*

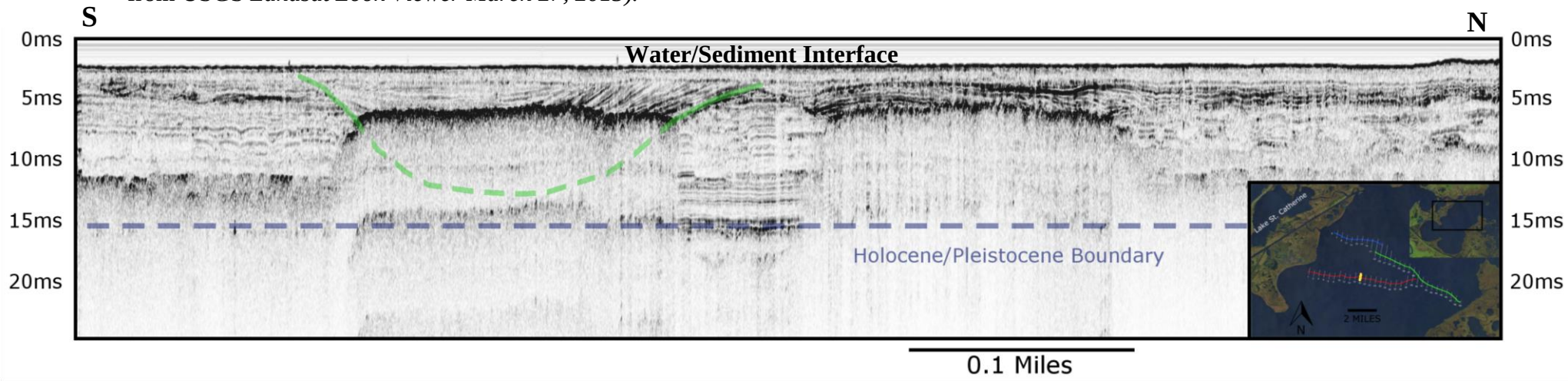


**Appendix C Figure 10.** Chirp seismic line #18. The green line represents the interpreted channel bottom and the dashed blue line represents where the approximate Holocene/Pleistocene age boundary is based on an isopach map from Kulp et al. (2002) (inset map from USGS *Landsat Look Viewer March 27, 2015).*

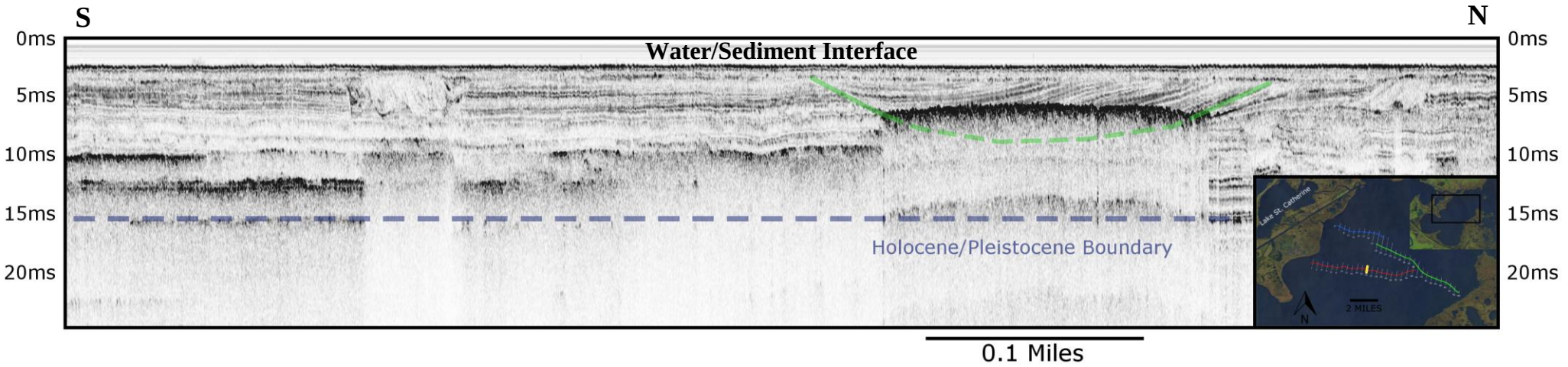


**Appendix C Figure 11.** Chirp seismic line #20. The green line represents the interpreted channel bottom and the dashed blue line represents where the approximate Holocene/Pleistocene age boundary is based on an isopach map from Kulp et al. (2002) (inset map from USGS *Landsat Look Viewer March 27, 2015).*

# Vita

Joseph Frank was born in Princeton, New Jersey and spent most of his youth exploring the Sourland Mountains, which surrounded his families' home. Before coming to the University of New Orleans to pursue a M.S. he earned a B.S. in geosciences (2013) from the Pennsylvania State University. While at Penn State he studied trace and major elements of volcanics ejected from an Argentinian caldera to understand where the magma was sourced from. After Graduating from Penn State he took an Environmental Science job at the engineering firm Charles P. Johnson located in the D.C. area.